DOI:10.14753/SE.2015.1764

A new method for identification and isolation of human embryonic stem cell-derived cardiac progenitors and cardiomyocytes

Ph.D. dissertation

Kornélia Szebényi

Semmelweis University
Doctoral School of Molecular Medicine

Doctoral supervisor: Dr. Balázs Sarkadi, member of HAS

Official opponents: Dr. Gábor Földes, Ph.D.
Dr. Melinda Pirity, Ph.D.

President of the examination committee: Dr. Erzsébet Ligeti, member of HAS
Members of the examination committee: Dr. Szabolcs Sipeki, Ph.D.
Dr. László Hiripi, Ph.D.

Budapest
2014

DOI:10.14753/SE.2015.1764

Table of Contents

DOI:10.14753/SE.2015.1764

DOI:10.14753/SE.2015.1764

1. List of Abbreviations

ACTB – human β-actin

AF – AlexaFluor

AFP – alpha-fetoprotein

ALCAM/CD166 - activated leukocyte cell adhesion molecule

APC - allophycocyanin

bFGF – basic fibroblast growth factor

βIII-Tub – beta-III tubulin

BMP4 - bone morphogenetic protein 4

CAPG – capping protein gelsolin-like

CD – cluster of differentiation

C-KIT/CD117 - tyrosine kinase Kit

CM – cardiomyocyte

CMSC – cardiomyocyte supporting cell

CMV - cytomegalovirus

CPC – cardiac progenitor cells

cTnI – cardiac troponin I

D - day

DM – differentiation medium

DMEM – Dulbecco's Modified Eagle's Medium

EB – embryoid body

EMT – epithelial-to-mesenchymal transition

END-2 - mouse visceral endoderm-like cells

END2-CM – END-2 conditioned medium

FACS - fluorescence activated cell sorting

FBS – fetal bovine serum

FITC - fluorescein isothiocyanate

GFP – green fluorescent protein

hESC – human embryonic stem cell

hiPSC – human induced pluripotent stem cell

hPSC – human pluripotent stem cell

ISL1 - insulin gene enhancer protein

KDR/VEGF-R - vascular endothelial growth factor receptor 2

MEF – mouse embryonic fibroblast

mESC – mouse embryonic stem cell

MTG – monothioglycerol

PAX6 - paired box 6

PDGFRA - platelet-derived growth factor receptor

PE - phycoerythrin

PECAM-1 – platelet endothelial cell adhesion molecule-1

PGK - phosphoglycerate kinase

PI - propidium iodide

QPCR - real-time quantitative PCR

RCM – ReproCardio Medium

rEBs – reaggregated embryoid bodies

SIRPA/CD47 - signal regulatory protein α

SMA – alpha-smooth muscle actin

SSEA4 - stage-specific embryonic antigen-4

TBX5 - T-Box Protein 5

TMRM - tetramethylrhodamine methyl ester perchlorate

TNNT2 - troponin T type 2

UbC - ubiquitinC

VCAM1/CD106 - vascular cell adhesion molecule 1

DOI:10.14753/SE.2015.1764

2. Introduction

Stem cells are capable of renewing themselves through cell division for unlimited times and divide asymmetrically, generating two different daughter cells. Under certain physiological or experimental conditions, stem cells can be induced to become tissue-specific cells with special functions through differentiation. Stem cells can have different potentials (e.g. toti-, pluri- or multipotency), limiting the number of tissue types that can be differentiated from them.

Features of pluripotency include the potential of unlimited cell growth and self-renewal, as well as the capacity to generate all cell types of the body. However, pluripotent cells are restricted in their potential compared to totipotent stem cells, since human pluripotent stem cells (hPSCs) cannot give rise to cells of the extra-embryonic tissues (amnion, chorion, yolk sac and the allantois). Multipotent stem cells have even lower potential and only give rise to tissue-specific cells. Therefore multipotent stem cells are often termed as multipotent progenitor cells of certain developmental lineages.

This dissertation will focus on hPSCs and their *in vitro* differentiation capabilities, with a specific focus on the cardiac lineage to provide a method for identifying and isolating cell types at different stages of cardiac commitment.

2.1. Human pluripotent stem cells

2.1.1 Generation of human pluripotent stem cells

The derivation of mouse pluripotent stem cell lines from blastocyst-stage embryos revolutionized biological research through allowing generation of knock-out animal models (2007 Nobel Prize) and opening new possibilities in studying early developmental events. The much awaited next step, the establishment of the first human embryonic stem cell (hESC) line was reported by Thomson *et al.* seventeen years later, in 1998[1]. The generation of hESC lines proved to be as revolutionary as the establishment of mouse ESC lines earlier, providing an excellent platform for human developmental studies and toxicological screenings, as well as the possibility of regenerative therapeutic applications.

DOI:10.14753/SE.2015.1764

Human ESC lines are usually derived from the inner cell mass of blastocyst stage embryos (see **Figure 1**). Unfortunately, ethical concerns regarding the use of *in vitro*-fertilized human embryos for research purposes strongly hinder the application of hESCs in basic research, drug development and medical therapy, even though the embryos are otherwise supposed to be destroyed. In addition to the ethical concerns, several other drawbacks exist. One of these is the potential immunological incompatibility that might limit the use of hESC-derived cells for regenerative purposes[2]. However, immunological problems may be prevented by hESC-banking[3, 4] or transplantation of encapsulated hESC-derivatives secreting the necessary factors to compensate for deficits[5].

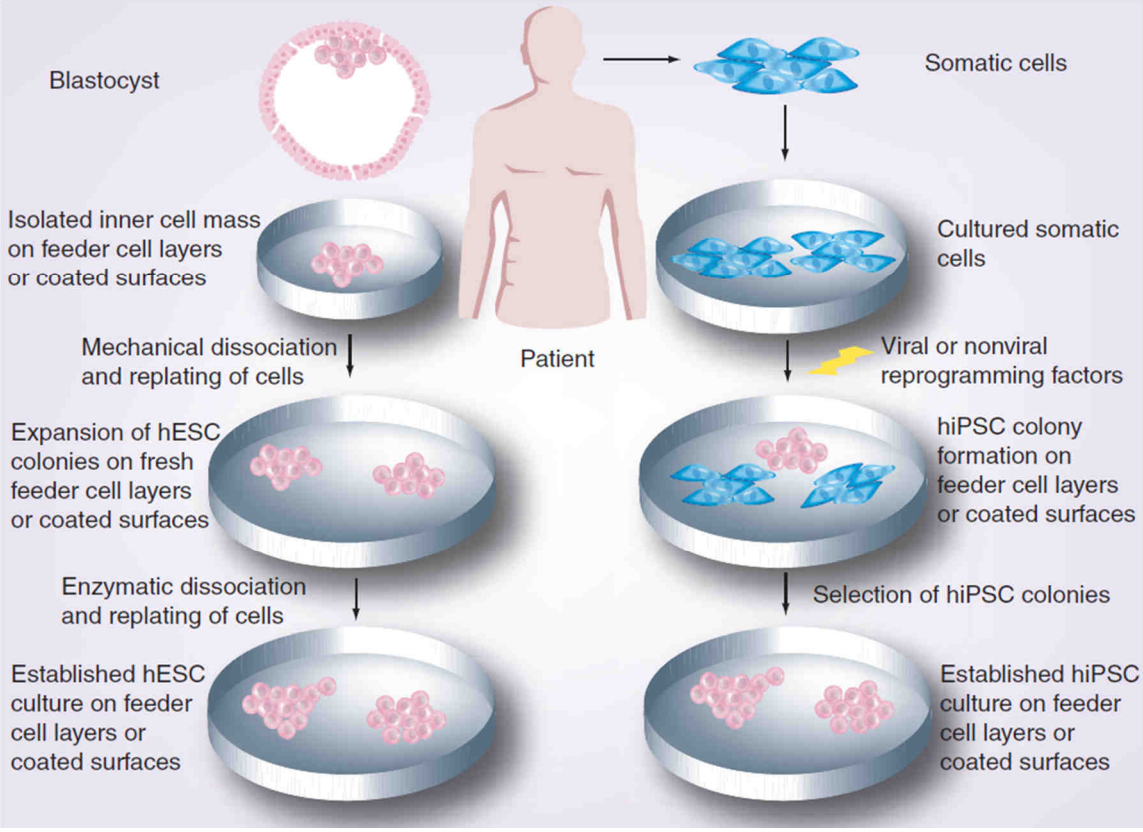

Figure 1. Methods for the generation and differentiation of human pluripotent stem cell lines. The image is taken from Szebényi *et al.*[6]

In 2006, another milestone of stem cell research was reached when induced pluripotent stem cells (iPSC) were generated from mouse fibroblast cultures by forced

expression of four transcription factors (Oct3/4, Sox2, Klf4 and c-Myc)[7]. This study was immediately followed by numerous others, documenting the generation of human induced pluripotent stem cells (hiPSCs) with viral or non-viral delivery of the reprogramming factors[8] (see **Figure 1**). The discovery that mature cells can be reprogrammed to become pluripotent was honoured by the 2012 Nobel Prize.

By now, hundreds of hPSC lines exist and many of them are available from tissue banks, while cell-line specific information has been collected and made accessible in Stem Cell Registries (reviewed by Borstlap *et al*.[9]).

2.1.2 Culture and characterization of human pluripotent stem cells

Human iPSCs are similar to hESCs regarding their morphological and proliferative characteristics, as well as cell surface marker and gene expression profiles or differentiation potential. Small colonies of hESCs and hiPSCs are usually maintained on mitotically inactivated feeder cells (mouse or human[10, 11]), or on extracellular matrix-coated surfaces (e.g. Matrigel[12], Laminin[13, 14] or Vitronectin[15, 16]) (see **Figure 1**). Feeder cells secrete necessary factors for maintaining the pluripotent state, therefore a special type of medium is needed for culturing hPSCs on extracellular matrix-coated surfaces (e.g. mTeSR, MEF conditioned medium or Essential 8 medium), to compensate for the absence of the feeder layer.

Several widely accepted markers for testing the undifferentiated (pluripotent) state of hPSC cultures exist, including alkaline phosphatase activity, expression of cell surface molecules (SSEA3, SSEA4, TRA1-60 TRA1-81, E-Cadherin), and transcription factors e.g. Nanog, Oct3/4 and Sox2 [17]. During long-term cell culture chromosomal abnormalities are frequently acquired, therefore methods to monitor and suppress abnormal karyotype acquisition are crucial[18-21]. The problem of large-scale production of high quality hPSCs has been also addressed, resulting in different solutions such as robotic systems[22] or 3D culture expansion in stirring suspension bioreactors[23-26].

Under adequate conditions hPSCs differentiate spontaneously to cells of all three primitive germ layers (endoderm, ectoderm and mesoderm)[27]. *In vivo* this leads to the

development of benign tumours (teratomas), containing a random mixture of partially developed tissues. *In vitro* hPSCs can spontaneously differentiate into specific cell types, including neurons, cardiomyocytes, epithelial and mesenchymal cells, although the output of each differentiation may vary depending on lot-to-lot variation of the reagents, e.g. foetal bovine serum (FBS), used to provide necessary differentiation signals. Therefore, several well-defined and reproducible methods for hPSC differentiation have been developed, allowing generation of cell populations by applying defined growth factors or chemical inducers instead of FBS or co-culture of hESCs with cells capable of lineage specific induction (more to this topic in Chapter 1.4)[28]. By using these methods, designated collectively as directed differentiation, clinically relevant cells types could be generated, including neural tissues[29, 30], cardiomyocytes[31], insulin producing islet cells[32, 33], and various blood cells[34]. However, it is important to emphasize, that *in vitro* developing cells usually reach a maturation status resembling rather the embryonic than the adult phenotype, therefore some studies aimed to develop techniques for maturation of specific cell types[35-38].

There is one key point where hiPSCs and hESCs may differ from each other, and that is the epigenetic memory of hiPSCs inherited from the reprogrammed somatic cells and gained through the reprogramming itself (reprogramming-specific epigenetic signature), eventually keeping away iPSCs from ground state pluripotency[39-41]. Even functional differences among hESC and hiPSC-derivatives have been reported[42, 43] . Therefore the existence of iPSC technology does not mean that there is no need for hESCs anymore - actually the use of hiPSCs makes hESCs indispensable as controls for hiPSCs-based models. A more technical issue is that development of new methods (genetic or non-genetic), allowing the isolation of a specific cell type, should be carried out on several types of hPSCs, since these methods have to be equally valid for hESCs and hiPSCs.

Still, hPSCs and their derivatives provide an excellent basis for studying early events of human development and for the establishment of human cellular drug screening model systems. New medical regenerative therapies based on various hESCs are already in clinical trials[44].

2.1.3 Application of human pluripotent stem cells and their derivatives

A major point where hiPSCs and hESCs are different is that the generation of hiPSCs does not require the use of human embryos, and therefore ethical concerns attenuate. An additional benefit of hiPSCs over hESCs is that the iPSC technology can provide patient- and disease-specific pluripotent stem cells and derivatives, allowing personalized *in vitro* disease modelling, drug screening, and even cellular replacement therapies without immunological problems.

The potential of hiPSCs in therapeutic approaches was examined in several proof-of-concept studies, e.g. in models of sickle cell anaemia[45], Fanconi anaemia[46] or Parkinson's disease[47]. In the case of the sickle cell anaemia model it was demonstrated that patient-derived hiPSCs can be corrected by targeted gene modification, while in the case of Fanconi anaemia the authors corrected patient-derived somatic cells before reprogramming and generated phenotypically normal haematopoietic progenitors of the myeloid and erythroid lineages from the corrected hiPSCs, thereby providing evidence for the potential of the iPSC technology in future therapeutic applications.

Disease-specific hPSC derivatives can also be used in screening applications to find drug candidate molecules allowing the rescue of the disease phenotype. In the case of hiPSCs derived from a patient with familial dysautonomia the authors revealed not only disease specific defects in neurogenesis but also found a compound that positively affected the otherwise defective migration of neural crest precursors[48].

Besides hiPSC-based disease models, disease-specific hESC lines also exist and are mostly derived from embryos diagnosed to carry mutations causing human diseases in Preimplantation Genetic Diagnosis[49]. Several hESC lines have been developed providing *in vitro* models for adrenoleukodystrophy, Duchenne and Becker muscular dystrophy, Fanconi anaemia, complementation group A, fragile-X syndrome, Huntington disease, Marfan syndrome, myotonic dystrophy, neurofibromatosis type I and thalassaemia[50].

Another application of hPSCs is to provide human cardiomyocytes (CMs) for the drug development process, in order to test for cardiac side effects of drugs. These effects are the most common causes of withdrawal of already approved drugs from the market,

and result from the species differences (e.g. in ion channel drug sensitivities) between humans and the animal models used for preclinical toxicity studies [51]. In addition, cardiac disease-specific human CMs can be used in screening applications, either aiming to find drug candidate molecules allowing to rescue the disease phenotype, or to detect disease-specific cardiotoxic side effects of any type of drugs.

Several hiPSC lines were derived from patients with cardiac channelopathies, such as the Long-QT syndrome type 1[52], Long-QT syndrome 2[53] and Timothy syndrome[54], while other congenital diseases affecting the heart such as the catecholaminergic polymorphic ventricular tachycardia[55], the arrhythmogenic right ventricular dysplasia/cardiomyopathy[56], the glycogen storage disease type II (Pompe) disease[57] or the LEOPARD syndrome[58] could also be modelled by hiPSC-derived CMs. A more detailed review of existing cardiac disease-specific iPSC lines can be found in the attached book chapter by Szebényi *et al.*, "Human Stem-Cell-Derived Cardiomyocytes in Drug Discovery and Toxicity Testing" (attached to the dissertation).

2.2. Generation of cardiomyocytes from human pluripotent stem cells

Human PSCs provide an unlimited source for differentiated cells through their unlimited self-renewal ability. However, directed differentiation protocols are needed to allow the enrichment of the cell type of particular interest, and to render its production economical, enabling the use of hPSC-derivatives in large-scale applications such as drug screening or therapeutic approaches.

DOI:10.14753/SE.2015.1764

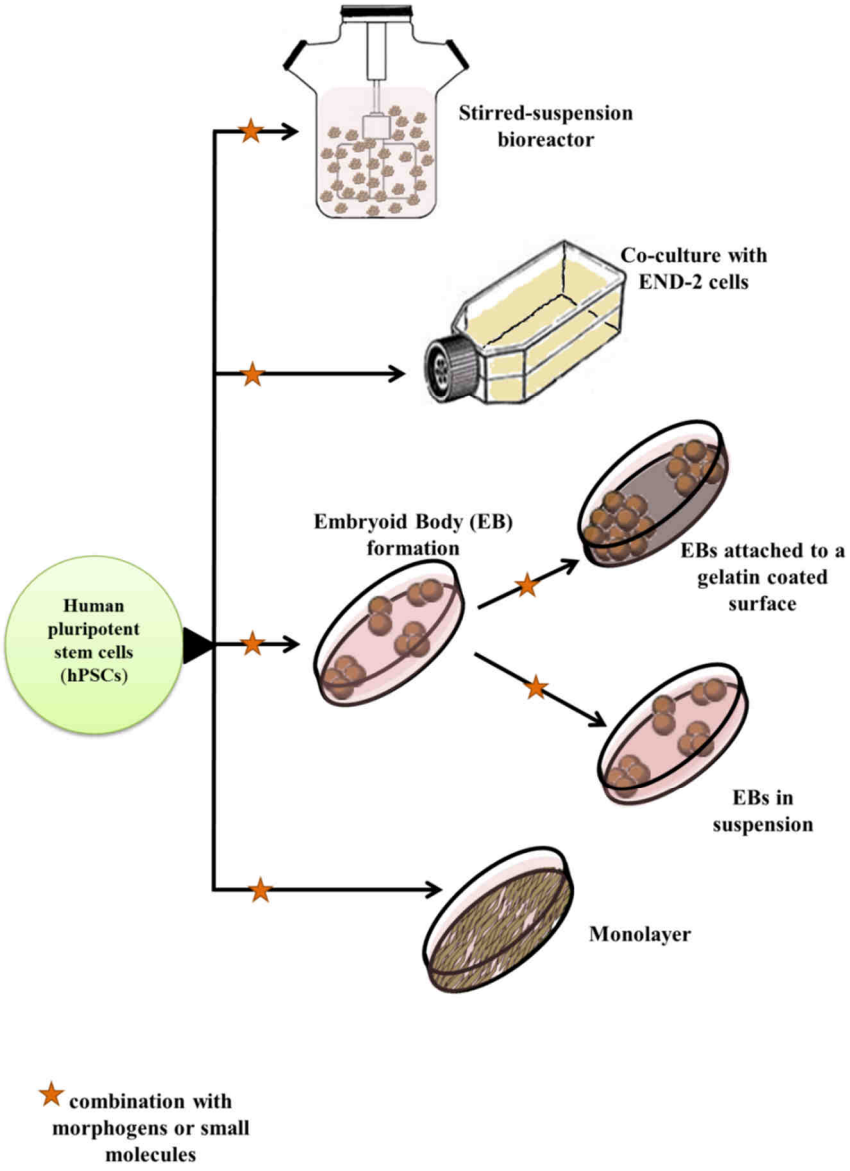

Figure 2. Differentiation methods to generate cardiomyocytes from human pluripotent stem cells.

Figure 2 shows various methods applied for cardiac differentiation of hPSCs. The most commonly used method to induce cardiomyocyte differentiation *in vitro* is the formation of three-dimensional aggregates, termed as embryoid bodies (EBs), consisting of cells representing the three germ layers[59] EBs are usually formed in suspension cultures in the presence of bovine or human serum, followed by either plating on a gelatine-coated surface or further differentiated in suspension culture. Serum is used to provide the necessary differentiation signals, however its lot-to-lot

variations result in stochastic output of the differentiation, usually with a low yield of cardiomyocytes. Therefore growth factors and morphogenes are often used to direct the differentiation of hPSCs[31, 60, 61], in the attempt to mimic the steps of *in vivo* cardiogenesis, namely mesoderm induction through Wnts, BMPs, or Nodal[62-64], patterning of the mesoderm towards cardiogenic mesoderm, formation of cardiogenic mesoderm presumably through Wnt inhibition[61] and Notch activity[65], and finally maturation to early cardiomyocytes. In addition, small molecules such as 5-azacytidine[60, 66-68], cyclosporin-A[69], or ascorbic acid[67] are also often used to enhance cardiomyocyte differentiation from hPSC.

In another widely used approach, undifferentiated hPSCs are co-cultured with mouse visceral endoderm-like (END-2) cells[70, 71]. While direct contact was reported to be important between END-2 cells and mouse ESCs or iPSCs for inducing cardiomyogenesis[72], cardiac differentiation of enzymatically passaged hESC lines could be enhanced in END-2 conditioned medium (END2-CM) as well[73], presumably due to factors secreted by END-2 cells. Biochemical analysis revealed elevated levels of prostaglandin I2 in END2-CM and its cardio-inductive effect was confirmed when a fully synthetic medium supplemented with prostaglandin I2 resulted in a cardiogenic activity equivalent to END2-CM[74].

An alternative protocol applied for cardiac differentiation is the monolayer culture of hPSCs on Matrigel-coated tissue culture plates in a feeder-free system[31]. To induce cardiac differentiation, MEF-conditioned medium used to maintain the pluripotent state is replaced with serum free RPMI-B27 medium supplemented with growth factors, such as BMP4 and activin A (as a mimic of Nodal).

Recently several scalable systems have been developed to adequately supply the large numbers of cardiac cells required for drug screening or therapeutic applications. These systems are usually based on the use of a stirred-suspension bioreactor, providing a stable physicochemical environment, well-controlled aggregate sizes and yielding an order of magnitude more CMs than conventional differentiation methods[75, 76].

Besides directed differentiation cultures, other methods also exist to guide the differentiation of hPSCs towards the cardiac lineage, e.g. transgenic modification

through the delivery of cardiac specific transcription factors[77] or recombinant proteins[78]. Since these methods are not closely related to the topic of the dissertation, further details are not provided here. However, a detailed review can be found in the attached book chapter Szebényi *et al.*, "Human Stem-Cell-Derived Cardiomyocytes in Drug Discovery and Toxicity Testing".

Another strategy to achieve an increased yield of CMs is to induce proliferation of mature hPSC-CMs that undergo progressive cell-cycle withdrawal during maturation[79]. Different cardiomyocyte cell-cycle reentry inducing extracellular factors have been reported, e.g. the fibroblast growth factor-1 (FGF-1) together with p38 MAP kinase inhibition[80], periostin[81] and Neuregulin-1β (NRG-1β)[82], a cardioactive growth factor released from endothelial cells of the ventricular endocardium[83]. After it was shown that Neuregulin-1, induces proliferation of mononucleated, but not binucleated CMs *in vivo*[82] another study demonstrated that inhibition of the signalling pathway involving NRG-1β and its tyrosine kinase receptor, ErbB4 enhances the proportion of cells showing nodal phenotype among hESC-derived CMs (60% nodal versus 40% ventricular subtype), while addition of exogenous NRG-1β resulted in the enhanced generation of CMs with ventricular phenotype (10% nodal versus 90% ventricular subtype)[84]. Direct differentiation of atrial and ventricular myocytes from hESCs has also been achieved by regulating Noggin and retinoid signals[85].

2.3. Systems allowing the isolation of human pluripotent stem cell-derived cardiac cells

Applicability of hPSC-derived cardiomyocytes depends not only on the large number of cells needed to be produced, but also on the purity of the cell population obtained at the end of differentiation. Therefore, the development of methods, allowing distinction between cardiac and other cell types is at least as relevant as the directed differentiation protocols. Isolation of living cells needed for drug screening, transplantation studies or basic research can be based on the use of genetically engineered reporter systems or cell surface markers. Genetically modified features are specially required when markers of the cell type of interest are not located on the cell surface (e.g. transcription factors or sarcomeric proteins) and therefore selection would not be possible without disruption of the cell membrane. This was the case for

cardiomyocytes for a long time, previously to the identification of several surface markers co-expressing with cardiac-specific transcription factors and sarcomeric proteins[72, 86, 87]. Moreover, a cardiac-specific reporter hESC line could be successfully used for identification of surface markers of the cardiac lineage[86, 88].

Increased yield of CMs as well as purification could also be achieved by isolation of progenitors (e.g. mesodermal, cardiac mesodermal, cardiovascular or cardiac progenitors, see **Figure 3**). Progenitors possess high proliferation capacity and restricted differentiation potential, allowing first the expansion of these cells by providing stage-specific renewal signals and then CM differentiation by cardio-inductive signals. A culture condition supporting continuous self-renewal and proliferation of cardiovascular progenitors by inhibition of BMP, Activin/Nodal and glycogen synthase kinase 3 (GSK3) pathways have already been described[89].

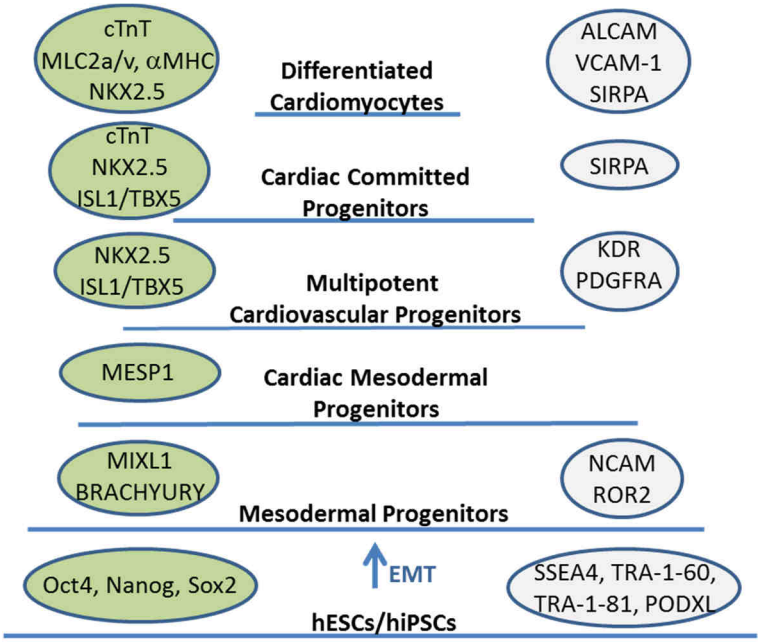

Figure 3. Proposed progenitor stages of the differentiation of human pluripotent stem cells into cardiomyocytes. The progenitor stages are identified by transcription factors and structural proteins (shown in green bubbles) and cell surface markers (shown in grey bubbles). The image is taken from Szebényi *et al.* [148], with some modifications.

1.3.1 Genetic methods for isolation of hPSC-derived cardiac cells

Genetic modification of stem cells is less efficient than that of tumour-derived or immortalized cell lines, therefore generation of reporter-expressing cardiomyocytes raises some technical challenges (for further review see the attached book chapter Szebényi *et al.*, "Human Stem-Cell-Derived Cardiomyocytes in Drug Discovery and Toxicity Testing"). However, by now several techniques have been documented to allow the generation of transgenic hPSC lines, without impairing self-renewal capacity and differentiation potential[6, 90-92]. Moreover, in most cases the studies demonstrated that the obtained cardiomyocytes were physiologically normal, regardless of the integration of the transgenes or the selection procedures applied for CM enrichment.

Constitutive promoters, such as ACTB, UbC, EF1α, PGK, CMV or the original variant of the CAG provide nearly uniform transgene expression in all tissues; therefore, theoretically, these types of promoters cannot be used for isolation of CMs. However, it was demonstrated in differentiated hESCs that the activity of several commonly used constitutive promoters can be restricted to specific cell lineages, since ACTB was only active in undifferentiated and neuronal cells, while UbC and PGK were inactive in endothelial cells [93]. Moreover, the CMV promoter became active only after mESCs differentiated into neuronal precursor cells [94], while the CAG promoter showed long-term activity during mESC differentiation towards mesoderm [95]. Still, reporter systems driven by various constitutive promoters (ACTB or CAG) could be reliable used for identification of transplanted transgenic hESC-derived CMs in infarcted mouse[96] and rat[97, 98] or healthy guinea pig heart[99] to provide evidence for successful and functional engraftment.

Cardiac tissue specific promoters allow the isolation of cardiomyocytes, while progenitors able to give rise to cardiac cells can be obtained when the promoter of an early mesoderm or cardiac lineage-specific gene is used. The first well-defined cells able to give rise to the cardiac (besides of hematopoietic, vascular, and skeletal muscle) lineage are mesodermal progenitors, expressing the T-box factor BRACHYURY and the homeodomain protein MIXL1 (see **Figure 3** for markers characteristic for specific stages of the cardiac differentiation). To allow selective isolation of mesodermal progenitors *GFP* expression cassette under the control of the *BRACHYURY* promoter

was randomly inserted into the genome[100] or were targeted into the *MIXL1* locus by homologous recombination[101]. More recently, a dual reporter system has been established where mesoderm posterior 1 (*MESP1),* a transcription factor characteristic for the pre-cardiac mesoderm is labelled with mCherry, while *NKX2.5* (expressed later than *MESP1*) is labelled with EGFP, allowing isolation of progenitors at different stages of cardiac commitment[102]. For this dual reporter system a previously established hESC reporter line provided the basis, in which the *GFP* cDNA was introduced into the *NKX2.5* locus by homologous recombination (*NKX2.5*$^{eGFP/w}$)[88]. This *NKX2.5*$^{eGFP/w}$ reporter cell line allows the selection of multipotent cardiovascular progenitors, displaying cardiac, endothelial and vascular smooth muscle potential, similarly to the *Cre/loxP* system-based labelling of *ISL1* expressing cells with the DsRed fluorescent reporter protein[103]. This system allows not only the selection of ISL^+ cells, but also the lineage tracing of these cells, since the labelling is irreversible and DsRed expression does not attenuate with the downregulation of ISL1 expression.

An alpha myosin heavy chain (*αMHC*) promoter-based system was used to follow maturation of hESC-derived cardiomyocytes over a year long[36], and also to identify hESC-derived early myocardial precursors (αMHC-GFP^{pos}) able to give rise to atrial ventricular and specialized conduction CM subtypes, but not to non-muscle cardiac cells[104]. Besides fluorescent proteins, drug resistance genes can also be used for enrichment of targeted cell populations. For example, hESC derived cardiomyocytes could be enriched to high purity (80-90%) when the puromycin resistance gene was driven by the αMHC promoter[105, 106].

Myosin light chain-2v (*MLC-2V*) is expressed later in CM differentiation than αMHC, therefore it does not allow the same insight into early CM differentiation, however, when the enhanced GFP was expressed under the control of the *MLC-2V* promoter, GFP expression-based identification and isolation of electrically active hESC-derived CMs was possible, according to Huber *et al.*[107]. It was also suggested that a short fragment of the cardiac troponin I (*TNNI3*) promoter in combination with the human cardiac alpha-actin enhancer is sufficient to identify hESC-derived CMs[108].

The disadvantage of these systems is that the activity of the transgene can only be detected at a certain stage of differentiation. To overcome this issue, Fu *et al.* applied

the combination of a constitutive and a tissue-specific promoter[109]. In this system GFP expression was driven by the constitutive *EF1α* promoter to allow selection of successfully transduced undifferentiated hESCs, while *MLC2V* promoter-driven dsRed expression was applied to enrich for CMs with ventricular phenotype[109109109109109106105].

Stage-specific reporter systems offer several advantages, for example these systems can be used as readouts of culture optimization in a stage-specific manner or can be utilized in the search for new cell-surface markers of the different stages of the cardiac lineage.

1.3.2 Non-genetic methods for isolation of cardiac cells

Mesodermal progenitors derived from hPSCs via epithelial-to-mesenchymal transition (EMT) can be selected not only by genetic methods, but also based on a cell surface marker combination, in which the neuronal cell adhesion molecule (NCAM or CD56) is used as positive, while the epithelial cell adhesion molecule (EpCAM or CD326) is used as negative marker[110]. However, the $CD56^{pos}CD326^{neg}$ marker combination was also documented to identify hESC-derived neuronal cells[111], suggesting that markers or marker combinations may identify a progenitor population only in a culture dependent manner and when the differentiation is directed into another lineage or not directed at all, than specificity of the markers may diminish. In addition, upregulation of the tyrosine kinase transmembrane receptor (ROR2) can also be used to identify and select mesodermal progenitors[112].

Similarly to the above mentioned marker combination, the stage-specific embryonic antigen-1 (SSEA-1) has also been proposed to be a suitable marker, in this case for isolation of multipotent cardiovascular progenitors[113], while others suggested SSEA-1 to be expressed on hESC-derived epithelial[1] or neuroectodermal committed cell types[114]. Thus SSEA-1 may only allow identification of multipotent cardiovascular progenitors when the differentiation has already been efficiently directed into the cardiac lineage.

It was shown that low level expression of the vascular endothelial growth factor receptor 2 (VEGFR-2/KDR) together with the absence of the mast/stem cell

growth factor receptor, also known as proto-oncogene c-Kit or tyrosine kinase Kit (C-KIT or CD117) identifies a population of cardiovascular progenitor cells (KDR^{low}C-KIT^{neg}), expressing *ISL1* and low levels of *NKX2-5* and *TBX5*[61]. This finding was verified not only on hESCs, but also in the case of hiPSCs[115] and showed that mouse models are not always adequate for establishing human protein expression profiles, since in mice cardiac progenitors are c-$Kit^{pos}$$Nkx2\text{-}5^{pos}$[116], while during human cardiac differentiation the emergence of a C-$KIT^{pos}$$NKX2\text{-}5^{pos}$ population could not be observed at all[117].

In addition, it was also suggested that cardiovascular progenitors can be identified based on the co-expression of KDR and PDGFRA[64]. However, the same research group demonstrated later that not all of the $KDR^{pos}PDGFRA^{pos}$ cells give rise to cells of the cardiac lineage[86]. In addition, isolation based on KDR expression may result in an impure population of cardiovascular progenitors, since KDR is also expressed on hPSCs[61].

The *NKX2-5*$^{eGFP/w}$ reporter system was used to screen for new cell-surface markers of the cardiac lineage, resulting in the discovery of two early CM markers, namely vascular cell adhesion molecule 1 (VCAM1) and signal regulatory protein α (SIRPA)[88]. Further experiments showed that VCAM1 positivity appears slightly later than SIRPA, and $NKX2\text{-}5^{pos}SIRPA^{pos}VCAM1^{pos}$ cardiomyocytes arose from an $NKX2\text{-}5^{pos}SIRPA^{pos}$ intermediate[117].

Upregulation of SIRPA happened parallel to the emergence of the first NKX2-5–GFP^{pos} cells (around day 8 of the differentiation), a day before the spontaneous contractile activity started in the differentiation cultures of HES2 hESCs[86]. Thus $SIRPA^{pos}$ cells isolated at EB day 8 were considered as cardiac precursors and were shown to be able to give rise to troponin expressing $SIRPA^{pos}$ CMs. Therefore it was concluded that SIRPA is a cell surface marker able to identify cardiac precursors and cardiomyocytes.

VCAM1 was shown to allow isolation of CMs but not cardiac progenitors, since troponin expression preceded VCAM1 appearance during differentiation[118]. VCAM1 expression based selection on day 11 of the differentiation resulted in a population of highly purified (>95%) CMs in the case of all four hPSC lines examined,

although VCAM1^{pos} cells represented only a subset within troponin T-positive cells (33.4%-63.5%).

The activated leukocyte cell adhesion molecule (ALCAM or CD166) is another marker, that have been suggested to enable isolation of hESC-derived CMs[87], and later it was also shown that ALCAM allows the high-purity enrichment of hiPSC-derived CMs as well[115]. In this latter work first KDR^{low}C-KIT^{neg} multipotent cardiovascular progenitors were isolated on EB day 6 and recultured as monolayer, than on day 20 of the differentiation CD166 was used to select CD166^{pos} CMs and CD166^{neg} smooth muscle cells. However, it is important to mention that there is only a short, early developmental stage-specific time window when ALCAM expression is restricted to cardiomyocytes, and beyond this particular developmental stage ALCAM expression is widespread among different types of tissues[115, 119-121].

The first non-genetic method reported in the literature allowing the isolation of living cardiomyocytes was based on the high mitochondrial content of CMs, resulting in that tetramethylrhodamine methyl ester perchlorate (TMRM), a fluorescent dye specifically labelling mitochondria could be used for cardiomyocyte enrichment with a purity of 99%[122]. However, it was shown that this method allows only the selection of late-stage CMs, while early CMs could not be discriminated from undifferentiated hESCs[88].

DOI:10.14753/SE.2015.1764

3. Aims

The goal of the research presented in the dissertation was to establish a novel *in vitro* method for the purification of human embryonic stem cell-derived cardiomyocytes and cardiac progenitors. In order to achieve this objective, the aims of the present study were:

1. To demonstrate that the CAG promoter provides the opportunity to identify cardiomyocytes in spontaneous differentiation cultures of human embryonic stem cells.

2. To induce cardiac differentiation of human embryonic stem cells in order to enrich the differentiation cultures for cardiac progenitors.

3. To demonstrate that the CAG promoter provides the possibility to identify and isolate cardiac progenitors during directed differentiation of human embryonic stem cells.

4. To find optimal culture conditions for isolated cardiac progenitors to maintain cardiac commitment during further differentiation.

5. To demonstrate that the isolated human embryonic stem cell-derived cardiac progenitors can be differentiated into relatively pure population of cardiomyocytes.

6. To optimize reaggregation and survival properties of isolated human embryonic stem cell-derived cardiac progenitors to enhance cardiomyocyte yield.

DOI:10.14753/SE.2015.1764

4. Materials and Methods

4.1. hESC culture and differentiation

The original HUES9 human embryonic cell line was kindly provided by Dr. Douglas Melton from the Harvard University, while BG01V was purchased from ATCC. The *Sleeping Beauty* (SB) transposon based gene delivery method was applied to genetically modify HUES9 and BG01V hESCs with a plasmid containing the cDNA of the fluorescent protein EGFP, under the control of a specific variant of the CAG promoter (SB-CAG-EGFP construct) [90]. This specific variant contains a CMV enhancer region, two sequences from the chicken β-actin promoter and one short part of the rabbit β1-globin promoter [90].

HUES9-CAG-EGFP and BG01V-CAG-EGFP hESC colonies were cultured on mitomycin-C treated mouse embryonic fibroblast (MEF) feeder cells (MERCK Millipore), in a medium consisting of Knockout DMEM (Life Technologies), supplemented with 20% Knockout Serum Replacement (Life Technologies), 2 mM glutamine, 0.1 mM nonessential amino acids, 0.1 mM β-Mercaptoethanol and 15 ng/ml recombinant human basic fibroblast growth factor (bFGF).

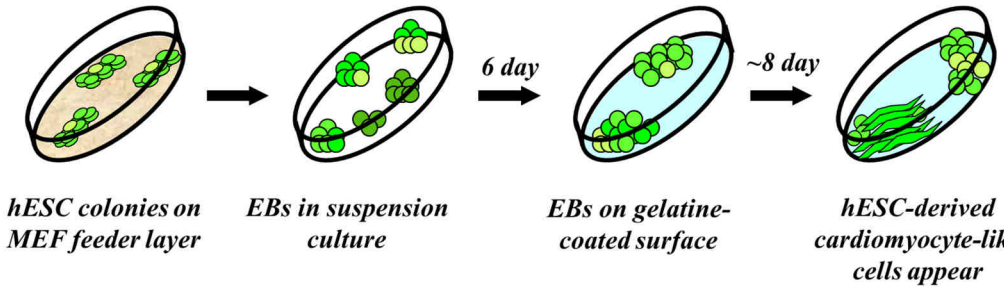

Figure 4. Schematic outline of spontaneous differentiation through the EB formation method.

Figure 4 shows the schematic outline of the spontaneous differentiation protocol, designated as the embryoid body (EB) formation method. Differentiation was initiated via EB formation under suspension culture conditions, ensured by an ultra-low

attachment surface of the culture plate and an EB medium containing Knockout DMEM, 20% ES-tested FBS (Life Technologies), 1% NEAA, 0,2% β-merkaptoethanol and 1% L-glutamin. On the 6th day of differentiation EBs were plated onto gelatine coated 24 well plates, in a density of 5-10 EBs/well. From this time point EBs were kept in differentiation medium (DM) containing DMEM (Life Technologies) and 10% EU-tested FBS (Life Technologies).

Directed differentiation of HUES9-CAG-EGFP and BG01V-CAG-EGFP cells was initiated via EB formation in suspension, as previously reported [61], with some modifications, as shown in the Results. Spontaneously contracting cardiomyocytes appeared at day 14-16 of the differentiation in both cases.

4.2. Flow cytometry

Undifferentiated HUES9-CAG-EGFP colonies were harvested from mouse feeder cells by enzymatic digestion with 0.05% trypsin-EDTA (Gibco), HUES9-CAG-EGFP EBs were dissociated with 0.25% trypsin-EDTA (Gibco). Single cell suspension was washed with PBS containing 0.5% bovine serum albumin and incubated for 30 min at 37 °C with the following directly labelled monoclonal antibodies: anti-human SSEA4-PE antibody (R&D System Inc., Minneapolis, MN) for specific labeling of pluripotent cells, anti-human CD166-A647 antibody (AbD Serotec) for specific labeling of activated cell adhesion molecule (ALCAM) expressing cells, CD106-PE for specific labeling of Vascular Cell Adhesion Molecule-1 (VCAM1) (BD Pharmingen) and anti-mouse Sca-1 (Ly-6A/E)-PECy5.5 (Beckton-Dickinson, San Jose, CA) antibody for specific labelling of mouse feeder cells in the case of undifferentiated cells (sample D0) and 6 day-old EBs (sample D6). The unconjugated monoclonal antibody SIRPA (BioLegend) was labelled with Alexa Fluor 647-conjugated goat anti-mouse IgG antibody (Invitrogen). For intracellular staining the cells were fixed and permeabilized with 4% paraformaldehyde (PFA) in PBS, subsequently the staining with anti-Troponin I (Monoclonal Anti-TNNI3, 1:500 dilution, Sigma) labelled with Alexa Fluor 647-conjugated goat anti-mouse IgG antibody (Invitrogen) was performed in PBS with 2% BSA and 0.75% Saponin (Sigma). Control staining with appropriate isotype-matched

control antibodies or background levels of fluorescence of the fluorochrome-conjugated secondary antibody was included. Dead cells were gated out based on 7AAD (Sigma) staining. HUES9 cells were measured to set the level for EGFP-positivity of undifferentiated HUES9-CAG-EGFP cells. Samples were analyzed by a FACSCalibur flow cytometer (Beckton-Dickinson, San Jose, CA) equipped with a 488 nm argon laser and a 635 nm red diode laser with BD CellQuest acquisition software (BDIS) or by FACSAria High Speed Cell Sorter (Beckton-Dickinson, San Jose, CA) with BD FACSDiva software.

4.3. Cell sorting

HUES9-CAG-EGFP EBs were dissected with 0.25% Trypsin-EDTA and single cell suspension was sorted into artificial fractions (low, mid and high) based on EGFP fluorescent signal intensity using the fluorescence based FACSAria High Speed Cell Sorter (Beckton-Dickinson, San Jose, CA). Minimum linear value within the CAG-EGFP^{low} fraction was 3000, maximum linear value was 15500; for the CAG-EGFP^{high} fraction minimum linear value was 29500, while maximum linear value was 262000.

Precision of the sorting procedure was monitored by EGFP expression profiling of the sorted fractions with flow cytometry, immediately after sorting (see Results). Cells obtained from the different fractions were washed with sterile PBS and either recultured or immediately resuspended in Trizol (Invitrogen, Carlsbad, CA, http://www.invitrogen.com) for further gene expression analysis. Isolated cells were placed into NUNC HydroCell Surface 96 well plates in a density of 30,000 cells/well, unless stated otherwise.

4.4. Fluorescence plate reader measurements

For fluorescence plate reader measurements a VICTOR X3 2030 Multilabel Reader (Perkin Elmer) was used. EBs reaggregated from the sorted cells (rEBs) were cultured in NUNC HydroCell Surface 96 well plates and fluorescence measured 3 and 20 days after sorting (see Results). Excitation wavelength was 490 nm, and a F535 emission

filter was used for detection of EGFP fluorescence. Fluorescence intensity levels were calculated as averages of 9 independent measurements.

Propidium iodide (PI) staining was carried out 3 and 20 days after sorting, in order to assess the growth of the rEBs and estimate changes in cell numbers. The rEBs were fixed with methanol on ice for 15 minutes and, after a washing step, were stained with PI. After incubation with PI for 15 minutes the rEBs were transferred into fresh PBS in a 96 well plate (Greiner). Excitation wavelength was 540 nm, and a F660 emission filter was used for detection of PI fluorescence. Fluorescence intensity levels were calculated as averages of 6 independent experiments.

4.5. Immuncytochemistry

For immunostaining, whole EBs were differentiated either on gelatin-coated 8 chamber dishes with glass bottom (Imaging chambers, PAA) or on 24 well culture plates, while EBs reaggregated from the sorted cells (rEBs), were plated onto gelatin-coated 8 chamber dishes with glass bottom, 6-7 days after the sorting procedure. To achieve adequate adherence of the rEBs, a 5 minute trypsinization procedure was performed with a 0.25% Trypsin-EDTA solution. EBs and rEBs were fixed with 4% paraformaldehyde in Dulbecco's modified Phosphate Buffered Saline (DPBS) for 15 min at room temperature. After three washing steps with DPBS, nonspecific antibody binding was blocked for 1 h at room temperature in DPBS containing 2 mg/ml bovine serum albumin, 1% fish gelatin, 5% goat serum and 0.1% Triton-X 100. The samples were then incubated for 1 h at room temperature with the primary antibodies. The primary antibodies used were: anti-Troponin I (Monoclonal Anti-TNNI3, 1:500 dilution, Sigma), Pecam (Anti-Human PECAM-1, 1:500 dilution, eBioscience), SMA (Monoclonal Anti-Actin, Alpha-Smooth Muscle, 1:100 dilution, Sigma), AFP (Monoclonal Anti-alpha-Fetoprotein, 1:500 dilution, Sigma), βIII-Tubulin (Monoclonal Anti-Neuron-specific beta-III Tubulin, 1:2000 dilution, R&D Systems). After washing with DPBS, the cells were incubated for 1 hour with the secondary antibodies at room temperature. Secondary antibodies were diluted in the blocking solution at 1:250 in each case. Alexa Fluor 568-conjugated goat anti-mouse IgG antibody (Invitrogen) was

applied to detect troponin I, AFP, βIII-Tubulin. DAPI (Invitrogen, Madison, WI) was used for nuclear staining (10 μM, 10 minute-long incubation in DPBS). Samples stained on 8 chamber dishes with glass bottom were examined by an Olympus FV500-IX confocal laser scanning microscope, while samples stained on 24 well plastic culture plates were examined by fluorescence microscopy. At least two independent samples were used in each measurement.

4.6. Real-time quantitative PCR analysis

Total RNA was isolated from cells using TRIzol™ Reagent (Invitrogen) following the manufacturer's instructions. cDNA samples were prepared from 0.2 μg total RNA using the Promega Reverse Transcription System Kit as specified by the manufacturer. For real-time quantitative PCR (QPCR) the following Pre-Developed TaqMan® assays were purchased from Applied Biosystems: *NANOG* as undifferentiated stem cell marker; *BRACHYURY* as early mesodermal marker; *ISL1*, *TBX5*, *NKX2.5* and *GATA4* as early markers of cardiac differentiation; *TNNT2, PLN* and *NPPA* as cardiac specific marker; *ALCAM* as stage specific cardiac marker; *MYL2* as ventricular-, *MYL7* as atrial-, *HCN4* as nodal subtype specific marker; *P0* ribosomal protein as endogenous control for quantification. QPCR analyses were carried out using the StepOne™ Real-Time PCR System (Applied Biosystems), according to the manufacturer's instructions. The fold-change of mRNA in experimental and control cells was determined using the $2^{-\Delta\Delta Ct}$ method. Relative mRNA levels were presented as mean values ± S.E.M. of 3 independent experiments. Levels of significance were calculated by the two-tailed Student t-test.

DOI:10.14753/SE.2015.1764

5. Results

5.1. The CAG promoter allows the identification of cardiomyocytes in spontaneous differentiation cultures of human embryonic stem cells

5.1.1. Characterization of the hESC lines HUES9-CAG-EGFP and BG01V-CAG-EGFP

EGFP expressing HUES9 and BG01V cells were generated by transfection with the SB-CAG-EGFP construct (see Materials and Methods). The genetic modification was carried out by the research group of Tamás Orbán. Transgenic hESC lines (HUES9-CAG-EGFP and BG01V-CAG-EGFP) were established through the enrichment of EGFP expressing hESCs by sorting or cloning. Several cell lines have been established with different EGFP expression intensities, either completely free of transgene-negative (CAG-EGFP^{neg}) cells or containing a small population of CAG-EGFP^{neg} cells.

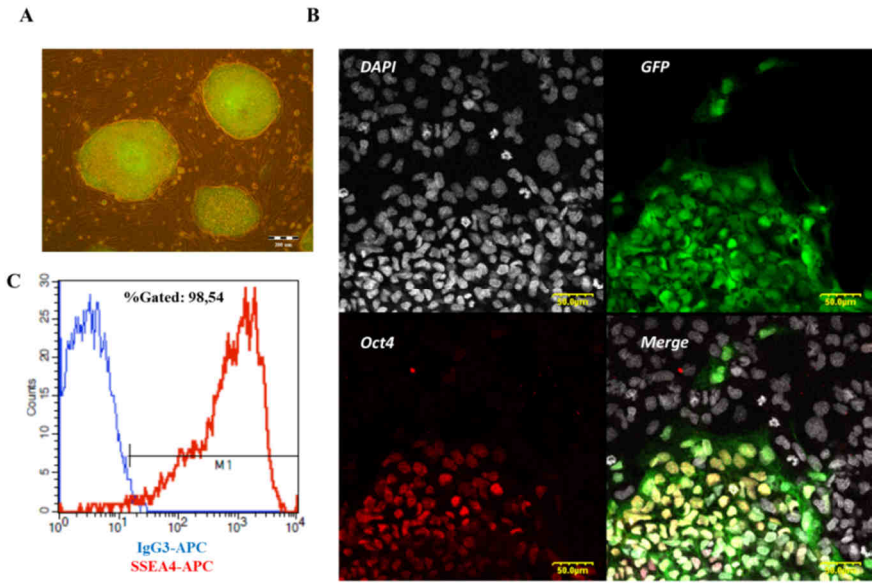

Figure 5. Characterization of HUES9-CAG-EGFP cells. (**A**) Fluorescence microscopy image of HUES9-CAG-EGFP colonies on MEF feeder layer, showing hESC-like morphology. (**B**) Confocal microscopy images of HUES9-CAG-EGFP colony on MEF feeder layer, showing expression of the pluripotency marker OCT4. (**C**) Flow cytometry measurement of SSEA4-APC and its isotype control IgG3-APC in HUES9-CAG-EGFP cells.

DOI:10.14753/SE.2015.1764

HUES9-CAG-EGFP cells were cultured on a mouse embryonic fibroblast (MEF) feeder layer and maintained pluripotency during long-term culture, as demonstrated by the colony (clump) morphology characteristic for pluripotent hESCs (**Figure 5A**), by immunostaining against the pluripotency marker OCT4 (**Figure 5B**) and by flow cytometry measurement detecting SSEA4 expression (**Figure 5C**).

Similarly to the HUES9-CAG-EGFP hESC line, BG01V-CAG-EGFP clumps were also cultured on MEF feeder layer (**Figure 6A**) and expressed OCT4 (**Figure 6B**) and SSEA4 (**Figure 6C**), respectively. Flow cytometry measurements detecting SSEA4 expression were routinely carried out to monitor the pluripotent state of hESCs during long term culture. Only hESCs with more than 95% SSEA4 positivity were used for experiments.

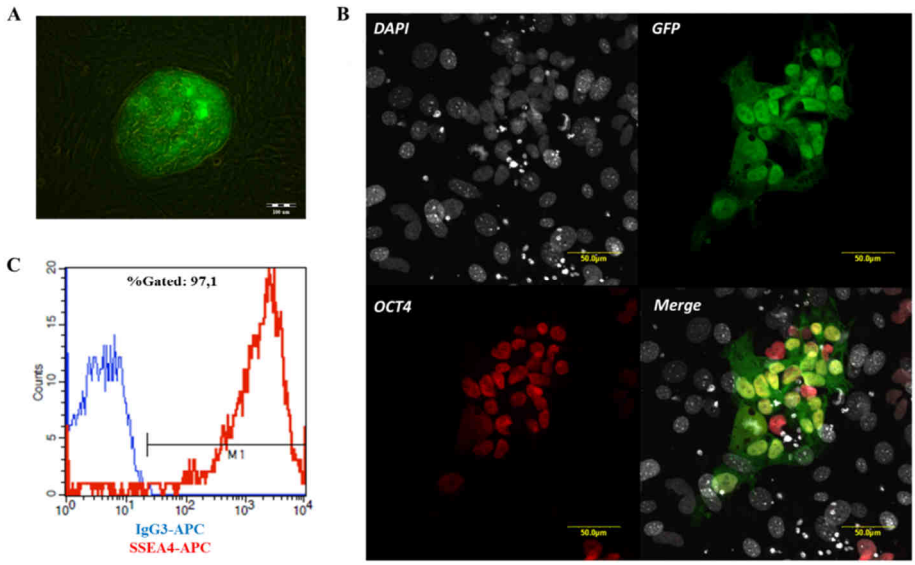

Figure 6. Characterization of BG01V-CAG-EGFP cells. (**A**) Fluorescence microscopy image of BG01V-CAG-EGFP colonies on MEF feeder layer, showing hESC-like morphology. (**B**) Confocal microscopy images of BG01V-CAG-EGFP colony on MEF feeder layer, showing expression of the pluripotency marker OCT4. (**C**) Flow cytometry measurement of SSEA4-APC and its isotype control IgG3-APC on BG01V-CAG-EGFP cells.

Pluripotency of hESC lines is also characterized by the ability of differentiating into the three germ layers, namely into the endoderm, ectoderm and mesoderm lineages.

DOI:10.14753/SE.2015.1764

HUES9-CAG-EGFP cells were differentiated through the EB method, which is often used for initiating spontaneous differentiation. Loss of pluripotency and mesodermal commitment was investigated by QPCR, detecting the downregulation of the pluripotency marker *NANOG* and the upregulation of the early mesodermal marker gene *BRACHYURY* during the first 12 days of differentiation (**Figure 7A**). Downregulation of *BRACHYURY* was followed by the upregulation of the early cardiac marker genes *GATA4*, *NKX2.5* and *ALCAM*, indicating the emergence of cardiac-committed cells in the differentiation culture around the10th day of the differentiation (**Figure 7B**).

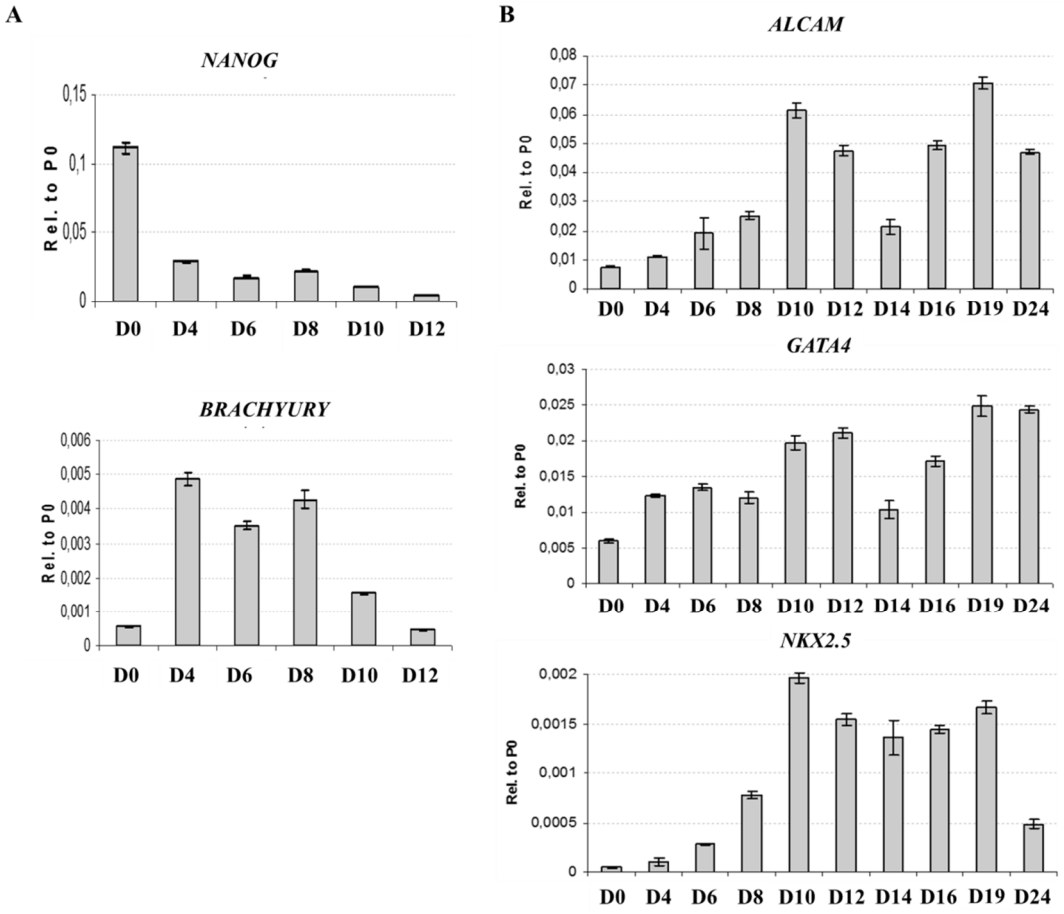

Figure 7. Transcriptional profile of spontaneous differentiation of HUES9-CAG-EGFP cells. (**A**) QPCR analysis of the mRNA expression of *NANOG* and *BRACHYURY* in whole EBs at early stages of differentiation. (**B**) QPCR analysis of the mRNA expression of *ALCAM*, *GATA4* and *NKX2.5* in whole EBs at different stages of spontaneous differentiation.

DOI:10.14753/SE.2015.1764

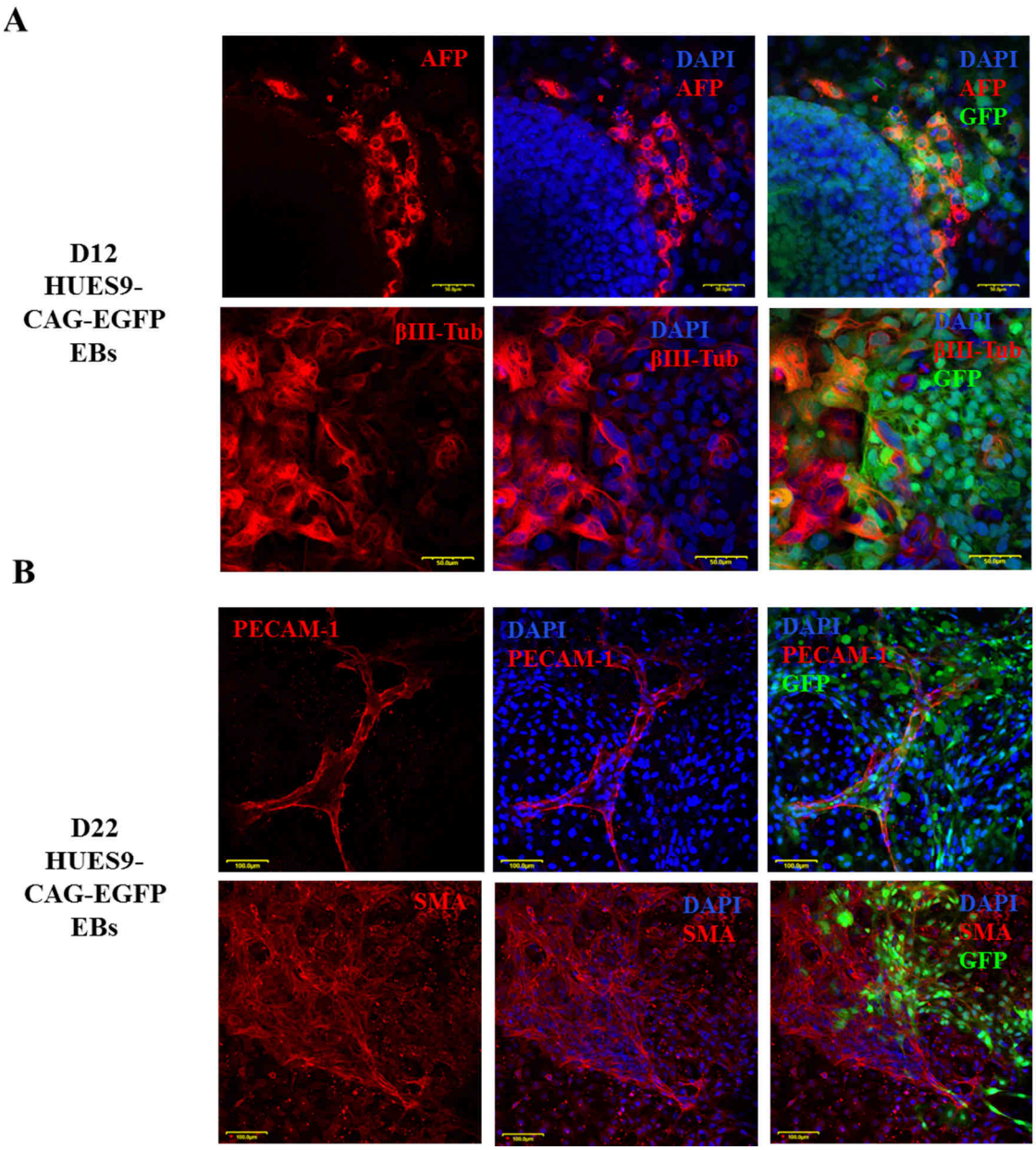

Figure 8. Immunocytochemistry analysis of spontaneously diffferentiating HUES-CAG-EGFP cells. Green: CAG-EGFP. Blue: DAPI. (**A**) Anti-alpha-fetoprotein (AFP) and anti-neuron-specific beta-III-tubulin (βIII-Tub) staining of HUES9-CAG-EGFP EBs on day 12 of the differentiation. (**B**) Anti-platelet endothelial cell adhesion molecule (PECAM-1) and anti-alpha-smooth muscle actin (SMA) staining of HUES9-CAG-EGFP EBs on day 22 of the differentiation. The image is taken from Szebényi *et al.*[123], with some modifications.

The emergence of cells of the other two germ layers was demonstrated by immunocytochemistry studies (**Figure 8A**). On day 12 of the differentiation (D12) EBs

were stained against the early endoderm marker alpha-fetoprotein (AFP) and the ectoderm marker beta-III-tubulin (βIII-Tub), and both endodermal and ectodermal cells were found to be present in the differentiation culture. Cells of the mesodermal lineages were identified based on the expression of alpha-smooth muscle actin (SMA), characteristic for smooth muscle cells and based on platelet endothelial cell adhesion molecule (PECAM-1) expression, characteristic for endothelial cells, respectively (**Figure 8B**). The expression of SMA and PECAM was investigated on day 22 (D22) of the differentiation, since cells positive for these markers emerge only at later stage of the differentiation. Besides smooth muscle and endothelial cells, cardiomyocytes are also of mesodermal origin. Cardiac differentiation was demonstrated by the emergence of numerous spontaneously contracting areas during later stage of differentiation (after 14 days).

5.1.2. In differentiation cultures of HUES9-CAG-EGFP and BG01V-CAG-EGFP cardiomyocytes show exceptionally high EGFP expression

Spontaneous differentiation of HUES9-CAG-EGFP hESCs usually resulted in numerous spontaneously contracting areas with extremely high EGFP fluorescence signal intensity, masking dimmer fluorescence of the surrounding tissues (**Figure 9**, white arrows pointing on the contracting areas with high EGFP signal). Extremely high EGFP expression intensities were predominantly observed onsite of the contracting areas (**Supplementary video 1**) and allowed the identification of cardiomyocytes in the differentiation culture based alone on their extremely high EGFP expression intensities. Two different hESC lines (HUES9-CAG-EGFP and BG01V-CAG-EGFP) and a mouse ESC line (R1-CAG-EGFP, kindly provided and differentiated by Elen Gócza) were used to demonstrate that this effect is cell line and species-independent (**Figure 9**). Moreover, it was shown by Tamás Orbán and co-workers that this phenomenon is exclusively dependent on the CAG promoter and independent of the transgene integration site and copy number, the transgene sequence, as well as the method of gene delivery. A detailed description of the experiments resulting in this conclusion can be found in the attached paper, Orbán *et al*.[90].

DOI:10.14753/SE.2015.1764

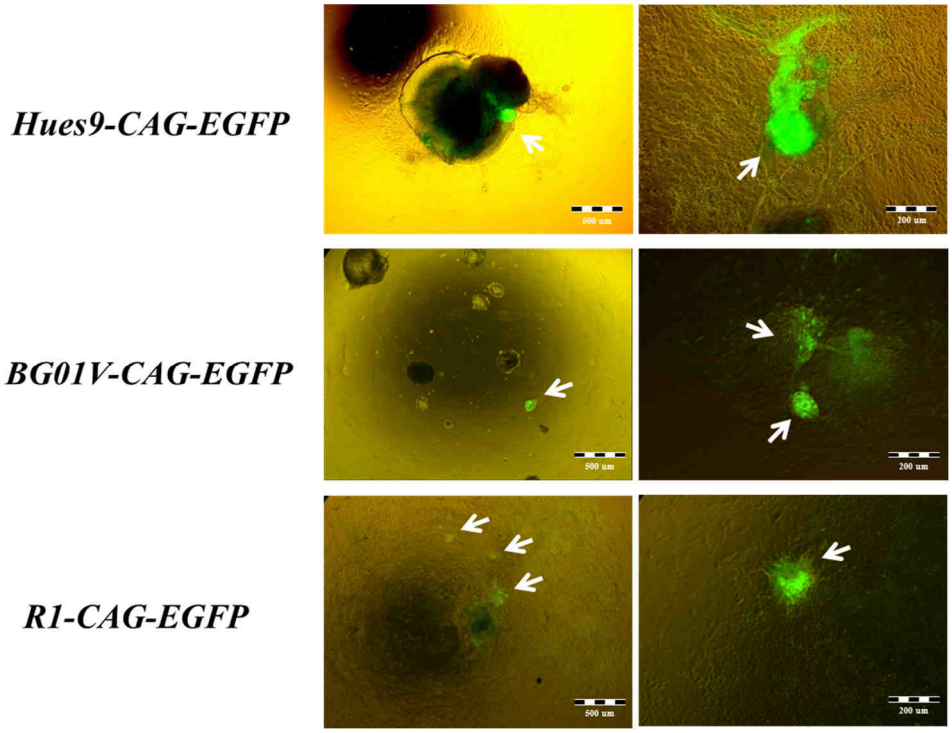

Figure 9. Fluorescence microscopy images of spontaneously contracting areas. The images show spontaneously contracting areas differentiated from two different human embryonic stem cell lines (HUES9-CAG-EGFP and BG01V-CAG-EGFP) and from a mouse embryonic stem cell line (R1-CAG-EGFP) at two different magnifications.

To elicit whether the extremely high EGFP expression intensities of cardiomyocytes are the result of higher transcription or translation rate, or certain posttranslational modifications, HUES9-CAG-EGFP differentiation cultures were separated into three fractions based on EGFP fluorescence by a FACSAria High Speed Cell Sorter at the 30th day of differentiation (**Figure 10A**). The data presented in **Figure 10** are the result of a differentiation, repeated independently from the experiments published by Orbán *et al.* In this particular experiment the applied HUES9-CAG-EGFP hESC line contained a subpopulation of EGFP negative cells (**Figure 10A**, yellow population), superseding the use of the HUES9 cell line as negative control for setting up the detection of the EGFP signal. EGFP negative cells were not included in further analysis since this population contained a mixture of all types of cells emerging during differentiation. The fraction containing cells with exceptionally high EGFP fluorescent signal intensity was designated as the CAG-EGFP^{high} subpopulation (**Figure**

10A, green), while cells with low EGFP intensity as the CAG-EGFP^{low} subpopulation (**Figure 10A**, blue). Cells between these two fractions were designated as CAG-EGFP^{mid} (**Figure 10A**, purple).

Sorted cells were resuspended in TRIzol Reagent to isolate total cellular RNA from each of the separated fractions. Real-time quantitative PCR analysis revealed that EGFP transcription levels closely correlated with the fluorescent signal intensities of the fractions, thereby providing evidence for increased transcription through increased promoter activity as the cause of enhanced EGFP fluorescent signal intensity (**Figure 10B**). Therefore higher nucleus-cytoplasm ratio in cardiomyocytes compared to other cell types could also be excluded as the cause of this phenomenon.

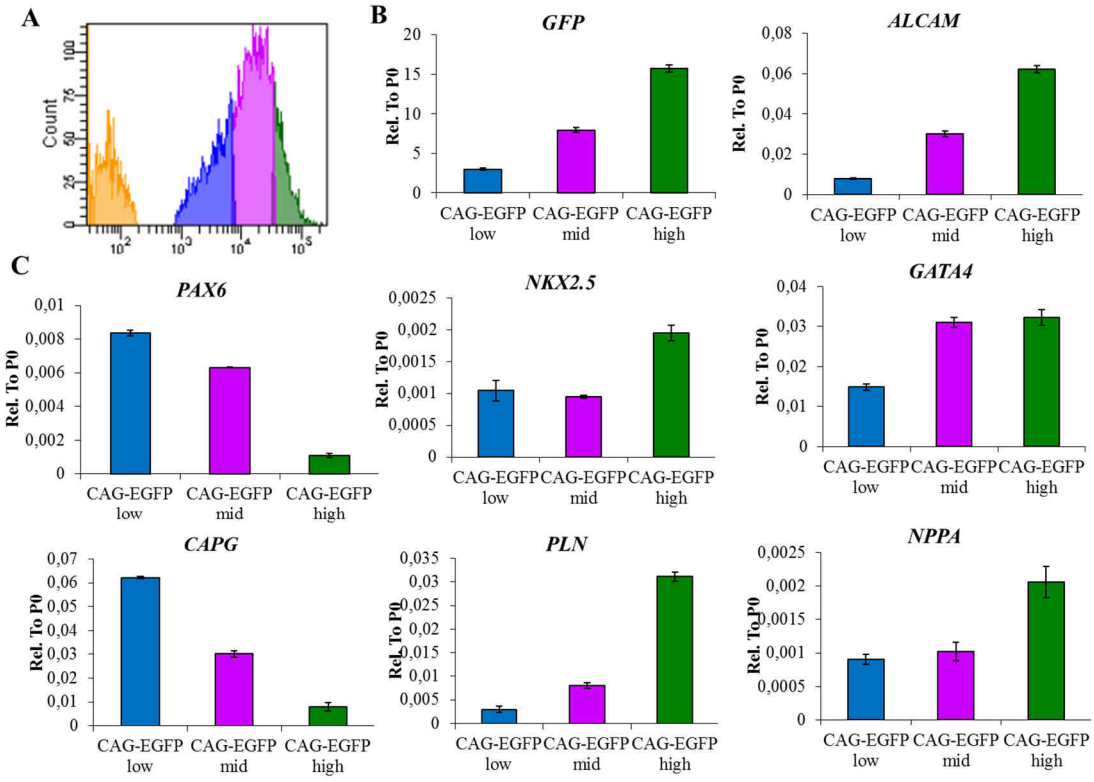

Figure 10. The CAG-EGFP^{high} subpopulation is enriched in cardiomyocytes. (A) Isolation of CAG-EGFP^{low} (blue), CAG-EGFP^{mid} (purple) and CAG-EGFP^{high} (green) fractions from HUES9-CAG-EGFP EBs based on the CAG-EGFP signal intensity on day 32 of the differentiation. (B) QPCR analysis of the mRNA expression of *GFP*, *ALCAM*, *NKX2.5*, *GATA4*, *PLN* and *NPPA* in EBs at day 32 of spontaneous differentiation. (C) QPCR analysis of the mRNA expression of *PAX6* and *CAPG* in EBs at day 32 of spontaneous differentiation.

DOI:10.14753/SE.2015.1764

Transcriptional profiles of cardiac-specific (*NKX2.5*, *GATA4*, *ALCAM*, *PLN* and *NPPA*), early neuron-specific (*PAX6*), and skin-specific (*CAPG*) marker genes measured by QPCR revealed that the CAG-EGFP^{high} fraction contained higher level of cardiac-specific mRNA than the other two fractions, while neuron and skin-specific mRNA was underrepresented in this sample compared to the other two fractions (**Figure 10B**). These findings proved that apart from being constitutively functional in all cell types (including undifferentiated hESCs, see **Figure 5 and 6**) this specific variant of the CAG promoter was transcriptional extremely active in cardiac tissues, providing the possibility for selection of transgene expressing hESCs and hESC-derived CMs, and therefore it was named as "double-feature" promoter[90].

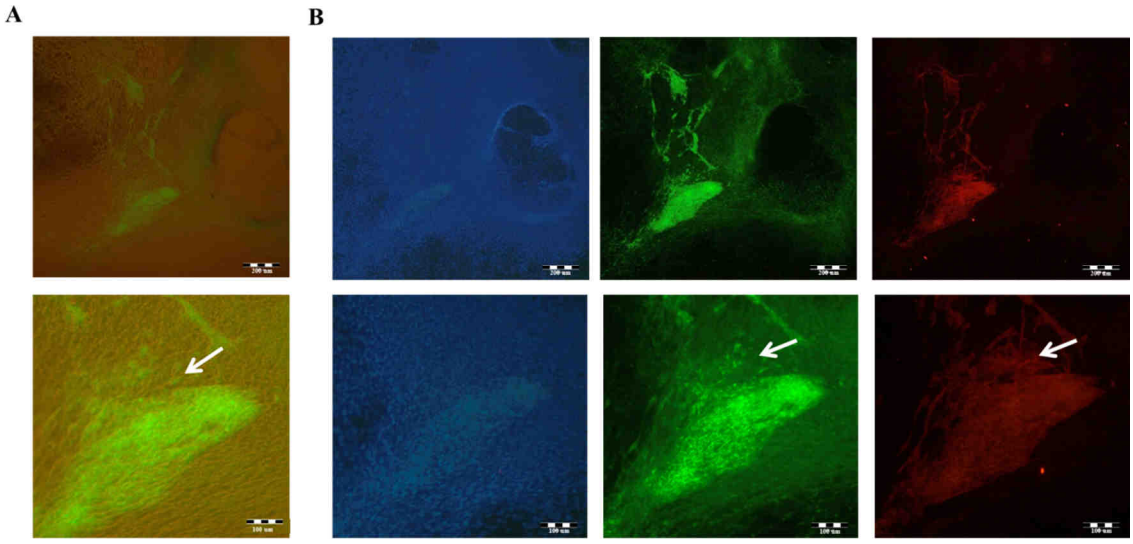

Figure 11. Non-contracting areas expressing CAG-EGFP at a very high intensity are cardiomyocytes, but not all of the cardiomyocytes express CAG-EGFP at an exceptionally high level. (**A**) Fluorescence microscopy images at two different magnifications of a non-contracting area expressing CAG-EGFP at an exceptionally high level. (**B**) Fluorescence microscopy images at two different magnifications of cardiac troponin I (cTnI) staining of the same area. Blue: DAPI. Green: CAG-EGFP. Red: cTnI. The white arrow indicates a cTnI positive area with lower EGFP signal intensity. The image is taken from Szebényi *et al.*[123], with some modifications.

Besides of numerous contracting areas several non-contracting areas with exceptionally high EGFP signal intensities were spotted by fluorescent microscopy during examination of the differentiation cultures, even at later stages of the differentiation (**Figure 11A**). To further support the previous finding, namely that the transcriptional activity of the CAG promoter is higher selectively in cardiomyocytes, wells of 24-well plates containing such non-contracting areas were stained against cardiac troponin I (cTnI). **Figure 11B** shows a representative cTnI staining, demonstrating good colocalization with the enhanced EGFP signal, as well as the existence of cardiomyocytes (cTnI positive cells) with lower EGFP signal intensity (**Figure 11B**, white arrow).

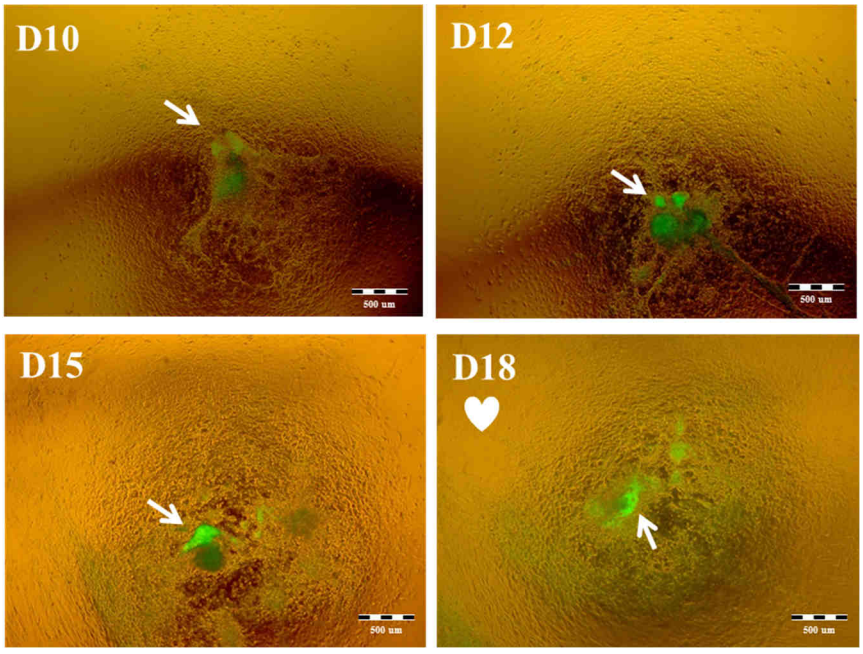

Figure 12. Fluorescence microscopy images of the same area showing exceptionally high EGFP expression during the course of spontaneous differentiation of HUES9-CAG-EGFP culture. Onset of the spontaneous contractile activity is denoted by a white heart symbol. White arrows indicate the areas with extremely high EGFP signal.

Next, the appearance of areas with exceptionally high EGFP signal was investigated by fluorescent microscopy at early stages of spontaneous differentiation and selected areas were followed during the course of differentiation to evaluate the

ability of the CAG promoter to identify progenitors of cardiomyocytes (**Figure 12**). This was important because the selection of mature cardiomyocytes is limited by their poor reaggregation and survival properties as single cells, while cardiac progenitors possess better reaggregation and survival properties. In addition, cardiomyocytes undergo progressive cell-cycle withdrawal during maturation[79], while progenitor cells are still able to divide, therefore cardiomyocyte yield of the differentiation can also be enhanced by selective propagation of cardiac progenitors.

Day 10 was found as the earliest time point when cells further differentiating to contracting cardiomyocytes could be identified based on their high EGFP expression (**Figure 12**). These findings suggested that the CAG promoter would allow not only the isolation of cardiomyocytes, but also that of cardiac progenitors, since the contractile activity, indicating the appearance of cardiomyocytes started only later, after day 14 in the differentiation cultures.

DOI:10.14753/SE.2015.1764

5.2. Directed cardiac mesoderm differentiation of CAG-EGFP expressing human embryonic stem cells

To facilitate the examination of the ability of the CAG promoter to identify cardiac progenitors, spontaneous differentiation was needed to be replaced by a differentiation protocol which is able to enrich the output of the differentiation for cells with mesoderm origin. The original protocol was obtained from the literature[61] and was optimized for CAG-EGFP expressing hESCs, however, some basic modifications were introduced to render it affordable for routine use in a small academic laboratory.

Figure 13 shows the outline of the protocol used to induce mesodermal differentiation. Bone morphogenetic factor-4 (BMP4), Activin A, ascorbic acid and monothioglycerol (MTG) was used to differentiate cells towards the mesoderm, while further commitment to the cardiac mesoderm was supported by the addition of ascorbic acid and MTG alone. Formation of cells of the cardiovascular lineages was achieved in differentiation medium (DM) supplemented with ascorbic acid and MTG, added until the 14th day of the differentiation.

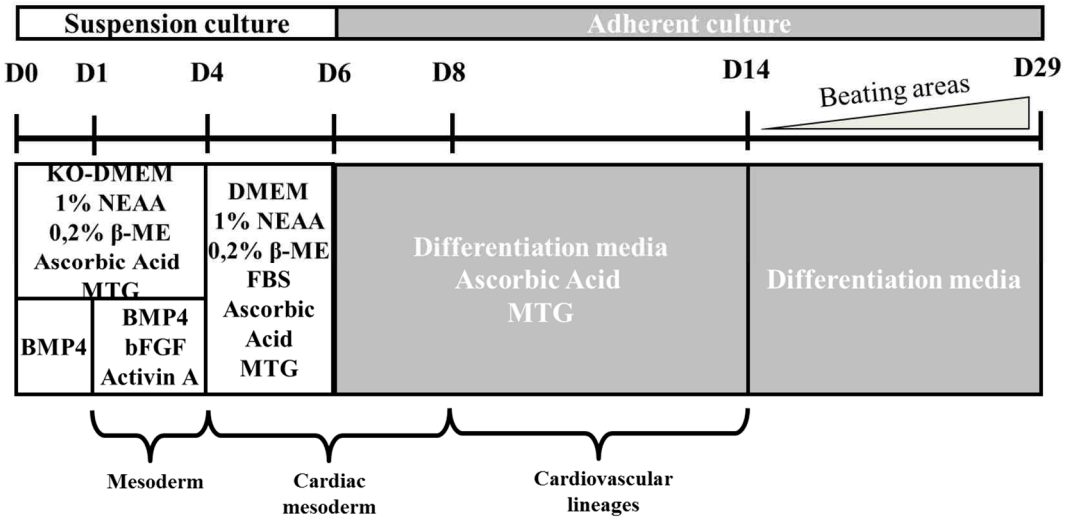

Figure 13. Schematic representation of the protocol for directed differentiation. The image is taken from Szebényi *et al.*[123], with some modifications.

Directed differentiation was monitored by fluorescence activated cell sorting (FACS) measurements and its kinetics was compared to that of spontaneous differentiation (**Figure 14**). The loss of pluripotency demonstrated by the decrease of SSEA4 expression could be detected earlier, already on day 6 in the directed differentiation culture, while during spontaneous differentiation SSEA4 expression started to decline only around D10 (**Figure 14A**).

ALCAM can be designated as a cardiomyocyte marker, but it is important to mention that ALCAM is expressed solely on cardiomyocytes at an early developmental stage-specific manner, while beyond this particular developmental stage ALCAM expression is widespread among different types of tissues[115, 119-121]. Therefore it was important to examine the kinetics of ALCAM expression during the course of differentiation of HUES9-CAG-EGFP cells. Directed differentiation resulted ALCAM positive cells around day 9, while during spontaneous differentiation ALCAM positive cells emerged later (around day 12).

To further examine mesoderm differentiation the cell surface expression of KDR (VEGF-R) and CD117 (C-KIT) was monitored during the first 12 days of the differentiation (**Figure 14B**), based on the paper of Yang *et al.*, showing that the $KDR^{low}/CD117^{neg}$ subpopulation indicate the presence of cardiovascular progenitors during directed differentiation of hESCs[61]. In the directed differentiation cultures increased presence of this population could be observed between day 6 and day 12, while in spontaneous differentiation cultures the $KDR^{low}/CD117^{neg}$ subpopulation evolved only later, around day 9 and composed a smaller fraction of the culture as shown in **Figure 14B**.

Counting of contracting areas served as a readout for cardiac differentiation efficiency. Directed differentiation resulted more contracting areas than spontaneous differentiation (**Figure 14C**). **Figure 14D** shows that this difference could be demonstrated by FACS measurement of undifferentiated (light grey) and differentiated HUES9-CAG-EGFP samples (dark grey for spontaneous or black for directed differentiation) stained against cTnI.

DOI:10.14753/SE.2015.1764

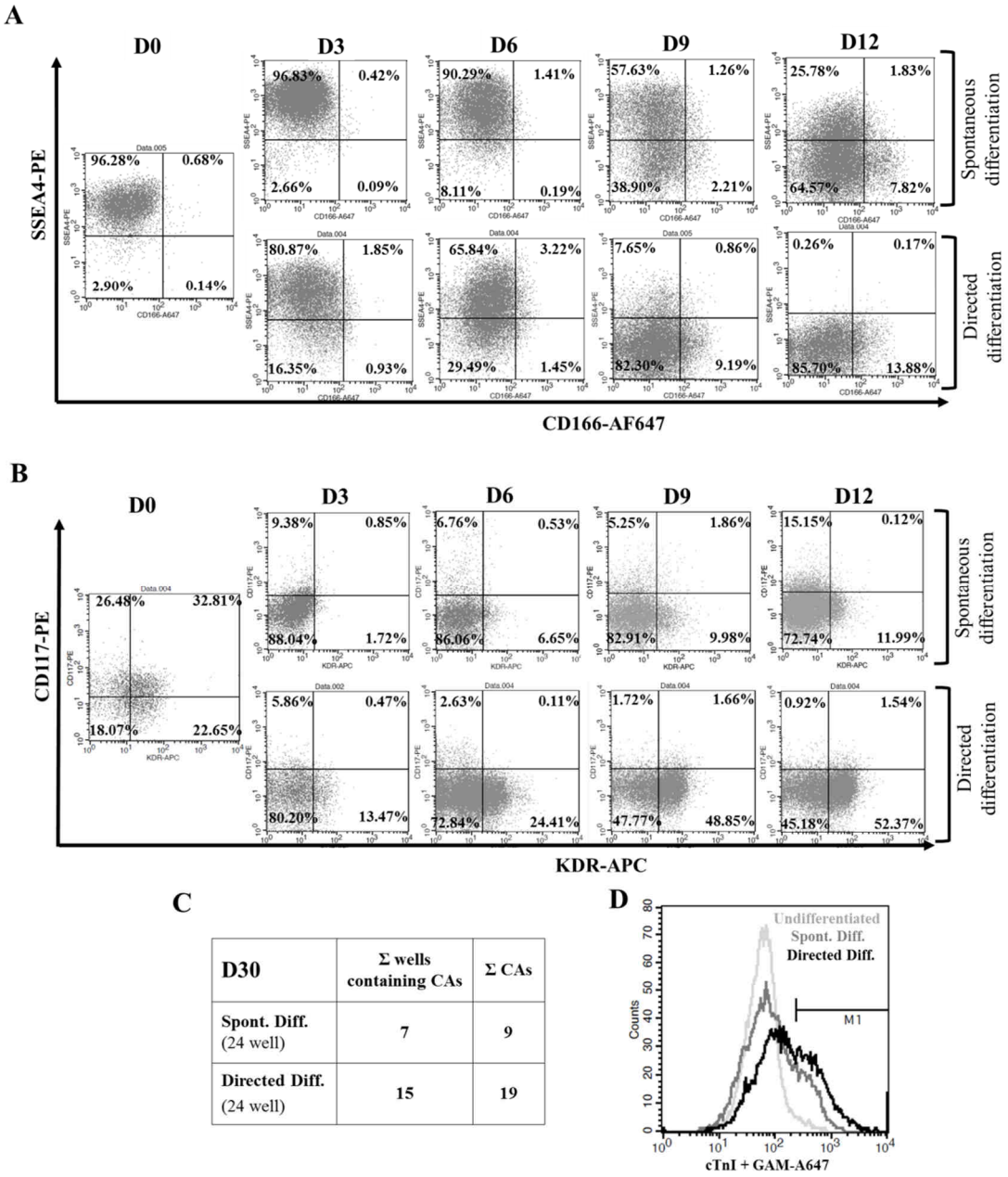

D30	Σ wells containing CAs	Σ CAs
Spont. Diff. (24 well)	7	9
Directed Diff. (24 well)	15	19

Figure 14. Comparison of spontaneous and directed differentiation. (A) Flow cytometry analysis of SSEA4 and ALCAM/CD166 on cells from whole HUES9-CAG-EGFP EBs at different stages of spontaneous (upper row) and directed differentiation (lower row). (B) Flow cytometry analysis of C-KIT/CD117 and KDR on cells from whole HUES9-CAG-EGFP EBs at different stages of spontaneous (upper row) and directed differentiation (lower row). (C) Table summarizing the outcome of a spontaneous and a directed differentiation in terms of contracting areas (CAs)-content on a 24 well plate at day 30 (D30). (D) Flow cytometry analysis of cardiac troponin I (cTnI) staining of undifferentiated and differentiated (spontaneous or directed) samples. For flow cytometry analysis the FACSCalibur flow cytometer was used; dot plot gates were set based on the isotype controls.

Figure 15 shows the transcriptional profile of directed differentiation measured by QPCR. By day 2 of the directed differentiation a rapid downregulation of the mRNA expression of the pluripotency gene *NANOG* was observed, followed by a transient upregulation of *BRACHYURY* mRNA level, implying the formation of the mesoderm (**Figure 15A**). *BRACHYURY* was already downregulated by day 8, while during spontaneous differentiation downregulation of the same gene happened only later, around day 12 (see **Figure 7**). Cardiac specific genes such as *ISL1*, *TBX5*, *NKX2.5*, *TNNT2* and *ALCAM* were used to confirm the emergence of cardiac mesoderm in the directed differentiation cultures (**Figure 15B**). *ISL1* expression was upregulated on day 6, preceding the upregulation of *TBX5* and *NKX2.5* expression on day 8. The expression of *TNNT2* mRNA become detectable at a low level on day 6, but a high level expression was associated with the emergence of spontaneous contractile activity and occurred around day 14. Upregulation of *ALCAM* mRNA levels overlapped with the upregulation of *ISL1*, and was maintained thereafter.

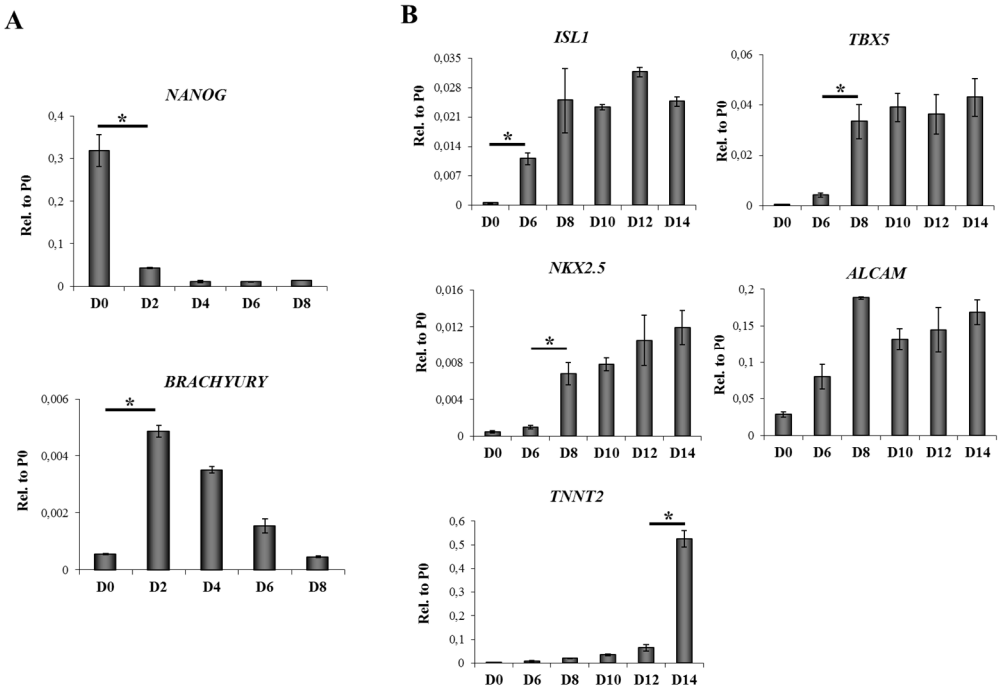

Figure 15. Transcriptional profile of directed differentiation of HUES9-CAG-EGFP cells. (A) QPCR analysis of the mRNA expression of *NANOG* and *BRACHYURY* in EBs at early stages of differentiation. (B) QPCR analysis of the mRNA expression of *ISL1*, *TBX5*, *NKX2.5*, *ALCAM* and *TNNT2* in EBs at different stages of directed differentiation. Levels of significance were calculated by the Student T-test; *: $p<0.05$, n=3. The image is taken from Szebényi *et al.*[123].

DOI:10.14753/SE.2015.1764

As shown in **Figure 16**, a well measurable EGFP expression could be detected by FACS in the pluripotent state (D0) of HUES9-CAG-EGFP cells, together with a high level of SSEA4 expression. Further analysis of HUES9-CAG-EGFP differentiation by FACS revealed a slight decrease in the EGFP signal during the suspension culture stage of the differentiation. However, on day 10 the formation of a subpopulation expressing EGFP at a very high level could be confirmed (**Figure 16**, black arrows). This CAG-EGFP^{high} subpopulation was negative for SSEA4 and its appearance on day 10 anticipated the onset of the spontaneous contractile activity (D14 and later) by four days at least. Therefore it was hypothesized that the ideal period for isolation of cardiac progenitors based on the CAG-EGFP signal is between day 10 and day 14 of the differentiation.

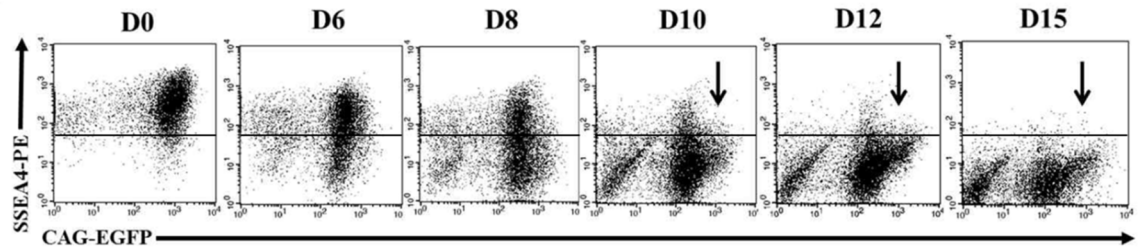

Figure 16. Flow cytometry analysis of the pluripotency marker SSEA4 and the CAG-EGFP on cells from whole HUES9-CAG-EGFP EBs at different stages of differentiation. Dot plot gate for SSEA4 expression was set based on the isotype control, IgG3-PE. Arrows indicate the evolving CAG-EGFP^{high}/SSEA4^{neg} subpopulation. The image is taken from Szebényi *et al.*[123], with some modifications.

DOI:10.14753/SE.2015.1764

5.3. The CAG promoter allows identification and isolation of human embryonic stem cell-derived cardiac progenitors

5.3.1. Isolation and mRNA expression profiling of the CAG-EGFP^{high} subpopulation

In order to assess whether the CAG-EGFP signal intensity allows the identification and isolation of cardiac progenitors, cell sorting was performed from the trypsinized cultures of differentiating HUES9-CAG-EGFP cells and transcriptional profile of the isolated samples were compared by QPCR.

As shown in **Figure 17** two separate cell populations, namely CAG-EGFP^{high} (indicated by blue colour) and CAG-EGFP^{low} (indicated by red colour) were isolated by a FACSAria High Speed Cell Sorter on day 10 (D10) and 12 (D12) of the differentiation. The sorted fractions were re-measured by FACS to establish sorting purity.

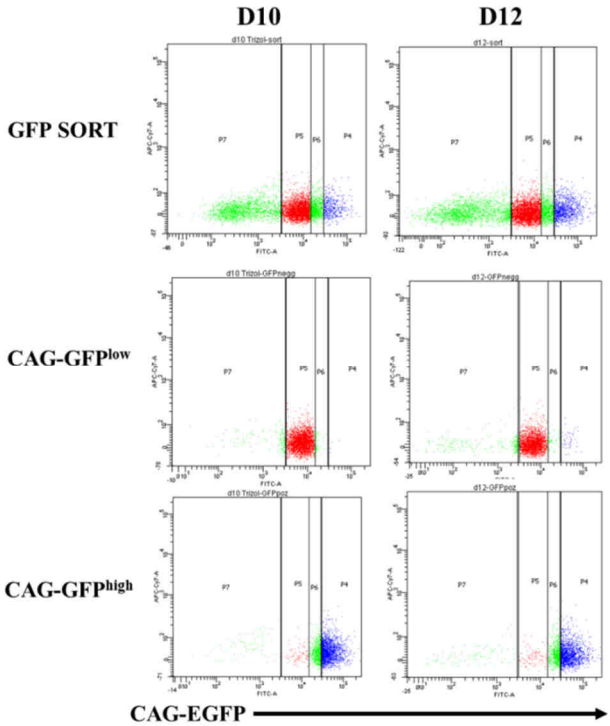

Figure 17. Isolation of CAG-EGFP^{low} (red) and CAG-EGFP^{high} (blue) fractions from HUES9-CAG-EGFP EBs based on the CAG-EGFP signal intensity on day 10 (D10) and day 12 (D12) of the differentiation. The sorted subpopulations were re-analyzed by FACS measurements to establish sorting purity of CAG-EGFP^{high} (lower row) and CAG-EGFP^{low} (middle row) cells. Green coloured cells were not analysed. The image is taken from Szebényi *et al.*[123].

QPCR analysis revealed that the CAG-EGFP^{high} samples expressed significantly higher levels of the cardiac specific genes *ISL1*, *TBX5* and *TNNT2* than the CAG-EGFP^{low} samples, while *NKX2.5* mRNA levels were higher in the CAG-EGFP^{low} fractions at both days of differentiation examined (D10 and D12) (**Figure 18A**). In CAG-EGFP^{high} samples expression levels of the *NKX2.5* transcripton slightly increased from day 10 to day 12, while in the case of CAG-EGFP^{low} cells a robust decrease was observed. **Figure 18A** also shows that expression levels of the *ALCAM* transcript were similar in the sorted fractions on day 10, but by day 12 the two fractions clearly separated from each other and CAG-EGFP^{high} cells expressed *ALCAM* at a significantly higher level than CAG-EGFP^{low} cells (**Figure 18A**).

Figure 18B shows that the early neuronal markers, SOX1 and PAX6, as well as the early endoderm marker AFP were expressed at higher levels in the CAG-EGFP^{low} samples. Expression of the pluripotency genes *OCT4* and *NANOG* was also investigated and two magnitude of order less transcript were found in isolated samples than in undifferentiated HUES9-CAG-EGFP cells, used as positive control (**Figure 18C**).

DOI:10.14753/SE.2015.1764

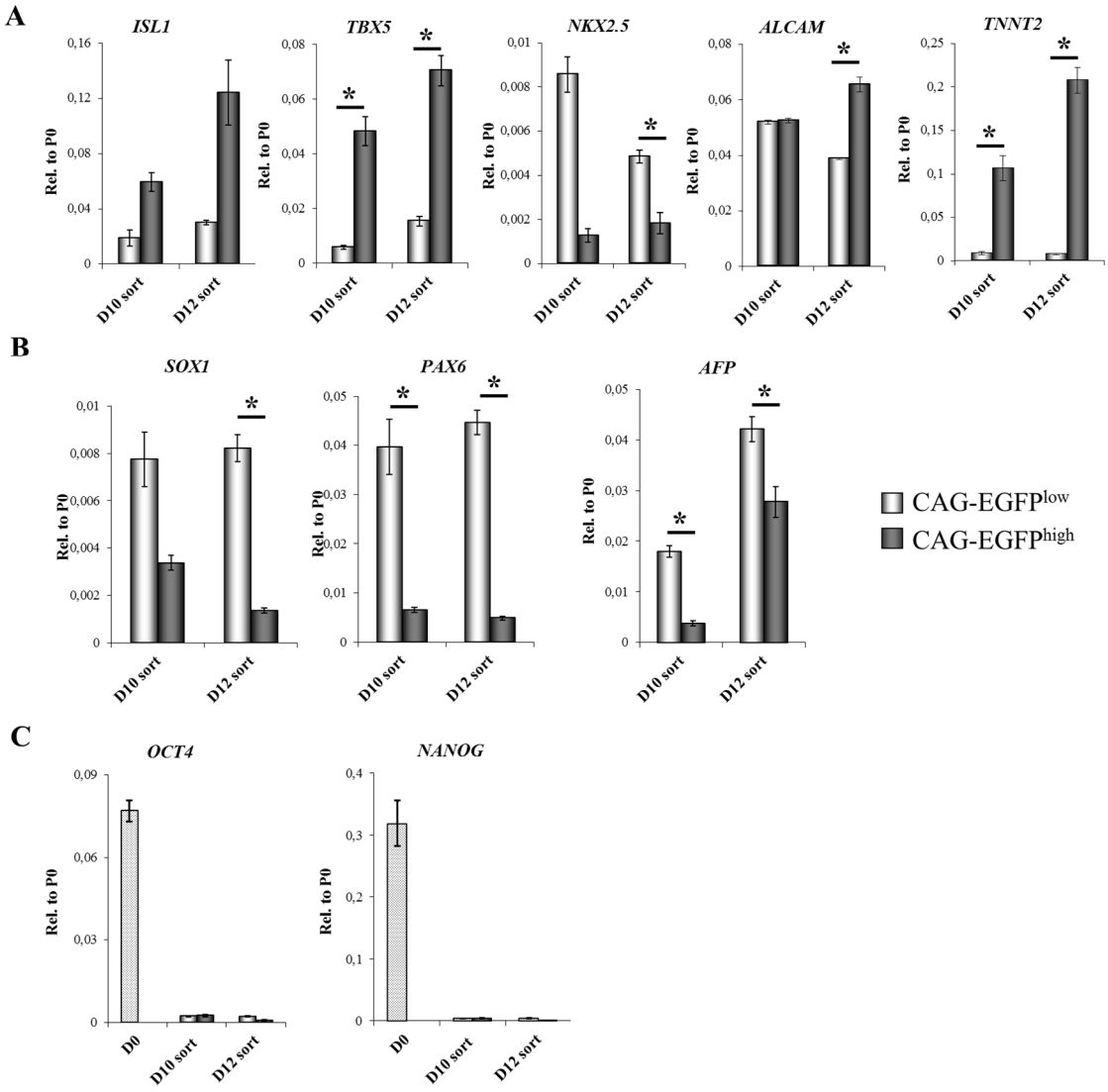

Figure 18. The CAG-EGFP^{high} subpopulation is enriched in cardiac progenitor cells. (**A**) QPCR analysis of the mRNA expression of *ISL1*, *TBX5*, *NKX2.5*, *ALCAM* and *TNNT2* in HUES9-CAG-EGFP^{low}(light grey columns) and HUES9-CAG-EGFP^{high} cells (dark grey columns), sorted at day 10 (D10 sort) or day 12 (D12 sort) of differentiation. (**B**): QPCR analysis of the mRNA expression of *SOX1*, *PAX6* and *AFP* in HUES9-CAG-EGFP^{low} (light grey columns) and HUES9-CAG-EGFP^{high} cells (dark grey columns), sorted at day 10 (D10 sort) or day 12 (D12 sort) of differentiation. (**C**) QPCR analysis of the mRNA expression of *OCT4* and *NANOG* in HUES9-CAG-EGFP^{low} and HUES9-CAG-EGFP^{high} cells, sorted at day 10 (D10 sort) or day 12 (D12 sort) of differentiation. Levels of significance were calculated by the Student T-test; *: $p<0.05$, n=3. The image is taken from Szebényi *et al.*[123], with some modifications.

DOI:10.14753/SE.2015.1764

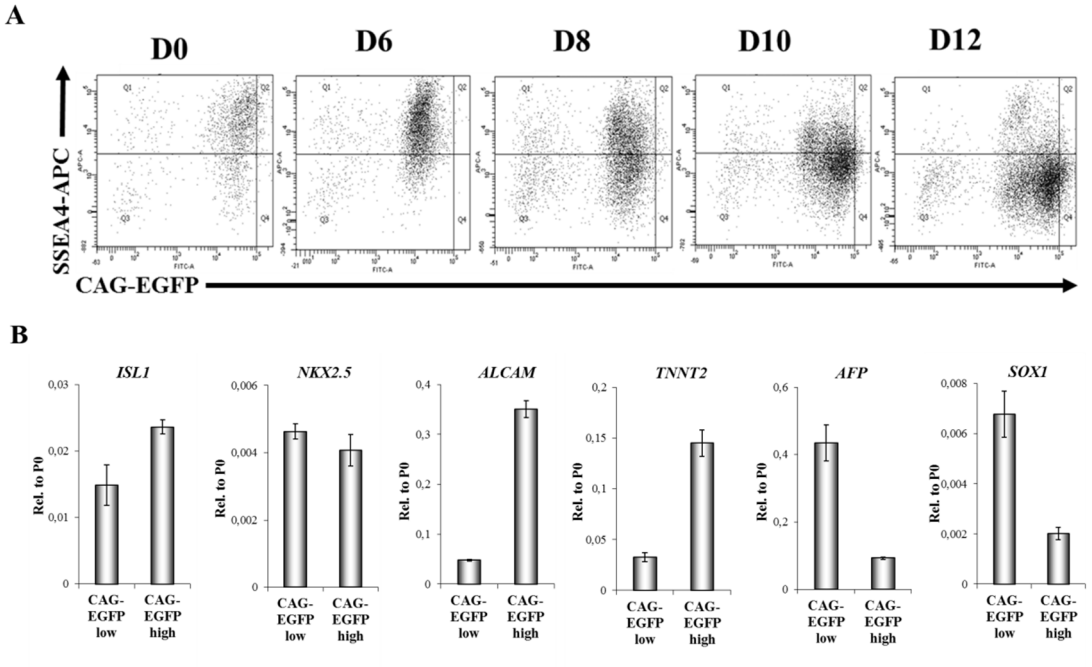

Figure 19. Analysis of directed differentiation of BG01V-CAG-EGFP hESCs. (**A**) Flow cytometry analysis of the pluripotency marker SSEA4 and CAG-EGFP on cells from whole BG01V-CAG-EGFP EBs at different stages of differentiation. Dot plot quadrant gates are set based on IgG3 isotype control for SSEA4 and EGFP fluorescence intensity of the undifferentiated BG01V-CAG-EGFP cells for CAG-EGFP. (**B**) QPCR analysis of cardiac lineage markers (*ISL1*, *NKX2.5*, *ALCAM* and *TNNT2*), the ectoderm marker *SOX1* and the early endoderm marker *AFP* in HUES9-CAG-EGFP^{low} and HUES9-CAG-EGFP^{high} cells sorted at day 12 of differentiation. The image is taken from Szebényi *et al.*[123], with some modifications.

To further confirm the ability of the CAG-EGFP system to identify cardiac progenitors, BG01V-CAG-EGFP hESCs were differentiated with the same directed differentiation protocol as used for differentiation of HUES9-CAG-EGFP cells (see **Figure 13**). BG01V-CAG-EGFP cells also started to form a CAG-EGFP^{high} subpopulation, however two days later than HUES9-CAG-EGFP cells (**Figure 19A**). This delay was presumably caused by an inherent feature of the BG01V hESC line, since this cell line was established from an embryo with Down syndrome causing congenital heart failure [124, 125]. Distribution of cardiac-specific mRNA levels between the two fractions sorted on day 12 were similar to that observed in the case of HUES9-CAG-EGFP cells (**Figure 19B**), since *ISL1*, *ALCAM* and *TNNT2* transcription levels

were higher in BG01V-CAG-EGFP^{high} samples, while *NKX2.5*, and the non-cardiac specific genes showed higher expression in BG01V-CAG-EGFP^{low} cells.

5.3.2. Comparing CAG-EGFP-based isolation of cardiac progenitors to other methods known from the literature

In good agreement with the increase of *ALCAM* transcription in D12 CAG-EGFP^{high} samples (see **Figure 18A**), CAG-EGFP^{high} cells started to express ALCAM at the protein level on day 12 of the differentiation (**Figure 20A**, black arrows indicate ALCAM^{pos}/CAG-EGFP^{high} cells). However, a clear co-expression of the two markers was first observed on day 14. The ability of ALCAM to identify solely cardiomyocytes is stage specific and it has not been indicated that ALCAM is suitable for the identification of cardiac progenitors; therefore it could be assumed that on day 12 CAG-EGFP^{high} cells identify CPCs that are becoming ALCAM positive CMs by day 14.

To further evaluate this possibility, half of the single cell suspension obtained by trypsinization from EBs was sorted into ALCAM positive (ALCAM^{pos}) and ALCAM negative (ALCAM^{neg}) fractions (**Figure 20A**), while the other half into CAG-EGFP^{high} and CAG-EGFP^{low} fractions (as shown in **Figure 17**). On day 12 *TNNT2* and *NKX2.5* transcriptional levels did not differ significantly between ALCAM^{pos} and ALCAM^{neg} samples, while by day 14 *TNNT*2 transcriptional levels of the ALCAM^{pos} and ALCAM^{neg} fractions became more distinct through a three-fold increase of *TNNT2* expression in the ALCAM^{pos} sample (**Figure 20B**). By day 14, the ALCAM^{pos} and ALCAM^{neg} populations became more distinct based on their *NKX2.5* transcriptional levels as well, however the ALCAM^{neg} fraction expressed a similar level of *NKX2.5* transcripts than the CAG-EGFP^{low} fraction, while CAG-EGFP^{high} cells expressed significantly lower levels of *NKX2.5* than all the other samples, irrespectively of the day of sorting. All these findings outlined that early cardiomyocytes expressed ALCAM on day 14, while a subpopulation of ALCAM^{pos} cells marked by the CAG-EGFP system expressed *TNNT2*, but only low levels of *NKX2.5*.

DOI:10.14753/SE.2015.1764

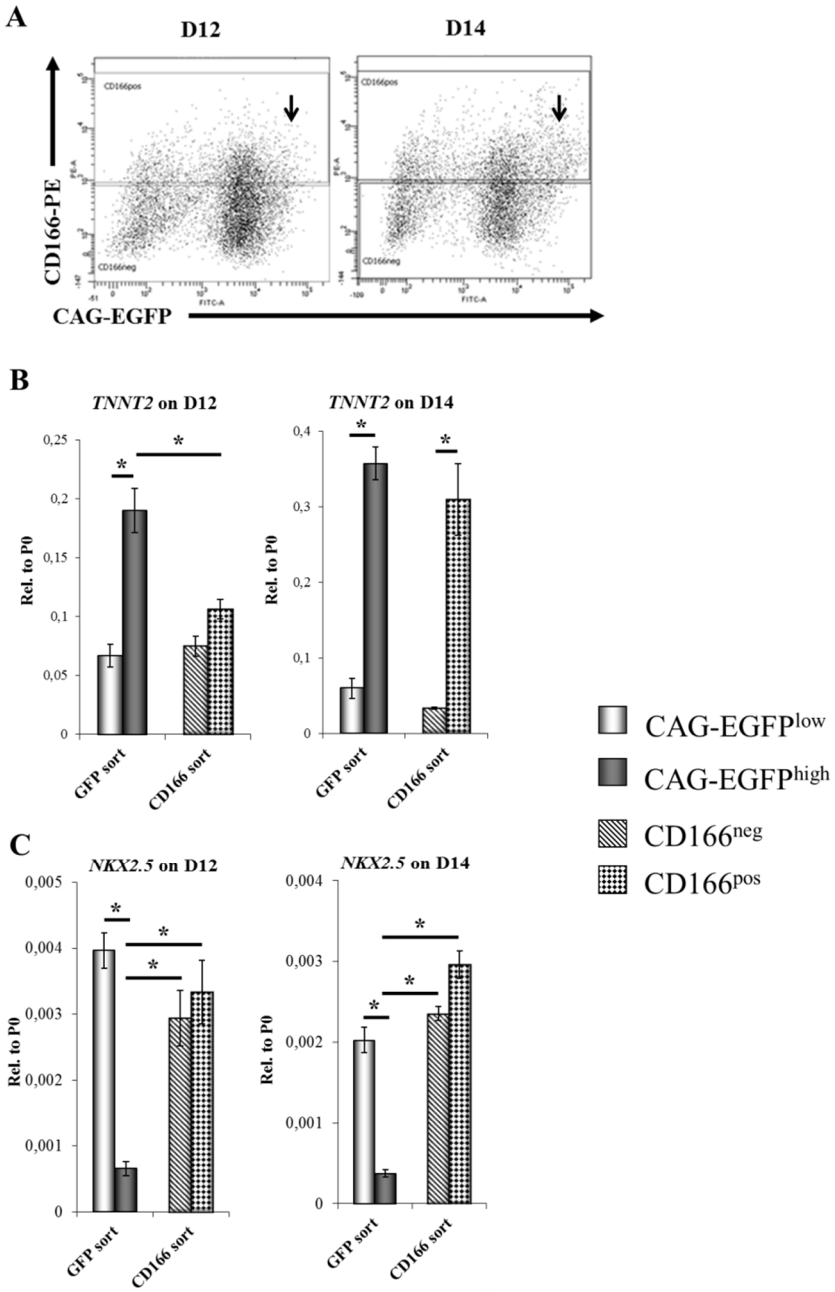

Figure 20. Analysis of the cardiac progenitors obtained by the CAG-EGFP separation system and those by the presence of CD166. (A): HUES9-CAG-EGFP EBs were sorted based on their CD166/ALCAM expression intensities into CD166 negative ($CD166^{neg}$) and positive ($CD166^{pos}$) fractions on day 12 (D12) and day 14 (D14) of the differentiation. Black arrows indicate $ALCAM^{pos}$/$CAG\text{-}EGFP^{high}$ cells. (B): QPCR analysis of the mRNA expression of TNNT2 and NKX2.5 in the different subpopulations (GFP sort: HUES9-$CAG\text{-}EGFP^{low}$ and HUES9-$CAG\text{-}EGFP^{high}$ cells; CD166 sort: $CD166^{neg}$ and $CD166^{pos}$ cells) sorted either at day 12 (left panel) or day 14 (right panel) of differentiation. Levels of significance were calculated by the Student T-test; *: $p<0.05$, n=3. The image is taken from Szebényi *et al.*[123].

DOI:10.14753/SE.2015.1764

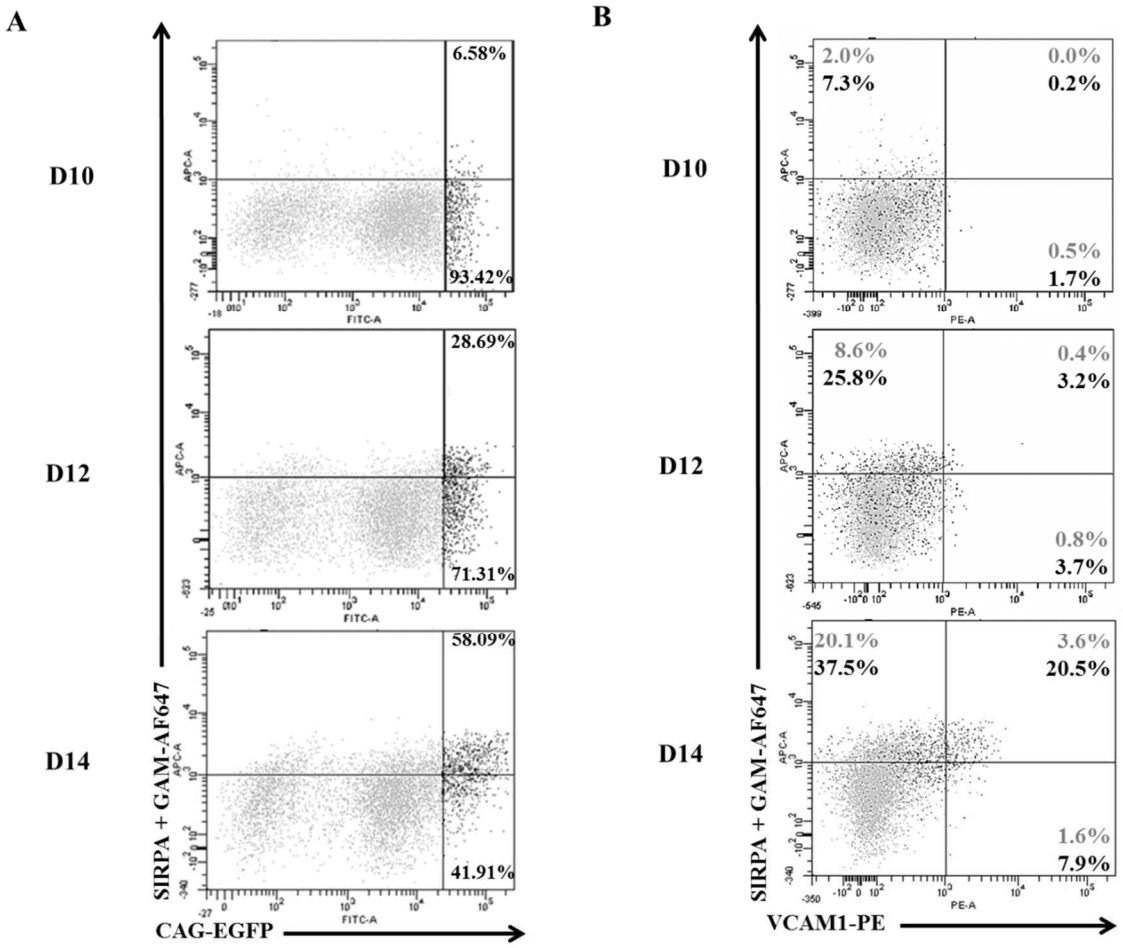

Figure 21. Comparison of the CAG-EGFP system with early cardiomyocyte markers SIRPA and VCAM1. (A) Flow cytometry analysis of SIRPA and CAG-EGFP in HUES9-CAG-EGFP EBs at day 10 (D10), day 12 (D12) and day 14 (D14) of differentiation. (B) Flow cytometry analysis of SIRPA and VCAM1 in HUES9-CAG-EGFP EBs at day 10 (D10), day 12 (D12) and day 14 (D14) of differentiation. Dot plot quadrant gates are set based on the background levels of fluorescence of Goat Anti-Mouse Alexa Fluor 647 (GAM-AF647) for SIRPA and IgG1kappa isotype control for VCAM1. Black coloured dots indicate CAG-EGFP^{high} cells. The image is taken from Szebényi *et al.*[123].

To further investigate CPCs (D12 cells) and early cardiomyocytes (D14 cells) identified by their high CAG-EGFP expression intensity, SIRPA and VCAM1 expression was investigated between day 10, the emergence of the CAG-EGFP^{high} subpopulation and day 14, the emergence of ALCAM^{pos}/CAG-EGFP^{high} early cardiomyocytes (**Figure 21**). CAG-EGFP^{high} cells started to express SIRPA on day 12

DOI:10.14753/SE.2015.1764

(28.69% of the CAG-EGFP^{high} cells were SIRPA^{pos}), and by day 14 58.09% were SIRPA^{pos}, further supporting that the CAG-EGFP^{high} population contains early cardiomyocytes (**Figure 21A**). As it was reported previously[88], expression of VCAM1 only partially overlapped with SIRPA, and accordingly to this approximately 36% of CAG-EGFP^{high} cells (indicated by black dots on **Figure 21B**) expressing SIRPA expressed VCAM1 by day 14.

5.4. Examining different culture conditions for isolated CAG-EGFP^{high} cardiac progenitors

To further investigate CAG-EGFP^{high} cells, culture conditions needed to be tested allowing re-culture and differentiation of the isolated cells. First, a cell line has been established by mechanically removing and enzymatically dissecting a contracting area and the surrounding tissues from a HUES9 (EGFP negative) differentiation culture. The dissected cells were re-cultured in DM and underwent several passages to generate a feeder cell line with fibroblast morphology, possibly able to support cardiac differentiation. The cell line was termed as cardiomyocyte supporting cells (CMSCs) and exhibited a mesenchymal stem cell-like phenotype[126, 127], since FACS measurements confirmed that CMSCs were positive for CD44, CD73, CD105, CD90, CD166 (ALCAM) and negative for CD45, CD34, CD31, CD56, CD61, SSEA4, respectively (**Figure 22**).

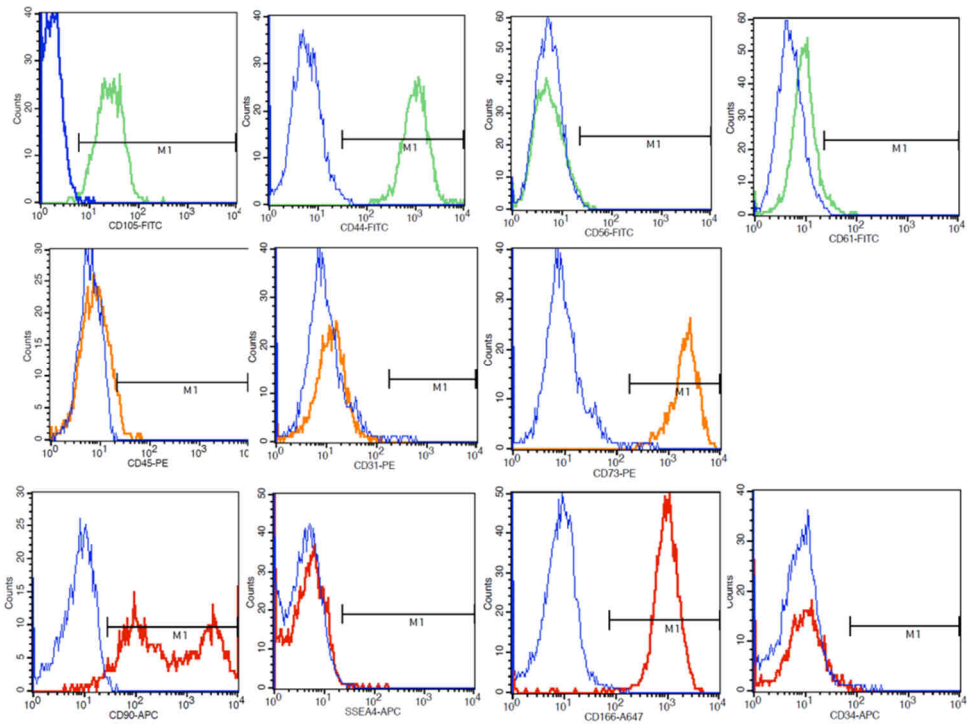

Figure 22. Characterization of the CMSC line established from a contracting area of a HUES9 differentiation culture. Green: CD105-FITC, CD44-FITC, CD56-FITC, CD61-FITC; orange: CD45-PE, CD31-PE, CD73-PE; red: CD90-APC, SSEA4-APC, CD166-AlexaFluor647, CD34-APC (from left to right). Blue lines indicate the signal of the isotype controls. The image is going to be published in Szebényi *et al*. (manuscript in preparation).

DOI:10.14753/SE.2015.1764

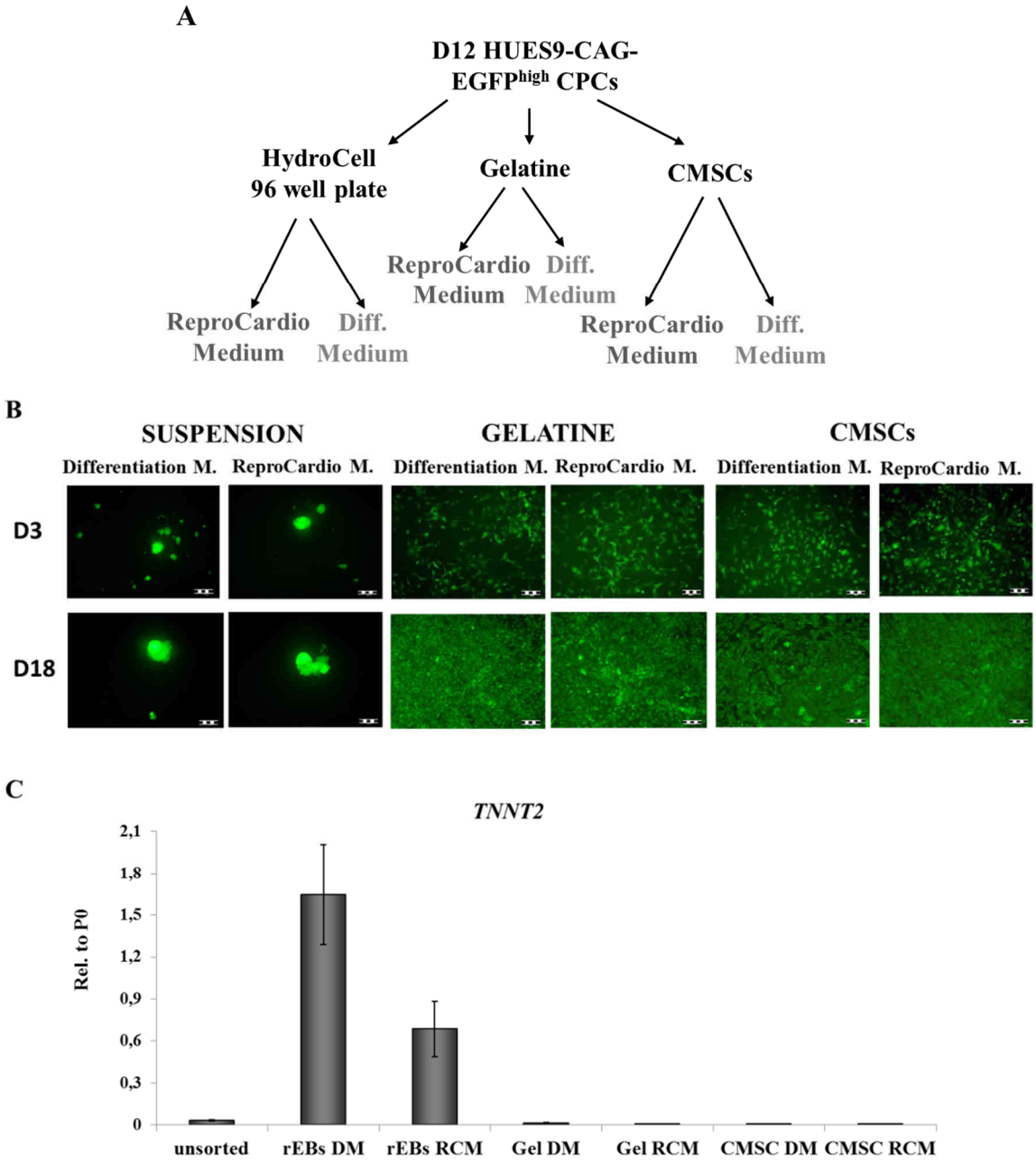

Figure 23. Comparison of different culture conditions for supporting cardiac differentiation of HUES9-CAG-EGFP^{high} cells. (A) Schematic outline of the different culture conditions applied. (B) Representative images of HUES9-CAG-EGFP^{high} cells under different culture conditions 3 and 18 days after sorting. Scale bars represent 200 µm. (C) QPCR analysis of the cardiac gene *TNNT2* in samples cultured for 18 days after sorting. The sorting was performed on day 12 of the differentiation. The unsorted sample was collected on day 30 of the differentiation. CPCs: cardiac progenitor cells; D: day; M: medium; rEBs: reaggregated embryoid bodies; DM: differentiation medium; RCM: ReproCardio medium; Gel: gelatin; CMSC: cardiomyocyte supporting cells. The image is going to be published in Szebényi *et al*. (manuscript in preparation).

DOI:10.14753/SE.2015.1764

Next, two different monolayers and a 3D suspension culture were tested in combination with two different culture media to compare their ability for supporting cardiac differentiation of CAG-EGFP^{high} cells (**Figure 23A**). HUES9-CAG-EGFP^{high} cells were isolated on day 12 and replated either in round bottom 96 well suspension (HydroCell) plates to form 3D aggregates or were cultured as monolayers on gelatine or on a layer of CMSCs (**Figure 23B**). Gelatine was tested based on previous reports, providing evidence for that gelatine-coated surfaces are able to support cardiac differentiation[128, 129]. In addition, the routinely used differentiation medium (DM) was compared to ReproCardio medium (RCM), under all of these above mentioned circumstances. RCM was tested because this medium is specially offered for culturing cardiomyocytes, hence it could be assumed that this medium would provide some benefit for cardiac progenitors as well.

CAG-EGFP^{high} cells cultured as monolayers exhibited mesenchymal morphology and were able to divide, demonstrated by the increased confluency of the cells after 18 days in culture (**Figure 23B**). Growth of reaggregated EBs (rEBs) was modest and at this time point was not further investigated (for detailed investigation of growth of rEBs see Chapter 6).

Samples were collected into TRIzol Reagent after 18 days of culture and *TNNT2* mRNA levels were compared by QPCR to evaluate the most potent culture condition in terms of cardiomyocyte differentiation efficiency (**Figure 23C**). Increased levels of *TNNT2* transcription could only be detected in the case of the 3D aggregates, while RCM did not show any advantages over the traditional DM in supporting cardiac differentiation of the isolated HUES9-CAG-EGFP^{high} cells.

DOI:10.14753/SE.2015.1764

5.5. CAG-EGFP^{high} cardiac progenitors give rise to a relative pure population of cardiomyocytes

In order to further examine the potential of the CAG-EGFP^{high} cells, isolated CAG-EGFP^{high} and CAG-EGFP^{low} cells were plated in suspension cultures either on day 10 or day 12, and maintained as rEBs for several weeks in the presence of 10% bovine serum. Spontaneous contractile activity was first detected at 25 days after the formation of CAG-EGFP^{high} rEBs (approx. 30% of CAG-EGFP^{high} rEBs contracted; see **Supplementary video 2**). CAG-EGFP^{low} rEBs did not show any contractile activity. **Figure 24** shows that after 30 days in culture CAG-EGFP^{high} rEBs expressed significantly higher levels of *TNNT2* and *NKX2.5* than CAG-EGFP^{low} rEBs, and these transcriptional levels were several fold higher than those of the initially isolated CAG-EGFP^{high} cells (D10 CAG-EGFP^{high} and D12 CAG-EGFP^{high}), implying maturation of the CPCs into CMs.

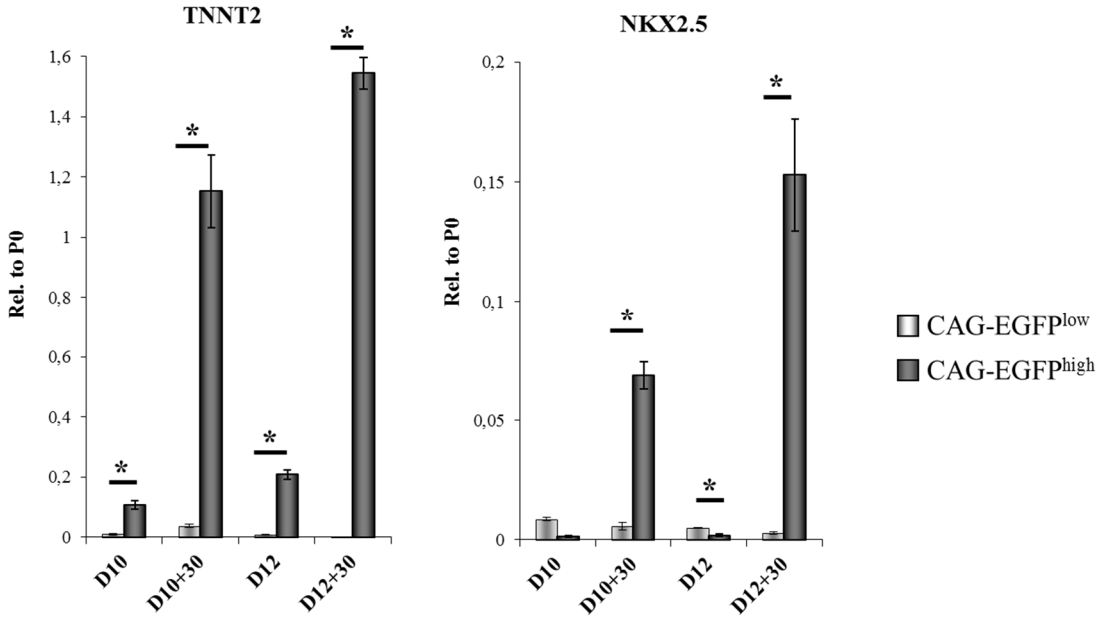

Figure 24. QPCR analysis of cardiac specific genes *NKX2.5* and *TNNT2*. HUES9-CAG-EGFP^{low} (light grey) and HUES9-CAG-EGFP^{high} (dark grey) cells were sorted either on day 10 (D10) or day 12 (D12) of differentiation and differentiated an additional 30 days long (D10+30 and D12+30 samples, respectively). Levels of significance were calculated by the Student T-test; *: $p<0.05$, n=6. The image is taken from Szebényi *et al.*[123].

DOI:10.14753/SE.2015.1764

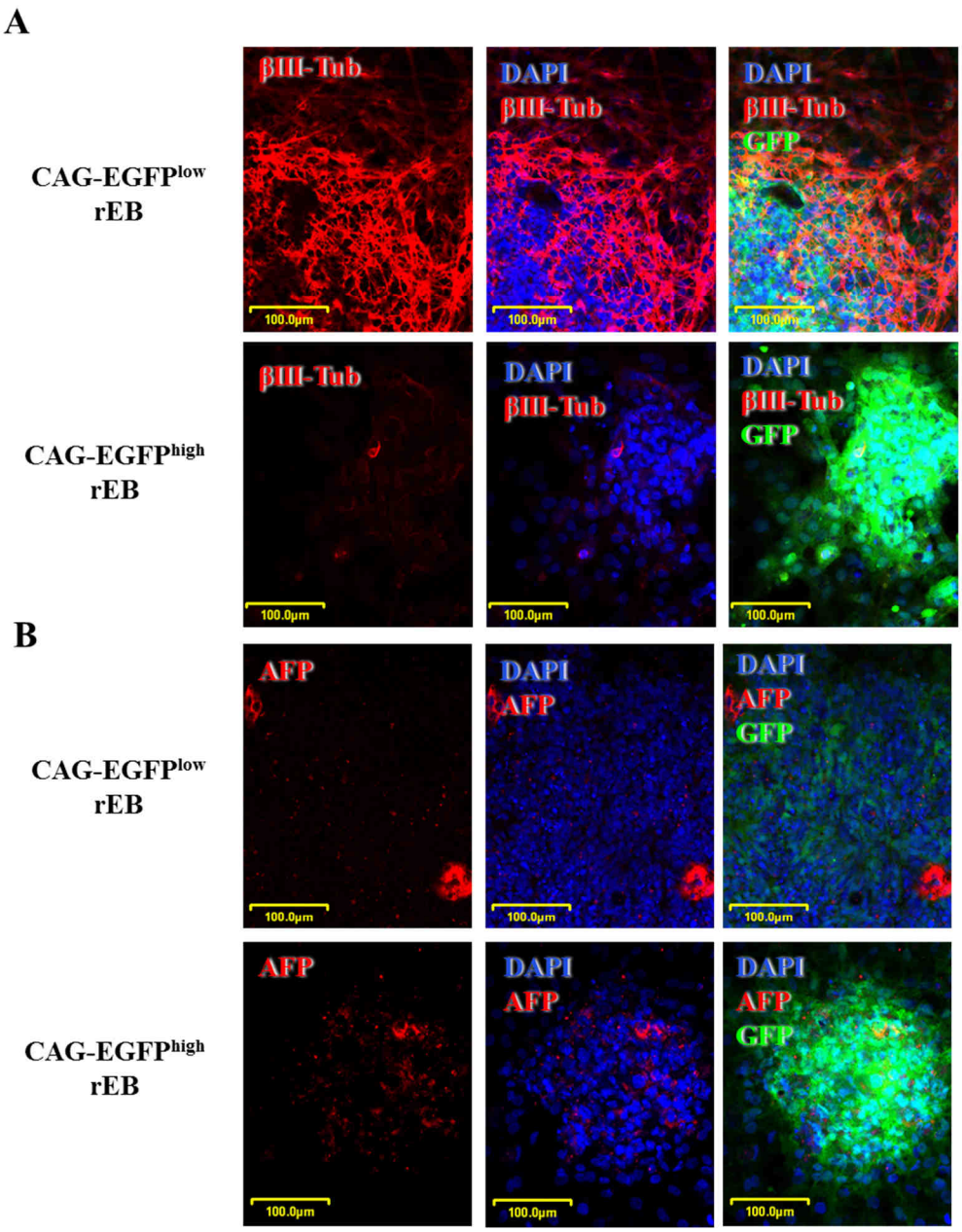

Figure 25. Immunocytochemical analysis of ectoderm and endoderm markers in 10 days old HUES9-CAG-EGFP^{low} and HUES9-CAG-EGFP^{high} rEBs. (A) Red: Anti-Neuron-specific beta-III Tubulin (βIII-Tub). (B) Red: the early endoderm marker Anti-alpha-Fetoprotein (AFP). The rEBs were generated from cells sorted on day 12 of the differentiation. Green: CAG-EGFP. Blue: DAPI. The image is taken from Szebényi *et al.*[123].

In order to examine the cell types present in the rEBs, immunocytochemistry analysis of the neuronal marker βIII Tubulin, the early endoderm marker AFP, the

endothelial cell marker PECAM, the smooth muscle cell marker SMA, as well as the cardiomyocyte marker troponin I was carried out on rEBs generated from D12 CAG-EGFP^{high} or CAG-EGFP^{low} cells (**Figure 25-27**). For immunostaining floating rEBs were seeded on confocal microscopy chambers, additionally CAG-EGFP^{high} rEBs needed a short trypsinization to achieve better adhesion.

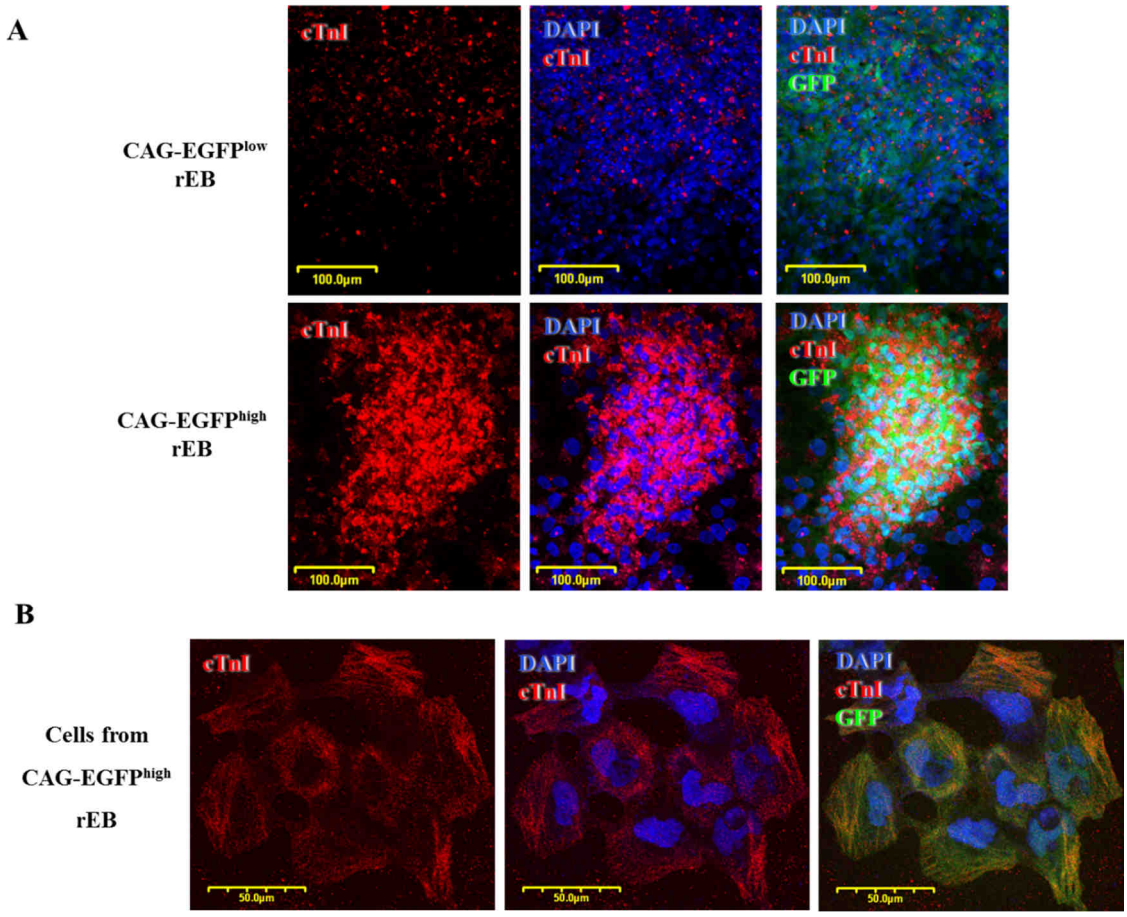

Figure 26. Cardiac troponin I (cTnI) immunostaining of 10 day-old HUES9-CAG-EGFP^{low} and HUES9-CAG-EGFP^{high} rEBs. The rEBs were generated from cells sorted on day 12 of the differentiation. Green: CAG-EGFP. Red: Anti-Human Cardiac Troponin I (cTnI). Blue: DAPI. The image is taken from Szebényi *et al.*[123].

In CAG-EGFP^{low} rEBs an appreciable amount of neuronal committed cells with high βIII Tubulin expression could be detected, while CAG-EGFP^{high} rEBs did not stained for βIII Tubulin (**Figure 25A**). AFP positive cells were detected in all rEBs

examined, however the extremely low yield showed that endoderm differentiation was not supported by the applied directed differentiation protocol (**Figure 25B**). Troponin I was only expressed in CAG-EGFP^{high} rEBs (**Figure 26A**) and in cells around them (**Figure 26B**), while cells around the rEBs often stained positive for SMA in both types of rEBs (**Figure 27A**). PECAM positive endothelial cells could not be found in either of the rEBs (**Figure 27B**).

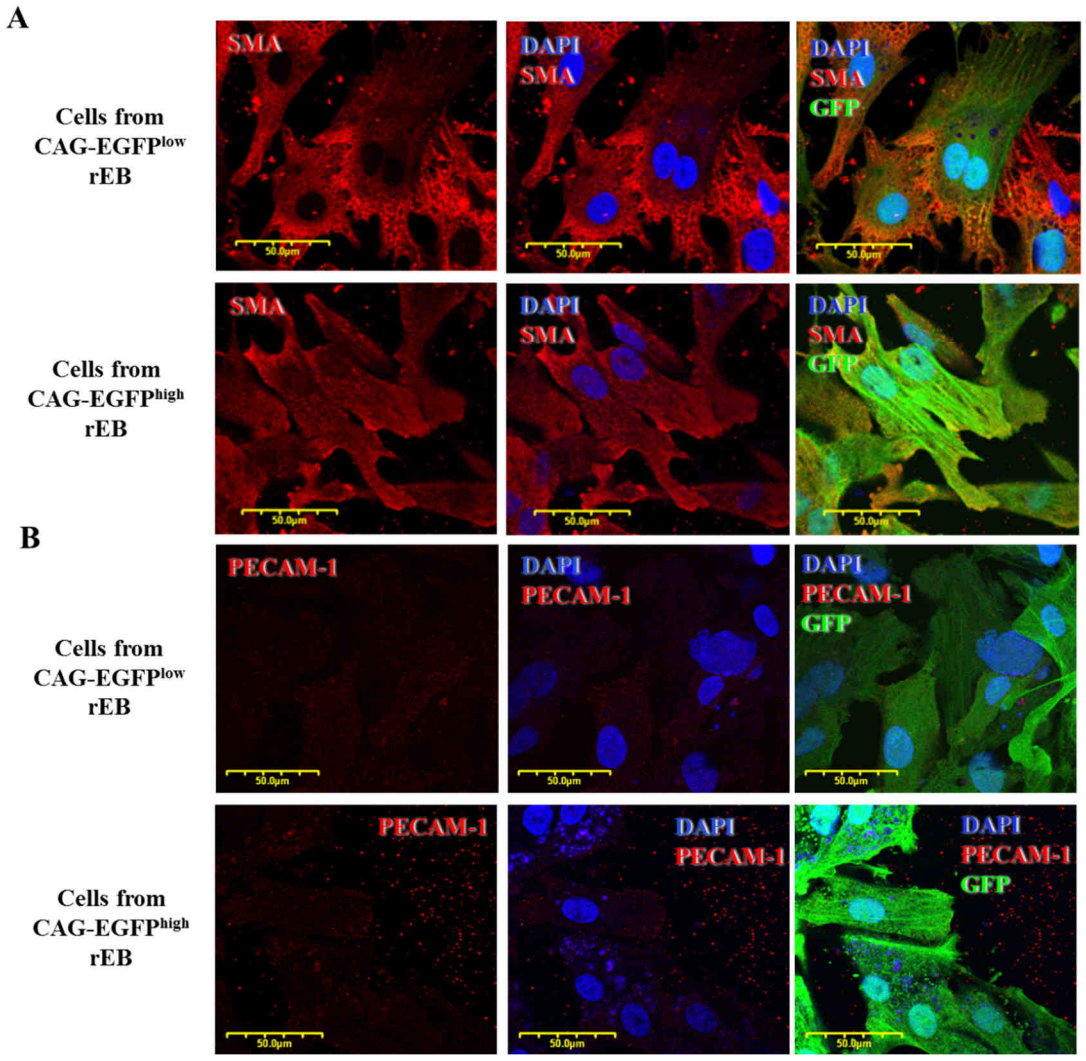

Figure 27. Immunocytochemical analysis of cardiovascular markers in 10 days old HUES9-CAG-EGFP^{low} and HUES9-CAG-EGFP^{high} rEBs. (A) Red: Anti-Alpha-Smooth Muscle Actin (SMA). (B) Red: Anti-Human Platelet endothelial cell adhesion molecule (PECAM). The rEBs were generated from cells sorted on day 12 of the differentiation. Green: CAG-EGFP. Blue: DAPI. The image is taken from Szebényi *et al.*[123], with some modifications.

DOI:10.14753/SE.2015.1764

Intracellular staining against Toponin I was detected by FACS and it was confirmed that more than 98% of the cells of CAG-EGFP^{high} rEBs were cardiomyocytes, indicating that approximately 2% of the cells present in CAG-EGFP^{high} rEBs are smooth muscle cells (**Figure 28**).

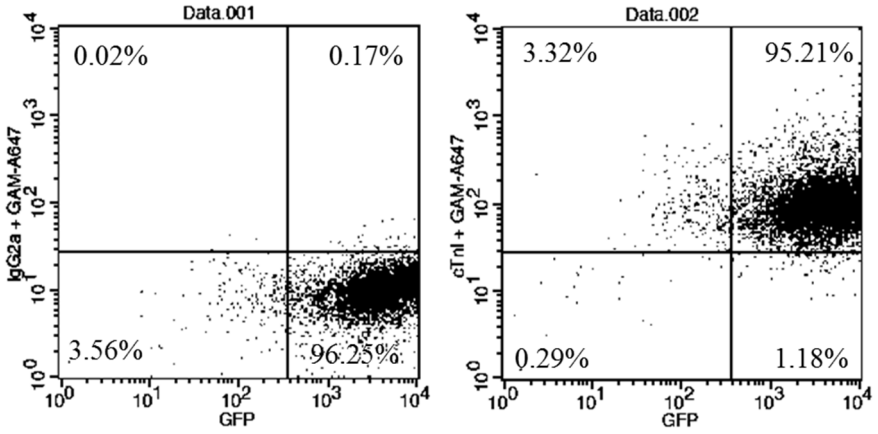

Figure 28. Flow cytometry analysis of cardiac troponin I (cTnI) expression on 20-day old HUES9-CAG-EGFP^{high} rEBs. The rEBs were generated from cells sorted on day 12 of the differentiation. Dot plot quadrant gate for cTnI (right panel) is set based on IgG2a isotype control (left panel), while the gate for EGFP fluorescence is set based on the fluorescence intensity of fixed undifferentiated CAG-EGFP cells. The image is taken from Szebényi *et al.* [123].

In order to determine the cardiac cell subtypes in present in CAG-EGFP^{high} rEBs, transcriptional levels of MYL2, a marker of ventricular CMs, MYL7, the marker of atrial CMs and HCN4, the earliest expressed nodal cell marker were analysed by QPCR (**Figure 29**). HCN4 and MYL2 were expressed at very low levels, whereas MYL7 showed high level expression in CAG-EGFP^{high} rEBs, indicating that cardiomyocytes derived from the isolated CAG-EGFP^{high} cells are mostly of atrial type. This observation may indicate a differential regulation of the CAG driven expression of EGFP in various CM types. This finding is further supported by one of the previous observation regarding the presence of troponin I positive areas with lower EGFP signal in the spontaneous differentiation cultures (see **Figure 11**).

DOI:10.14753/SE.2015.1764

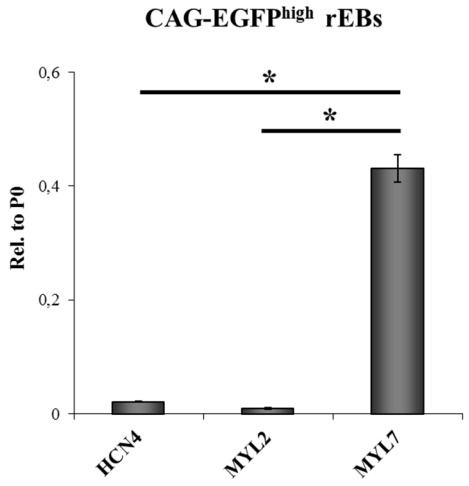

Figure 29. QPCR analysis of the mRNA expression of *HCN4*, *MYL2*, and *MYL7* in HUES9-CAG-EGFP^{high} rEBs, generated from cells sorted on day 12 of differentiation. Levels of significance were calculated by the Student T-test; *: $p<0.05$, n=3.The image is taken from Szebényi *et al.*[123].

5.6. Enhanced culture conditions for supporting the growth of CAG-EGFP^{high} rEBs without losing cardiac commitment

5.6.1. Modest growth of 3D aggregates generated from isolated CAG-EGFP^{high} cells

Next, the ability of CAG-EGFP^{high} rEBs to grow was investigated by fluorescence imaging (**Figure 30**) and fluorescence plate reader measurements (**Figure 31**). **Figure 30** shows representative images of rEBs 3 and 20 days after isolation of CAG-EGFP^{high} (**Figure 30A**) and CAG-EGFP^{low} (**Figure 30B**) cells on day 10 and day 12, respectively. Fluorescent microscopy data suggested, that CAG-EGFP^{high} cells sorted on day 10 exhibited slightly better aggregation and/or proliferation properties than the cells isolated on day 12, since CAG-EGFP^{high} rEBs generated from cells isolated on day 12 (D12 CAG-EGFP^{high} rEBs) were slightly smaller at the end of the differentiation than those generated from cells isolated on day 10 (D10 CAG-EGFP^{high} rEBs) (**Figure 30A**). Additionally, several differences between CAG-EGFP^{high} and CAG-EGFP^{low} rEBs were observed, for example in the ability to grow and in their shape as well, since CAG-EGFP^{low} cells formed perfect spheroids (while CAG-EGFP^{high} rEBS were more spindle-shaped) and exhibited higher proliferation capacity resulting larger rEBs (**Figure 30B**).

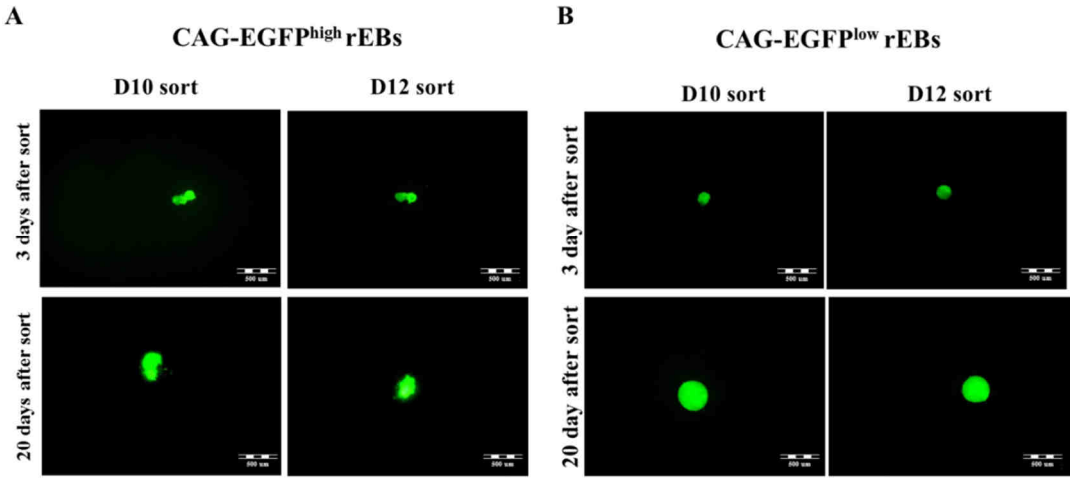

Figure 30. Representative fluorescent images of reaggregated embryoid bodies (rEBs) 3 and 20 days after sorting. (A) HUES9-CAG-EGFP^{high} rEBs and (B) HUES9-CAG-EGFP^{low} rEBs. The cells were either sorted on day 10 (D10 sort) or day 12 (D12 sort) of the differentiation. EGFP expression was detected by fluorescence microscopy**.** The image is taken from Szebényi *et al.*[123].

DOI:10.14753/SE.2015.1764

In order to allow better quantification of the growth of CAG-EGFP^{high} rEBs, fluorescence plate reader measurements were performed 3 and 20 days after cell sorting (**Figure 31**). Plate reader measurements were carried out to detect fluorescence of either the CAG-EGFP signal (**Figure 31A**) or that of the propidium iodide (PI) staining of fixed rEBs (**Figure 31B**). Both methods confirmed the growth of rEBs during 20-day-long culture, additionally the PI staining-based method provided evidence about modest, but significant growth of the rEBs (**Figure 31B**). Fluorescence intensities of the PI staining of 3 day old rEBs sorted on day 10 (D10 sort) and day 12 (D12 sort) were similar, corresponding to the identical number of cells seeded on the wells three days before the measurement (30,000 cells/well) and suggesting similar reaggregation properties among CAG-EGFP^{high} cells sorted either on day 10 or day 12.

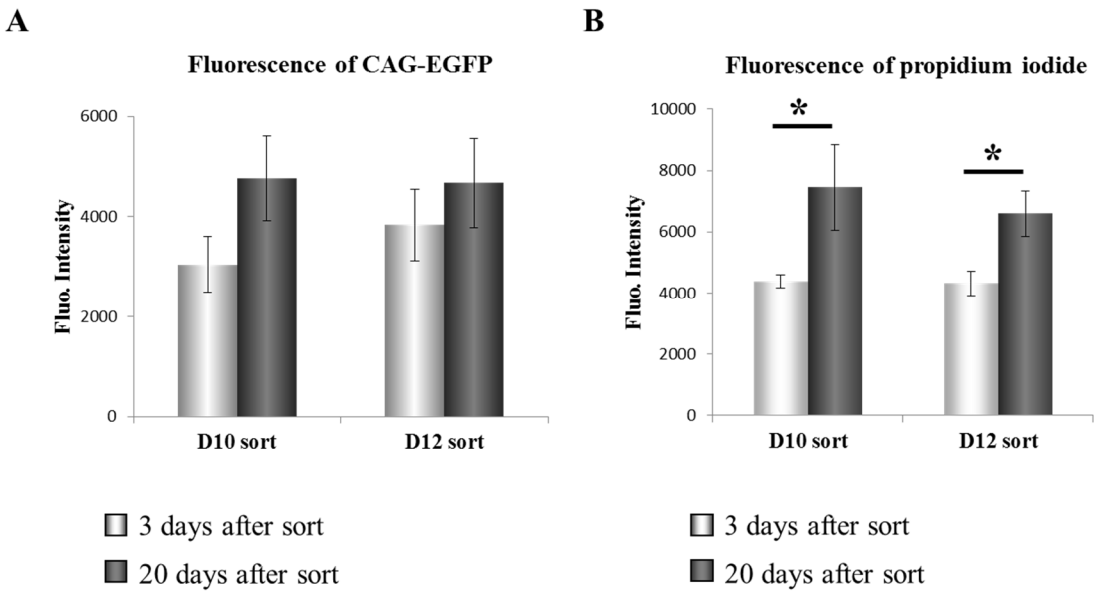

Figure 31. Quantification of the growth of CAG-EGFP^{high} reaggregated embryoid bodies (rEBs). (A) Fluorescence intensity of HUES9-CAG-EGFP^{high} rEBs measured by fluorescence plate reader 3 and 20 days after sorting. (B) Fluorescence intensity of propidium iodide staining in HUES9-CAG-EGFP^{high} rEBs measured by fluorescence plate reader 3 and 20 days after sorting. Sorting was performed either on day 10 (D10 sort) or day 12 (D12 sort) of differentiation. Levels of significance were calculated by the Student T-test; *: $p<0.05$, n=6. The image is taken from Szebényi *et al.*[123].

DOI:10.14753/SE.2015.1764

5.6.2. Thiazovivin enhances reaggregation and survival of the sorted cells

Reaggregation properties of isolated cells were relatively poor, since one day after the sorting procedure a large amount of single cells was detectable, floating around the forming CAG-EGFP^{high} rEBs (**Figure 32**, Differentiation Medium panel, upper left image). To enhance survival and reaggregation ability of CAG-EGFP^{high} cells, culture conditions were optimized.

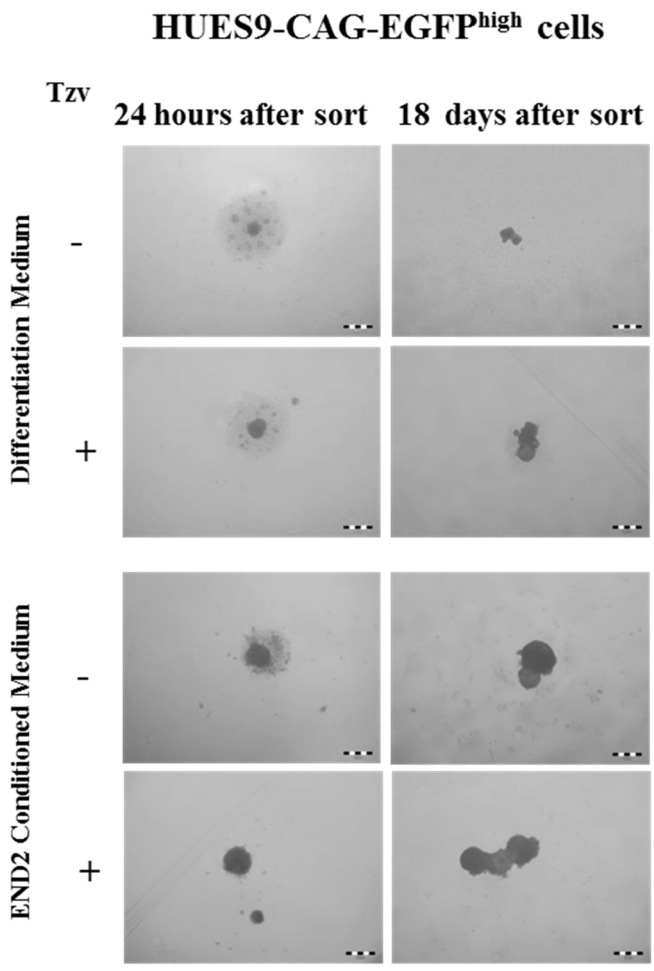

Figure 32. Representative images of HUES9-CAG-EGFP^{high} reaggregated embryoid bodies (rEBs) 1 and 18 days after sorting, cultured either in differentiation or in END-2 conditioned medium. The rEBs were generated from cells sorted on day 12 of the differentiation. Tzv: thiazovivin. „+": with treatment. „-": without treatment. Scale bars represent 500 μm. The image is going to be published in Szebényi *et al*. (manuscript in preparation).

Isolated CAG-EGFP^{high} cells were plated in HydroCell 96 well plates either in DM or in END2-CM, and in the absence or presence of Thiazovivin (**Figure 32**). Thiazovivin is a cell permeable small molecule, able to reduce apoptosis and support single cell survival of hESCs after enzymatic dissociation, through stabilizing E-cadherin and inhibiting Rho-associated kinase (ROCK) activity[130]. A similar ROCK inhibitor, Y-27632 was reported to improve survival of hESC-derived cardiomyocytes after enzymatic dissociation[131], therefore Thiazovivin seemed to be an interesting candidate for optimization studies aiming to improve reaggregation and survival properties of the isolated CAG-EGFP^{high} cells after sorting.

Isolated cells were treated with 2 μM Thiazovivin right after the sorting procedure to promote cell survival during reaggregation. After 24 hours clear differences could be observed between control and Thiazovivin treated wells, as well as between rEBs cultured in DM or in END2-CM (**Figure 32**). In END2-CM CAG-EGFP^{high} cells showed enhanced reaggregation compared to cells recultured in DM, while treatment with Thiazovivin further reduced the amount of free-floating cells in END2-CM. The effect of Thiazovivin was also observable in the case of CAG-EGFP^{high} cells replated in DM.

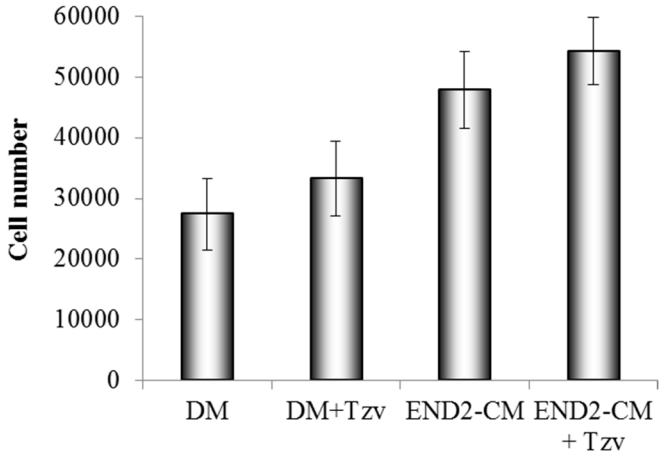

Figure 33. Comparison of the effect of different culture conditions on the survival of HUES9-CAG-EGFP^{high} cells after sorting. Cell number was counted by trypan blue staining of trypsinized HUES9-CAG-EGFP^{high} reaggregated embryoid bodies one day after sort. The rEBs were generated from cells sorted on day 12 of the differentiation. The image is going to be published in Szebényi *et al*. (manuscript in preparation).

DOI:10.14753/SE.2015.1764

To quantify the observed effects cell counting by Trypan Blue was used after enzymatic dissociation of some of the newly formed rEBs (n=3) (**Figure 33**). This method was chosen instead of the previously applied detection of PI staining of fixed rEBs, because after fixation PI staining was not feasible for distinguishing between living and dead cells, while the PI staining of living rEBs and floating cells around it could not be distinguished from the background signal of PI. The trypan blue staining showed that enhanced aggregation properties were coupled to increased survival of the sorted cells (**Figure 33**). The first medium change was carried out two days after sort and this resulted in the final clearing of wells from free-floating cells in every culture condition tested.

After 18 days in culture, the size of the rEBs were found to be more increased in END2-CM, than in DM; this was confirmed by light microscopy (**Figure 32**) and by plate reader measurements detecting the CAG-EGFP signal (**Figure 34**). Enhanced survival and reaggregation properties provided by Thiazovivin treatment resulted in further size increase of CAG-EGFP^{high} rEBs (**Figure 32 and 34**).

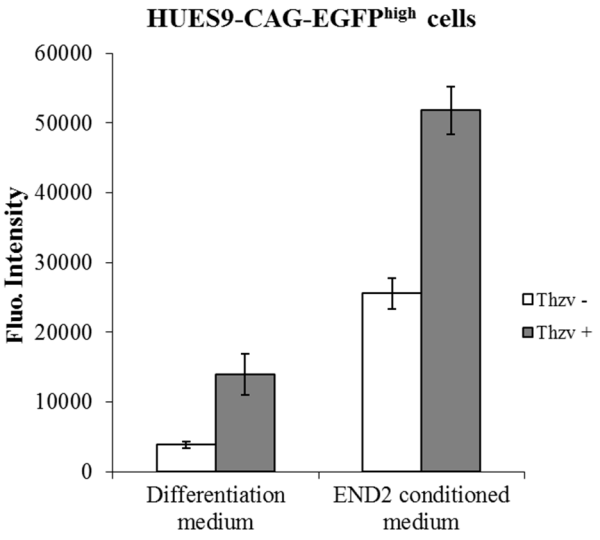

Figure 34. Comparison of the effect of different culture conditions on the growth of HUES9-CAG-EGFP^{high} reaggregated embryoid bodies (rEBs). Fluorescence plate reader measurement of the fluorescence intensity of HUES9-CAG-EGFP^{high} rEBs after 18 days in culture either in differentiation or END-2 conditioned medium. The rEBs were generated from cells sorted on day 12 of the differentiation. Tzv-: thiazovivin treatment was not applied. Tzv+: thiazovivin treatment was applied. The image is going to be published in Szebényi *et al.* (manuscript in preparation).

However, TNNT2 and Phospholamban (PLN) transcription levels were lower in rEBs cultured in END2-CM than in DM, regardless of Thiazovivin treatment, suggesting that non-CM derivatives of the CPCs overgrow cardiomyocytes during the culture period (**Figure 35**). Since previous data suggest (see Szebényi *et al*. and **Figure 27**) that CAG-EGFP^{high} CPCs are able to give rise to SMA positive, but not to PECAM positive cells, it can be assumed that these non-CM derivatives are presumably smooth muscle cells. Regardless of the type of the non-CM population, aim of the further studies was to promote cardiomyocyte differentiation under the END2-CM+Tzv culture condition (allowing the most growth of rEBs) to increase the cardiomyocyte yield of the initial method (CAG-EGFP^{high} rEBs cultured in DM).

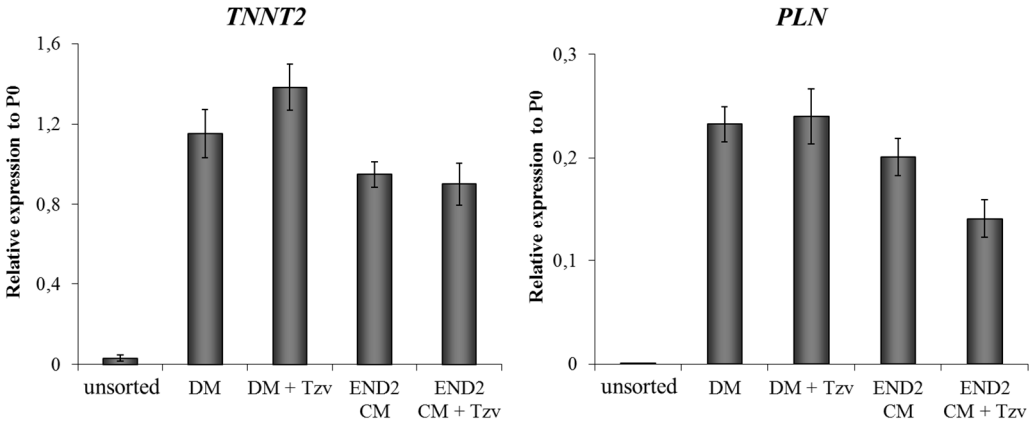

Figure 35. QPCR analysis of cardiac specific genes *TNNT2* and *PLN*. HUES9-CAG-EGFP^{high} reaggregated embryoid bodies (rEBs) were cultured either in differentiation medium (DM) or in END-2 conditioned medium (END2-CM) for 18 days. The rEBs were generated from cells sorted on day 12 of the differentiation. The unsorted sample was collected on day 30 of the differentiation. Tzv: thiazovivin. The image is going to be published in Szebényi *et al*. (manuscript in preparation).

5.6.3. Isoproterenol enhances cardiac differentiation of CAG-EGFP^{high} cells cultured in END-2 conditioned medium

As discussed in the Introduction, the addition of exogenous NRG-1β, a cardioactive growth factor resulted in enhanced generation of ventricular CMs[84] and induced proliferation of mononucleated CMs *in vivo*[82]. NRG-1β acts on ErbB4, a tyrosine kinase receptor required for normal cardiac differentiation during embryonic development[132]. Therefore NRG-1β was tested to enhance cardiomyocyte differentiation of CAG-EGFP^{high} CPCs in END2-CM, after Thiazovivin treatment.

Besides of NRG-1β, Isoproterenol treatment was also tested. Isoproterenol is a β1- and β2-adrenoreceptor (AR) agonist and structurally similar to adrenaline. Isoproterenol can possess arrhythmogenic effects on hESC-CMs [133] and can cause cellular hypertrophy or apoptotic cell death through the β1-AR subtype, whereas stimulation of the β2-AR inhibits apoptosis[134-136]. It was suggested in the case of a rat myoblast cell line (H9c2), often used in toxicological studies, that undifferentiated myoblasts are less prone to the cardiotoxic effect of Isoproterenol than CMs differentiated from them[137]. The idea that cardiac precursors and mature CMs react diversely on β-adrenergic stimulation is further supported by Khan *et al*., demonstrating that survival and proliferation of mouse and human CPCs derived from the heart is promoted by adrenerg stimuli through β2-AR, while further maturation leads to significant β1-AR expression and thereby to sensitization to isoproterenol-induced cell death[138]. Moreover, Yan *et al.* demonstrated that β-adrenergic stimulation with 10 μM Isoproterenol during differentiation of mouse ESCs significantly enhances the cardiomyocyte yield[139]. All these data suggested that Isoproterenol might have the ability to enhance the cardiomyocyte yield of CAG-EGFP^{high} CPCs when differentiated in END2-CM, after Thiazovivin treatment.

NRG-1β was used with 100 ng/ml final concentration (Nrg), based on the work of Zhu *et al.* applying NRG-1β during hESC differentiation [84], while Isoproterenol was used with 10 μM final concentration (Iso). The first treatment was applied two days after sorting, and during the following 12 days the treatment was repeated in every third day when the medium was changed. After 18 days in culture, the size of CAG-EGFP^{high}

rEBs were found to be similar, irrespective of whether the rEBs were cultured under treated (END2-CM+Tzv+Nrg and END2-CM+Tzv+Iso) or control (END2-CM+Tzv) conditions (**Figure 36A**). This finding was also confirmed by plate reader measurements detecting the CAG-EGFP signal (**Figure 36B**). While the treatments did not modify the ability of rEBs to grow, enhanced transcription of *TNNT2* demonstrated that CM-differentiation abilities increased in Isoproterenol treated rEBs (**Figure 36C**). The *TNNT2* transcript level measured in rEBs cultured in END2-CM and treated with Thiazovivin and Isoproterenol was similar to that of rEBs cultured in DM (**Figure 35**). NRG-1β failed to achieve increased cardiomyocyte differentiation, moreover, it seemed that NRG-1β decreased cardiomyocyte generation efficiency (**Figure 36C**).

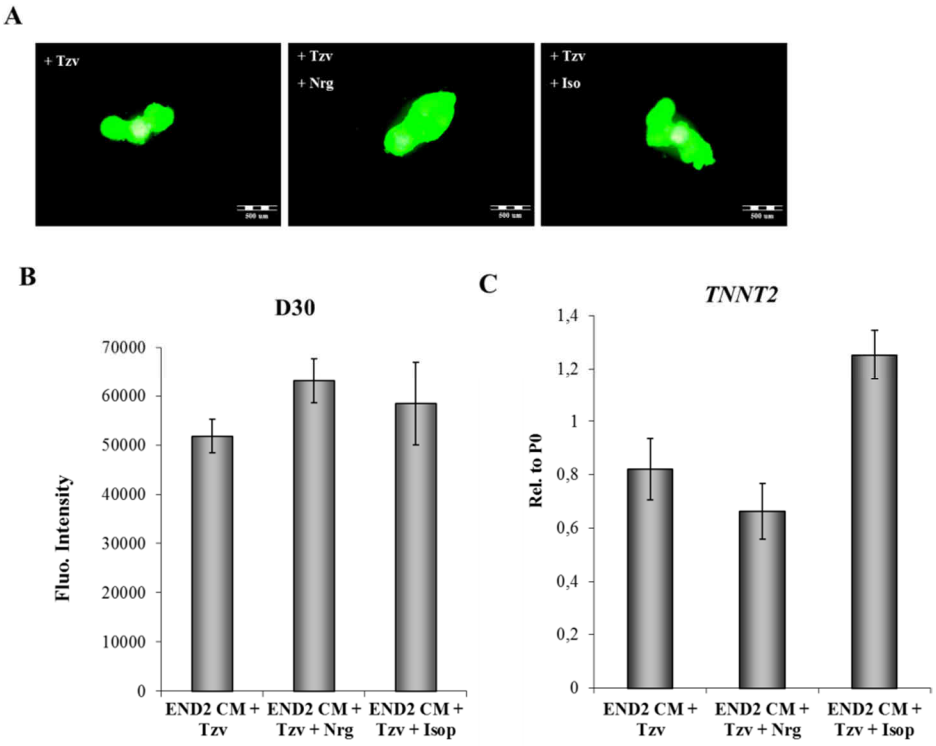

Figure 36. The effect of Neuregulin (Nrg) and Isoproterenol (Iso) on HUES9-CAG-EGFP^{high} reaggregated embryoid bodies (rEBs) cultured in END-2 conditioned medium (END2-CM) for 18 days. (A) Representative images of HUES9-CAG-EGFP^{high} rEBs cultured under different culture conditions. (B) Fluorescence plate reader measurement of the fluorescence intensity of HUES9-CAG-EGFP^{high} rEBs cultured under different culture conditions. (C) QPCR analysis of the cardiac specific gene *TNNT2* in HUES9-CAG-EGFP^{high} rEBs cultured under different culture conditions. The rEBs were generated from cells sorted on day 12 of the differentiation. Tzv: thiazovivin. The image is going to be published in Szebényi *et al.* (manuscript in preparation).

DOI:10.14753/SE.2015.1764

6. Discussion

The promise of human embryonic and induced pluripotent stem cells providing an inexhaustible source of human cardiomyocytes for medical applications was initially limited by inefficient differentiation protocols (resulting in low cardiomyocyte yield), lack of methods for purification of living cardiomyocytes, and the immature state of the derived CMs. Our research group joined the field of stem cell biology with the aim to address the generation of large amounts of pure cardiomyocytes and progenitors of the cardiac lineage.

In the last decade several transgenic reporter systems have been established, allowing the identification and selection of cardiomyocytes and precursors of the cardiac lineage[148]. This effort was motivated by the lack of known cell surface markers allowing the isolation of cardiomyocytes (and cardiac progenitors) without the disruption of their cell membranes. However, most of these studies described cardiac-specific promoter based reporter hESC lines, where the stable integration of the transgene could only be detected when the hESCs differentiated into the cardiac lineage[148]. Our research group established a "double feature" system, allowing the detection and isolation of transgene expressing hESCs (**Figure 5 and 6**) and their cardiomyocyte progeny (**Figure 9 and 10**) based on the CAG promoter driven EGFP expression.

The original CAG promoter is an artificial promoter constructed from the CMV enhancer, the chicken β-actin and the rabbit β1-globin sequences, while the version used here contains a CMV enhancer region, two sequences from the chicken β-actin promoter and one short part of the rabbit β1-globin promoter[90]. The cardiac reporter feature is presumably a specific property of the variant of the CAG promoter that was used[90], resulting in that CAG-EGFP expressing hESCs giving rise to cardiomyocytes with exceptionally high EGFP signal (**Figure 9**).

Next, we verified the CAG-EGFP system for allowing the identification of cardiac progenitors by monitoring the emergence and fate of CAG-EGFP^{high} cells during differentiation (**Figure 12 and 16**) and by QPCR analysis of sorted CAG-EGFP^{high} cells (**Figure 18 and 19**). We confirmed by QPCR (**Figure 24 and 29**),

immunocytochemical analysis (**Figure 25-27**) and by flow cytometry measurements (**Figure 28**) that the isolated CAG-EGFP^{high} cells mostly give rise to cardiomyocytes when cultured as 3D aggregates (**Figure 23**). These findings were also supported by the observed spontaneous contraction in 30% of the CAG-EGFP^{high} rEBs.

It is important to emphasize that a key step during our work was to recognize the need to set up a cardiac-directed differentiation protocol (**Figure 13**). The use of the directed differentiation protocol allowed us to enrich for cardiac progenitors (**Figure 14**), thereby not only the amount, but also the sorting purity of CAG-EGFP^{high} cells could be enhanced. Directed differentiation synchronized and hastened the differentiation of individual cells (SSEA4 expression declined earlier than during spontaneous differentiation, see **Figure 14A**), hence contamination of the CAG-EGFP^{high} population by SSEA4 positive cells could be avoided already on day 10 of the differentiation (**Figure 16**). This was important because some of the undifferentiated cells possessed similar CAG-EGFP signal intensity than CAG-EGFP^{high} CPCs (**Figure 16 and 19A**).

To identify the maturity status of CAG-EGFP^{high} CPCs, we compared the CAG-EGFP system to recently discovered cardiomyocyte- and cardiac precursor cell surface markers such as SIRPA and VCAM1. Comparison of different systems is always difficult due to variation in differentiation capabilities of hESC lines [125]and due to differences in the kinetics of the differentiation caused by the variety of differentiation protocols applied. In addition, these cell surface marker-based systems show some leakiness, since according to the original articles 17.2% of the SIRPA negative cells are also troponin T positive[86], while 25.8% of troponin T positive cells are VCAM1 negative [118] at around the time when the beating activity starts (day 9). Still, sorting based on SIRPA expression on day 8 or on VCAM1 expression on day 11 resulted pure population of CMs according to these articles. The relation between SIRPA and VCAM1 positive cells was also extensively studied and it was shown that SIRPA^{pos} cells give rise to the VCAM1^{pos}/SIRPA^{pos} population[88, 117].

Based on our findings, CAG-EGFP^{high} cells emerge earlier (on day 10) than SIRPA positive cells (around day 12), however, these two population overlapped partially already on day 12, while on day 14 the majority of CAG-EGFP^{high} cells

expressed SIRPA (**Figure 21A**). Moreover, one third of SIRPA positive CAG-EGFP^{high} cells already expressed VCAM1 at this time point (**Figure 21B**). These findings also supported our previous findings regarding the identity of CAG-EGFP^{high} cells as progenitors of the cardiac lineage and suggested a less mature progenitor state for CAG-EGFP^{high} CPCs than represented by SIRPA^{pos} cardiac precursor cells.

The directed differentiation kinetics of HUES9-CAG-EGFP cells differs from that of shown by Dubois *et al.*, since in our system SIRPA expression upregulates on day 12 (day 7 in Dubois *et al*) and spontaneous contractile activity starts around day 14 (day 9 in Dubois *et al.*). Accordingly, emergence of SIRPA positive cells precedes the onset of spontaneous contractile activity by two days in both systems. Therefore, we assumed that day 12 conditions in our system might be most comparable to day 7 conditions documented by Dubois *et al.*[86].

Dubois *et al.* reported [86] that on day 8 of differentiation only half of the SIRPA positive cells were NKX2.5-GFP positive, while at the same time, 98% of the SIRPA positive cells expressed cTnT. This means that at this stage (one day before the contractile activity onsets) there is a SIRPA^{pos}/cTnT^{pos}/NKX2.5^{neg} subpopulation in the differentiation culture. In accordance with this finding, day 12 CAG-EGFP^{high} cells showed upregulated *TNNT2* transcription and low levels of *NKX2.5* transcripts (**Figure 18A and Figure 20B**), while some of the CAG-EGFP^{high} cells already expressed SIRPA on day 12 (**Figure 21A**). By day 14 SIRPA expression became even more characteristic for the CAG-EGPF^{high} population (**Figure 21A**), while *NKX2.5* transcription levels remained low (**Figure 20C**).

The expression of ALCAM was also monitored during the differentiation of HUES9-CAG-EGFP hESCs (**Figure 14A and 20A**). We found that the majority of CAG-EGFP^{high} cells became ALCAM positive by day 14, while on day 12 the ratio of ALCAM positive to negative cells was only slightly higher in the CAG-EGFP^{high} than in the CAG-EGFP^{low} population (**Figure 20A**), still resulting in a significant difference of their *ALCAM* mRNA levels (**Figure 18A**). However, we did not expect a clear separation between day 12 ALCAM^{neg} and ALCAM^{pos} samples regarding *TNNT2* or *NKX2.5* transcription levels (**Figure 20B and C**), since the ALCAM protein is a stage-specific marker of cardiomyocytes, and does not allow the specific identification of

cardiac progenitors. At the same time, on day 12, the CAG-EGFP system already provided excellent separation, demonstrated by the significantly higher *TNNT2* transcription level of the CAG-EGFP^{high} sample compared to the CAG-EGFP^{low} sample (**Figure 18A and 20B**).

Expression of ALCAM on day 14 CAG-EGFP^{low} cells has to be discussed more thoroughly, since it can be interpreted in two different ways: 1) the CAG-EGFP^{low}/ALCAM^{pos} subpopulation represents CMs (CAG-EGFP^{low} cells can also give rise to CMs, see **Figure 11**) or 2) ALCAM does not allow the identification of CMs in our system. The second possibility could be excluded based on the QPCR analysis of samples sorted on day 14, showing elevated levels of *TNNT2* transcripts in ALCAM^{pos} compared to ALCAM^{neg} samples (**Figure 20B**). Interestingly, the day 14 ALCAM^{pos} sample showed only a slightly lower level of *TNNT2* mRNA, than the CAG-EGFP^{high} sample. This finding, on one hand, can suggests that not only the CAG-EGFP^{high}/ALCAM^{pos} cells, but the majority of CAG-EGFP^{low}/ALCAM^{pos} and CAG-EGFP^{neg}/ALCAM^{pos} cells are CMs by day 14, but can also refer to a less pure ALCAM^{pos} population containing proportionally more mature CMs (expressing higher levels of *TNNT2* mRNA) than the CAG-EGFP^{high} fraction (possibly containing proportionally more immature CMs).

A key issue was to interpret the data obtained by the QPCR analysis about *NKX2.5* expression. *NKX2.5* mRNA level of ALCAM^{pos} and ALCAM^{neg} samples were similar to that of the CAG-EGFP^{low} sample, and was significantly higher than observed in the CAG-EGFP^{high} fraction both in day 12 and in day 14 experiments (**Figure 20C**). These results were especially contradictory in the case of day 14 samples, when the QPCR analysis of *TNNT2* mRNA showed elevated expression both in ALCAM^{pos} and in CAG-EGFP^{high} samples compared to ALCAM^{neg} and CAG-EGFP^{low} samples, respectively (**Figure 20B**). We assumed that a pure ALCAM^{pos} population containing mostly CMs of a particular phenotype would have resulted in significant differences in distribution of *NKX2.5* mRNA levels between the ALCAM^{neg} and ALCAM^{pos} sample. However, this was not the case, therefore we concluded that the ALCAM^{pos} population has to contain ALCAM^{pos}/*NKX2.5*^{high} cells to compensate for the significantly low *NKX2.5* levels of CAG-EGFP^{high} cells (a subpopulation of the ALCAM^{pos} fraction),

resulting in a lowered average *NKX2.5* mRNA level of the ALCAM^{pos} sample. The ALCAM^{pos}/*NKX2.5*^{high} phenotype can represent a more mature stage of CM differentiation, since day 12 CAG-EGFP^{high} CPCs expressing *NKX2.5* mRNA at low levels are also able to give rise to *NKX2.5*^{high} CMs (**Figure 24**).

However, these results, together with the fact that the CAG-EGFP^{high} rEBs gave rise mainly to atrial myocytes (**Figure 29**), suggest that not only the maturity status of the cardiac cells differs from each other, but there may also be a subtype-specificity of the CAG-EGFP system involved. In this case CAG-EGFP^{high} cells would identify *NKX2.5*^{low} atrial progenitors, able to give rise to atrial myocytes and smooth muscle cells (**Figure 26 and 27**). This is in good accordance with the report of Nakano *et al.*, demonstrating that a pool of cells of the second heart field located in the venous pole of the heart tube (from where the atria arise) give rise solely to atrial cardiomyocytes and smooth muscle cells during mouse embryogenesis[140]. These *Isl1* and sarcolipin positive cells could be isolated and after 4 days of *in vitro* differentiation most of the colonies expressed low levels of *Nkx2.5*.

It has also been shown in atrial *Nkx2.5* conditional knockout mice that *Nkx2.5* serves as a negative regulator for proliferation of atrial myocytes[141]. Zebra fish studies also suggested a role for the Nkx2.5 transcription factor in limiting atrial cell number and promoting ventricular cell number, while loss of *nkx2.5* function resulted in the opposite effect[142]. This study also demonstrated that nkx2.5 is responsible for sustaining ventricular myocyte attributes through repression of atrial chamber identity and that loss of Nkx gene function can cause ventricular myocytes to transform into atrial myocytes.

Human embryonic stem cells, unlike mouse ESCs, show low survival rate as single cells due to disruption of E-cadherin signalling caused by enzymatic dissociation[143]. The same is true for early derivatives of hESCs[131, 144]. In accordance with these findings, our experiments indicated that the CAG-EGFP^{high} CPCs are not able to survive as single cells, at least not under suspension culture conditions (**Figure 32**).

In order to enhance overall CM yield we had to enhance survival of CAG-EGFP^{high} cells after the sorting procedure. This could be performed by supporting the reaggregation of the isolated cells with Thiazovivin treatment or applying an END-2 conditioned medium (**Figure 32**). Better reaggregation ability resulted in CAG-

EGFP^{high} rEBs with increased size (**Figure 34**), but with decreased cardiac mRNA levels (**Figure 35**). Long-term administration of Isoproterenol enhanced *TNNT2* levels of CAG-EGFP^{high} rEBs cultured in END2 conditioned medium, while the size of the rEBs were not affected (**Figure 36**). This optimized culture method generates CAG-EGFP^{high} rEBs with increased cell number, but similar troponin levels as that of rEBs cultured under basic conditions (**Figure 24 and 35**).

Neuregulin was suggested to enhance proliferation of CMs[82], to increase CM yield from mESCs[145-147] and to enhance the proportion of ventricular myocytes among the generated CMs (10% nodal versus 90% ventricular subtype)[84]. However, in our system, Neuregulin failed to enhance *TNNT2* levels of the CAG-EGFP^{high} rEBs, but this may reflect that Neuregulin-dependent regulation of subtype specification happens at earlier stages of differentiation.

DOI:10.14753/SE.2015.1764

7. Conclusions

1. The CAG promoter-driven EGFP reporter system enables the selection of transgene-expressing hESCs. Moreover, cardiomyocytes differentiated from CAG-EGFP expressing hESCs can be easily identified based on their extremely high EGFP expression due to the cardiac tissue-specific transcriptional upregulation of the CAG promoter. These two features of this CAG promoter variant led to the designation as a "double feature promoter".

2. Directed differentiation of human embryonic stem cells results in enrichment of CAG-EGFP^{high} progenitors.

3. The CAG-EGFP system offers the advantage to isolate *NKX2.5*^{low} cardiac progenitor cells. During differentiation CAG-EGFP^{high} cardiac progenitor cells upregulate cardiomyocyte markers, such as SIRPA, VCAM1 and ALCAM.

4. Isolated CAG-EGFP^{high} cardiac progenitors are able to maintain their cardiac commitment during differentiation when cultured as 3D aggregates in conventional differentiation medium.

5. CAG-EGFP^{high} progenitor cells can generate spontaneously contracting 3D aggregates. These rEBs contain more than 90% of mature cardiomyocytes and show enhanced NKX2.5 and MYL7 transcription. CAG-EGFP^{high} cells possess a more restricted differentiation potential than previously described cardiovascular progenitor cells, since CAG-EGFP^{high} cardiac progenitor cells give rise to smooth muscle cells and atrial myocytes, but fail to differentiate into endothelial cells under 3D culture conditions.

6. Reaggregation and survival properties of CAG-EGFP^{high} CPCs can be enhanced by Thiazovivin or by the use of an END-2 conditioned medium, resulting rEBs with larger size than under control conditions. In our hands the cardioinductive effect of END-2 was not detectable and Isoproterenol, a beta-adrenerg agonist was needed to support the cardiogenic potential of CAG-EGFP^{high} CPCs when cultured in END-2 conditioned medium as 3D aggregates.

DOI:10.14753/SE.2015.1764

The application of this ‘‘double-feature’’ promoter provides a unique opportunity to examine the selective markers, including cell surface proteins of the cardiac lineage from early CPCs to late CMs and allows purification and enrichment of cardiac cells.

DOI:10.14753/SE.2015.1764

8. Summary

The achievements displayed in the dissertation include characterization of a novel *in vitro* method for identification and isolation of human embryonic stem cell-derived cardiomyocytes and cardiac progenitors, characterization of the cardiac progenitors identified by this method and introduction of an optimized culture condition for cardiac progenitors to enhance overall cardiomyocyte yield.

The method utilizes the special, double-feature characteristics of the CAG promoter, driving the expression of the green fluorescent protein (GFP) in undiffereniated stem cells and providing exceptionally high GFP expression in hESC-derived cardiomyocytes, while its activity in other cell types remains modest. This exceptionally high GFP signal is also characteristic for cardiac progenitors, allowing the isolation of progenitor cells, which are still capable to divide and differentiate into atrial type cardiomyocytes and, to a lesser extent, into smooth muscle cells. Cardiac commitment of the progenitors could be best maintained by supporting the initiation of direct cell-cell contacts through 3D culture. Enhanced survival of cardiac progenitors after isolation could be achieved, and by applying a specific combination of treatments cardiomyocyte yield could also be enhanced.

DOI:10.14753/SE.2015.1764

9. Összefoglalás

A doktori disszertációban részletezett tudományos munka eredményeként megszületett egy olyan új módszer, amely humán embrionális őssejt eredetű szívizomsejtek és azok előalakjainak, az ún. szívizom progenitorsejteknek a felismerését és kiválogatását teszi lehetővé. A munka részét képezte az ilyen módon kiválogatható szívizom progenitorsejtek jellemzése, valamint egy olyan tenyésztési körülmény kidolgozása is, ami a progenitorsejtek osztódását és szívizom irányú elköteleződését egyaránt támogatja.

A módszer a CAG promóter egy variánsának különleges, kétarcú tulajdonságán alapul, amely egyrészt “megszólaltatja” a zöld fluoreszcens fehérjét (GFP) differenciálatlan őssejtekben, másrészt különösen erős GFP kifejeződést biztosít az őssejtekből keletkező szívizomsejtekben, míg más sejttípusok esetében aktivitása lényegesen gyengébb. Ez a különösen erős GFP jel a szívizom progenitorsejtekre is jellemző, így ezek a még osztódásra képes sejtek is kiválogathatók az őssejtek különböző típusú utódsejtjeit tartalmazó tenyészetekből. A kiválogatott progenitorsejtekből főleg pitvari típusú szívizomsejtek keletkeznek, de képesek simaizom típusú sejtek létrehozására is. A kiválogatott progenitorsejtek túlélését és szívizomirányú elköteleződését is elősegíti, ha sejt-sejt kapcsolatok kialakítására alkalmas 3D struktúrában tenyésznek, míg a megfelelő kezelések alkalmazásával az előállított szívizomsejtek mennyisége növelhető.

10. References

1. Thomson JA, Itskovitz-Eldor J, Shapiro SS, Waknitz MA, Swiergiel JJ, Marshall VS & Jones JM. (1998) Embryonic stem cell lines derived from human blastocysts. Science, 282: 1145-1147.
2. Charron D, Suberbielle-Boissel C & Al-Daccak R. (2009) Immunogenicity and allogenicity: a challenge of stem cell therapy. J Cardiovasc Transl Res, 2: 130-138.
3. Cabrera CM, Cobo F, Nieto A & Concha A. (2006) Strategies for preventing immunologic rejection of transplanted human embryonic stem cells. Cytotherapy, 8: 517-518.
4. Taylor CJ, Bolton EM & Bradley JA. (2011) Immunological considerations for embryonic and induced pluripotent stem cell banking. Philos Trans R Soc Lond B Biol Sci, 366: 2312-2322.
5. Kroon E, Martinson LA, Kadoya K, Bang AG, Kelly OG, Eliazer S, Young H, Richardson M, Smart NG, Cunningham J, Agulnick AD, D'Amour KA, Carpenter MK & Baetge EE. (2008) Pancreatic endoderm derived from human embryonic stem cells generates glucose-responsive insulin-secreting cells in vivo. Nat Biotechnol, 26: 443-452.
6. Szebenyi K, Erdei Z, Pentek A, Sebe A, Orban TI, Sarkadi B & Apati A. (2011) Human pluripotent stem cells in pharmacological and toxicological screening: new perspectives for personalized medicine. Pers Med, 8: 347-364.
7. Takahashi K & Yamanaka S. (2006) Induction of pluripotent stem cells from mouse embryonic and adult fibroblast cultures by defined factors. Cell, 126: 663-676.
8. Malik N & Rao MS. (2013) A review of the methods for human iPSC derivation. Methods Mol Biol, 997: 23-33.
9. Borstlap J, Luong MX, Rooke HM, Aran B, Damaschun A, Elstner A, Smith KP, Stein GS & Veiga A. (2010) International stem cell registries. In Vitro Cell Dev Biol Anim, 46: 242-246.

10. Stacey GN, Cobo F, Nieto A, Talavera P, Healy L & Concha A. (2006) The development of 'feeder' cells for the preparation of clinical grade hES cell lines: challenges and solutions. J Biotechnol, 125: 583-588.
11. Stojkovic P, Lako M, Stewart R, Przyborski S, Armstrong L, Evans J, Murdoch A, Strachan T & Stojkovic M. (2005) An autogeneic feeder cell system that efficiently supports growth of undifferentiated human embryonic stem cells. Stem Cells, 23: 306-314.
12. Ludwig TE, Bergendahl V, Levenstein ME, Yu J, Probasco MD & Thomson JA (2006) Feeder-independent culture of human embryonic stem cells. Nat Methods, 3: 637-646.
13. Li Y, Powell S, Brunette E, Lebkowski J & Mandalam R. (2005) Expansion of human embryonic stem cells in defined serum-free medium devoid of animal-derived products. Biotechnol Bioeng, 91: 688-698.
14. Rodin S, Domogatskaya A, Strom S, Hansson EM, Chien KR, Inzunza J, Hovatta O & Tryggvason K. (2010) Long-term self-renewal of human pluripotent stem cells on human recombinant laminin-511. Nat Biotechnol, 28: 611-615.
15. Beers J, Gulbranson DR, George N, Siniscalchi LI, Jones J, Thomson JA & Chen G. (2012) Passaging and colony expansion of human pluripotent stem cells by enzyme-free dissociation in chemically defined culture conditions. Nat Protoc, 7: 2029-2040.
16. Chen G, Gulbranson DR, Hou Z, Bolin JM, Ruotti V, Probasco MD, Smuga-Otto K, Howden SE, Diol NR, Propson NE, Wagner R, Lee GO, Antosiewicz-Bourget J, Teng JM & Thomson JA. (2011) Chemically defined conditions for human iPSC derivation and culture. Nat Methods, 8: 424-429.
17. Adewumi O, Aflatoonian B, Ahrlund-Richter L, Amit M, Andrews PW, Beighton G, Bello PA, Benvenisty N, Berry LS, Bevan S, Blum B, Brooking J, Chen KG, Choo AB, Churchill GA, Corbel M, Damjanov I, Draper JS, Dvorak P, Emanuelsson K, Fleck RA, Ford A, Gertow K, Gertsenstein M, Gokhale PJ, Hamilton RS, Hampl A, Healy LE, Hovatta O, Hyllner J, Imreh MP, Itskovitz-Eldor J, Jackson J, Johnson JL, Jones M, Kee K, King BL, Knowles BB, Lako M, Lebrin F, Mallon BS, Manning D, Mayshar Y, McKay RD, Michalska AE,

Mikkola M, Mileikovsky M, Minger SL, Moore HD, Mummery CL, Nagy A, Nakatsuji N, O'Brien CM, Oh SK, Olsson C, Otonkoski T, Park KY, Passier R, Patel H, Patel M, Pedersen R, Pera MF, Piekarczyk MS, Pera RA, Reubinoff BE, Robins AJ, Rossant J, Rugg-Gunn P, Schulz TC, Semb H, Sherrer ES, Siemen H, Stacey GN, Stojkovic M, Suemori H, Szatkiewicz J, Turetsky T, Tuuri T, van den Brink S, Vintersten K, Vuoristo S, Ward D, Weaver TA, Young LA & Zhang W. (2007) Characterization of human embryonic stem cell lines by the International Stem Cell Initiative. Nat Biotechnol, 25: 803-816.

18. Baker DE, Harrison NJ, Maltby E, Smith K, Moore HD, Shaw PJ, Heath PR, Holden H & Andrews PW. (2007) Adaptation to culture of human embryonic stem cells and oncogenesis in vivo. Nat Biotechnol, 25: 207-215.
19. Cowan CA, Klimanskaya I, McMahon J, Atienza J, Witmyer J, Zucker JP, Wang S, Morton CC, McMahon AP, Powers D & Melton DA. (2004) Derivation of embryonic stem-cell lines from human blastocysts. N Engl J Med, 350: 1353-1356.
20. Draper JS, Smith K, Gokhale P, Moore HD, Maltby E, Johnson J, Meisner L, Zwaka TP, Thomson JA & Andrews PW. (2004) Recurrent gain of chromosomes 17q and 12 in cultured human embryonic stem cells. Nat Biotechnol, 22: 53-54.
21. Rosler ES, Fisk GJ, Ares X, Irving J, Miura T, Rao MS & Carpenter MK. (2004) Long-term culture of human embryonic stem cells in feeder-free conditions. Dev Dyn, 229: 259-274.
22. Terstegge S, Laufenberg I, Pochert J, Schenk S, Itskovitz-Eldor J, Endl E & Brustle O. (2007) Automated maintenance of embryonic stem cell cultures. Biotechnol Bioeng, 96: 195-201.
23. Abbasalizadeh S, Larijani MR, Samadian A & Baharvand H. (2012) Bioprocess development for mass production of size-controlled human pluripotent stem cell aggregates in stirred suspension bioreactor. Tissue Eng Part C Methods, 18: 831-851.
24. Badenes SM, Fernandes TG, Rodrigues CA, Diogo MM & Cabral JM. (2014) Scalable Expansion of Human-Induced Pluripotent Stem Cells in Xeno-Free Microcarriers. Methods Mol Biol, Online Ahead of Print.

25. Fan Y, Hsiung M, Cheng C & Tzanakakis ES. (2014) Facile engineering of xeno-free microcarriers for the scalable cultivation of human pluripotent stem cells in stirred suspension. Tissue Eng Part A, 20: 588-599.
26. Kehoe DE, Jing D, Lock LT & Tzanakakis ES. (2010) Scalable stirred-suspension bioreactor culture of human pluripotent stem cells. Tissue Eng Part A, 16: 405-421.
27. Itskovitz-Eldor J, Schuldiner M, Karsenti D, Eden A, Yanuka O, Amit M, Soreq H & Benvenisty N. (2000) Differentiation of human embryonic stem cells into embryoid bodies compromising the three embryonic germ layers. Mol Med, 6: 88-95.
28. Murry CE & Keller G. (2008) Differentiation of embryonic stem cells to clinically relevant populations: lessons from embryonic development. Cell, 132: 661-680.
29. Joannides AJ, Fiore-Heriche C, Battersby AA, Athauda-Arachchi P, Bouhon IA, Williams L, Westmore K, Kemp PJ, Compston A, Allen ND & Chandran S. (2007) A scaleable and defined system for generating neural stem cells from human embryonic stem cells. Stem Cells, 25: 731-737.
30. Kang SM, Cho MS, Seo H, Yoon CJ, Oh SK, Choi YM & Kim DW. (2007) Efficient induction of oligodendrocytes from human embryonic stem cells. Stem Cells, 25: 419-424.
31. Laflamme MA, Chen KY, Naumova AV, Muskheli V, Fugate JA, Dupras SK, Reinecke H, Xu C, Hassanipour M, Police S, O'Sullivan C, Collins L, Chen Y, Minami E, Gill EA, Ueno S, Yuan C, Gold J & Murry CE. (2007) Cardiomyocytes derived from human embryonic stem cells in pro-survival factors enhance function of infarcted rat hearts. Nat Biotechnol, 25: 1015-1024.
32. D'Amour KA, Bang AG, Eliazer S, Kelly OG, Agulnick AD, Smart NG, Moorman MA, Kroon E, Carpenter MK & Baetge EE. (2006) Production of pancreatic hormone-expressing endocrine cells from human embryonic stem cells. Nat Biotechnol, 24: 1392-1401.
33. Pagliuca FW, Millman JR, Gurtler M, Segel M, Van Dervort A, Ryu JH, Peterson QP, Greiner D & Melton DA. (2014) Generation of Functional Human Pancreatic beta Cells In Vitro. Cell, 159: 428-439.

34. Olsen AL, Stachura DL & Weiss MJ. (2006) Designer blood: creating hematopoietic lineages from embryonic stem cells. Blood, 107: 1265-1275.

35. Gieseck RL, 3rd, Hannan NR, Bort R, Hanley NA, Drake RA, Cameron GW, Wynn TA & Vallier L. (2014) Maturation of induced pluripotent stem cell derived hepatocytes by 3D-culture. PLoS One, 9: e86372.

36. Otsuji TG, Minami I, Kurose Y, Yamauchi K, Tada M & Nakatsuji N. (2010) Progressive maturation in contracting cardiomyocytes derived from human embryonic stem cells: Qualitative effects on electrophysiological responses to drugs. Stem Cell Res, 4: 201-213.

37. Yang X, Pabon L & Murry CE (2014) Engineering adolescence: maturation of human pluripotent stem cell-derived cardiomyocytes. Circ Res, 114: 511-523.

38. Yao R, Wang J, Li X, Da J, Qi H, Kee KK & Du Y. (2014) Hepatic Differentiation of Human Embryonic Stem Cells as Microscaled Multilayered Colonies Leading to Enhanced Homogeneity and Maturation. Small, 10: 4311-23.

39. Kim K, Doi A, Wen B, Ng K, Zhao R, Cahan P, Kim J, Aryee MJ, Ji H, Ehrlich LI, Yabuuchi A, Takeuchi A, Cunniff KC, Hongguang H, McKinney-Freeman S, Naveiras O, Yoon TJ, Irizarry RA, Jung N, Seita J, Hanna J, Murakami P, Jaenisch R, Weissleder R, Orkin SH, Weissman IL, Feinberg AP & Daley GQ. (2010) Epigenetic memory in induced pluripotent stem cells. Nature, 467: 285-290.

40. Ruiz S, Diep D, Gore A, Panopoulos AD, Montserrat N, Plongthongkum N, Kumar S, Fung HL, Giorgetti A, Bilic J, Batchelder EM, Zaehres H, Kan NG, Scholer HR, Mercola M, Zhang K & Izpisua Belmonte JC. (2012) Identification of a specific reprogramming-associated epigenetic signature in human induced pluripotent stem cells. Proc Natl Acad Sci U S A, 109: 16196-16201.

41. Vaskova EA, Stekleneva AE, Medvedev SP & Zakian SM. (2013) "Epigenetic memory" phenomenon in induced pluripotent stem cells. Acta Naturae, 5: 15-21.

42. Feng Q, Lu SJ, Klimanskaya I, Gomes I, Kim D, Chung Y, Honig GR, Kim KS & Lanza R. (2010) Hemangioblastic derivatives from human induced pluripotent stem cells exhibit limited expansion and early senescence. Stem Cells, 28: 704-712.

43. Foldes G, Matsa E, Kriston-Vizi J, Leja T, Mioulane M, Vauchez K, Ketteler R, Schneider MD, Denning C & Harding SE. (2013) Key differences in hypertrophic signalling between hESC- and hIPSC-derived cardiomyocytes. Eur Heart J, 34: 279-279.

44. Ramsden CM, Powner MB, Carr AJ, Smart MJ, da Cruz L & Coffey PJ. (2013) Stem cells in retinal regeneration: past, present and future. Development, 140: 2576-2585.

45. Sebastiano V, Maeder ML, Angstman JF, Haddad B, Khayter C, Yeo DT, Goodwin MJ, Hawkins JS, Ramirez CL, Batista LF, Artandi SE, Wernig M & Joung JK. (2011) In situ genetic correction of the sickle cell anemia mutation in human induced pluripotent stem cells using engineered zinc finger nucleases. Stem Cells, 29: 1717-1726.

46. Raya A, Rodriguez-Piza I, Guenechea G, Vassena R, Navarro S, Barrero MJ, Consiglio A, Castella M, Rio P, Sleep E, Gonzalez F, Tiscornia G, Garreta E, Aasen T, Veiga A, Verma IM, Surralles J, Bueren J & Izpisua Belmonte JC. (2009) Disease-corrected haematopoietic progenitors from Fanconi anaemia induced pluripotent stem cells. Nature, 460: 53-59.

47. Sanchez-Danes A, Richaud-Patin Y, Carballo-Carbajal I, Jimenez-Delgado S, Caig C, Mora S, Di Guglielmo C, Ezquerra M, Patel B, Giralt A, Canals JM, Memo M, Alberch J, Lopez-Barneo J, Vila M, Cuervo AM, Tolosa E, Consiglio A & Raya A. (2012) Disease-specific phenotypes in dopamine neurons from human iPS-based models of genetic and sporadic Parkinson's disease. EMBO Mol Med, 4: 380-395.

48. Lee G, Papapetrou EP, Kim H, Chambers SM, Tomishima MJ, Fasano CA, Ganat YM, Menon J, Shimizu F, Viale A, Tabar V, Sadelain M & Studer L. (2009) Modelling pathogenesis and treatment of familial dysautonomia using patient-specific iPSCs. Nature, 461: 402-406.

49. Aran B, Sole M, Rodriguez-Piza I, Parriego M, Munoz Y, Boada M, Barri PN, Izpisua JC & Veiga A. (2012) Vitrified blastocysts from Preimplantation Genetic Diagnosis (PGD) as a source for human Embryonic Stem Cell (hESC) derivation. J Assist Reprod Genet, 29: 1013-1020.

50. Verlinsky Y, Strelchenko N, Kukharenko V, Rechitsky S, Verlinsky O, Galat V & Kuliev A. (2005) Human embryonic stem cell lines with genetic disorders. Reprod Biomed Online, 10: 105-110.

51. O'Hara T & Rudy Y. (2012) Quantitative comparison of cardiac ventricular myocyte electrophysiology and response to drugs in human and nonhuman species. Am J Physiol Heart Circ Physiol, 302: H1023-1030.

52. Moretti A, Bellin M, Welling A, Jung CB, Lam JT, Bott-Flugel L, Dorn T, Goedel A, Hohnke C, Hofmann F, Seyfarth M, Sinnecker D, Schomig A & Laugwitz KL. (2010) Patient-specific induced pluripotent stem-cell models for long-QT syndrome. N Engl J Med, 363: 1397-1409.

53. Itzhaki I, Maizels L, Huber I, Zwi-Dantsis L, Caspi O, Winterstern A, Feldman O, Gepstein A, Arbel G, Hammerman H, Boulos M & Gepstein L. (2011) Modelling the long QT syndrome with induced pluripotent stem cells. Nature, 471: 225-229.

54. Yazawa M, Hsueh B, Jia X, Pasca AM, Bernstein JA, Hallmayer J & Dolmetsch RE. (2011) Using induced pluripotent stem cells to investigate cardiac phenotypes in Timothy syndrome. Nature, 471: 230-234.

55. Jung CB, Moretti A, Mederos y Schnitzler M, Iop L, Storch U, Bellin M, Dorn T, Ruppenthal S, Pfeiffer S, Goedel A, Dirschinger RJ, Seyfarth M, Lam JT, Sinnecker D, Gudermann T, Lipp P & Laugwitz KL. (2012) Dantrolene rescues arrhythmogenic RYR2 defect in a patient-specific stem cell model of catecholaminergic polymorphic ventricular tachycardia. EMBO Mol Med, 4: 180-191.

56. Kim C, Wong J, Wen J, Wang S, Wang C, Spiering S, Kan NG, Forcales S, Puri PL, Leone TC, Marine JE, Calkins H, Kelly DP, Judge DP & Chen HS. (2013) Studying arrhythmogenic right ventricular dysplasia with patient-specific iPSCs. Nature, 494: 105-110.

57. Huang HP, Chen PH, Hwu WL, Chuang CY, Chien YH, Stone L, Chien CL, Li LT, Chiang SC, Chen HF, Ho HN, Chen CH & Kuo HC. (2011) Human Pompe disease-induced pluripotent stem cells for pathogenesis modeling, drug testing and disease marker identification. Hum Mol Genet, 20: 4851-4864.

58. Carvajal-Vergara X, Sevilla A, D'Souza SL, Ang YS, Schaniel C, Lee DF, Yang L, Kaplan AD, Adler ED, Rozov R, Ge Y, Cohen N, Edelmann LJ, Chang B, Waghray A, Su J, Pardo S, Lichtenbelt KD, Tartaglia M, Gelb BD & Lemischka IR. (2010) Patient-specific induced pluripotent stem-cell-derived models of LEOPARD syndrome. Nature, 465: 808-812.

59. Kurosawa H. (2007) Methods for inducing embryoid body formation: in vitro differentiation system of embryonic stem cells. J Biosci Bioeng, 103: 389-398.

60. Xu C, Police S, Rao N & Carpenter MK. (2002) Characterization and enrichment of cardiomyocytes derived from human embryonic stem cells. Circ Res, 91: 501-508.

61. Yang L, Soonpaa MH, Adler ED, Roepke TK, Kattman SJ, Kennedy M, Henckaerts E, Bonham K, Abbott GW, Linden RM, Field LJ & Keller GM. (2008) Human cardiovascular progenitor cells develop from a KDR+ embryonic-stem-cell-derived population. Nature, 453: 524-528.

62. Gadue P, Huber TL, Paddison PJ & Keller GM. (2006) Wnt and TGF-beta signaling are required for the induction of an in vitro model of primitive streak formation using embryonic stem cells. Proc Natl Acad Sci U S A, 103: 16806-16811.

63. Lindsley RC, Gill JG, Kyba M, Murphy TL & Murphy KM. (2006) Canonical Wnt signaling is required for development of embryonic stem cell-derived mesoderm. Development, 133: 3787-3796.

64. Kattman SJ, Witty AD, Gagliardi M, Dubois NC, Niapour M, Hotta A, Ellis J & Keller G. (2011) Stage-specific optimization of activin/nodal and BMP signaling promotes cardiac differentiation of mouse and human pluripotent stem cell lines. Cell Stem Cell, 8: 228-240.

65. Chen VC, Stull R, Joo D, Cheng X & Keller G. (2008) Notch signaling respecifies the hemangioblast to a cardiac fate. Nat Biotechnol, 26: 1169-1178.

66. Gai H, Leung EL, Costantino PD, Aguila JR, Nguyen DM, Fink LM, Ward DC & Ma Y. (2009) Generation and characterization of functional cardiomyocytes using induced pluripotent stem cells derived from human fibroblasts. Cell Biol Int, 33: 1184-1193.

67. Wang Y, Chen G, Song T, Mao G & Bai H. (2010) Enhancement of cardiomyocyte differentiation from human embryonic stem cells. Sci China Life Sci, 53: 581-589.

68. Yoon BS, Yoo SJ, Lee JE, You S, Lee HT & Yoon HS. (2006) Enhanced differentiation of human embryonic stem cells into cardiomyocytes by combining hanging drop culture and 5-azacytidine treatment. Differentiation, 74: 149-159.

69. Fujiwara M, Yan P, Otsuji TG, Narazaki G, Uosaki H, Fukushima H, Kuwahara K, Harada M, Matsuda H, Matsuoka S, Okita K, Takahashi K, Nakagawa M, Ikeda T, Sakata R, Mummery CL, Nakatsuji N, Yamanaka S, Nakao K & Yamashita JK. (2011) Induction and enhancement of cardiac cell differentiation from mouse and human induced pluripotent stem cells with cyclosporin-A. PLoS One, 6: e16734.

70. Mummery C, Ward-van Oostwaard D, Doevendans P, Spijker R, van den Brink S, Hassink R, van der Heyden M, Opthof T, Pera M, de la Riviere AB, Passier R & Tertoolen L. (2003) Differentiation of human embryonic stem cells to cardiomyocytes: role of coculture with visceral endoderm-like cells. Circulation, 107: 2733-2740.

71. Mummery C, Ward D, van den Brink CE, Bird SD, Doevendans PA, Opthof T, Brutel de la Riviere A, Tertoolen L, van der Heyden M & Pera M. (2002) Cardiomyocyte differentiation of mouse and human embryonic stem cells. J Anat, 200: 233-242.

72. Uosaki H, Andersen P, Shenje LT, Fernandez L, Christiansen SL & Kwon C. (2012) Direct contact with endoderm-like cells efficiently induces cardiac progenitors from mouse and human pluripotent stem cells. PLoS One, 7: e46413.

73. Mummery CL, Ward D & Passier R. (2007) Differentiation of human embryonic stem cells to cardiomyocytes by coculture with endoderm in serum-free medium. Curr Protoc Stem Cell Biol, Chapter 1: Unit 1F 2.

74. Xu XQ, Graichen R, Soo SY, Balakrishnan T, Rahmat SN, Sieh S, Tham SC, Freund C, Moore J, Mummery C, Colman A, Zweigerdt R & Davidson BP.

(2008) Chemically defined medium supporting cardiomyocyte differentiation of human embryonic stem cells. Differentiation, 76: 958-970.

75. Lam AT, Chen AK, Li J, Birch WR, Reuveny S & Oh SK. (2014) Conjoint propagation and differentiation of human embryonic stem cells to cardiomyocytes in a defined microcarrier spinner culture. Stem Cell Res Ther, 5: 110.
76. Niebruegge S, Bauwens CL, Peerani R, Thavandiran N, Masse S, Sevaptisidis E, Nanthakumar K, Woodhouse K, Husain M, Kumacheva E & Zandstra PW. (2009) Generation of human embryonic stem cell-derived mesoderm and cardiac cells using size-specified aggregates in an oxygen-controlled bioreactor. Biotechnol Bioeng, 102: 493-507.
77. Dixon JE, Dick E, Rajamohan D, Shakesheff KM & Denning C. (2011) Directed differentiation of human embryonic stem cells to interrogate the cardiac gene regulatory network. Mol Ther, 19: 1695-1703.
78. Fonoudi H, Yeganeh M, Fattahi F, Ghazizadeh Z, Rassouli H, Alikhani M, Mojarad BA, Baharvand H, Salekdeh GH & Aghdami N. (2013) ISL1 protein transduction promotes cardiomyocyte differentiation from human embryonic stem cells. PLoS One, 8: e55577.
79. Snir M, Kehat I, Gepstein A, Coleman R, Itskovitz-Eldor J, Livne E & Gepstein L. (2003) Assessment of the ultrastructural and proliferative properties of human embryonic stem cell-derived cardiomyocytes. Am J Physiol Heart Circ Physiol, 285: H2355-2363.
80. Engel FB, Schebesta M, Duong MT, Lu G, Ren S, Madwed JB, Jiang H, Wang Y & Keating MT. (2005) p38 MAP kinase inhibition enables proliferation of adult mammalian cardiomyocytes. Genes Dev, 19: 1175-1187.
81. Kuhn B, del Monte F, Hajjar RJ, Chang YS, Lebeche D, Arab S & Keating MT. (2007) Periostin induces proliferation of differentiated cardiomyocytes and promotes cardiac repair. Nat Med, 13: 962-969.
82. Bersell K, Arab S, Haring B & Kuhn B. (2009) Neuregulin1/ErbB4 signaling induces cardiomyocyte proliferation and repair of heart injury. Cell, 138: 257-270.

83. Meyer D & Birchmeier C. (1995) Multiple essential functions of neuregulin in development. Nature, 378: 386-390.

84. Zhu WZ, Xie Y, Moyes KW, Gold JD, Askari B & Laflamme MA. (2010) Neuregulin/ErbB signaling regulates cardiac subtype specification in differentiating human embryonic stem cells. Circ Res, 107: 776-786.

85. Zhang Q, Jiang J, Han P, Yuan Q, Zhang J, Zhang X, Xu Y, Cao H, Meng Q, Chen L, Tian T, Wang X, Li P, Hescheler J, Ji G & Ma Y. (2011) Direct differentiation of atrial and ventricular myocytes from human embryonic stem cells by alternating retinoid signals. Cell Res, 21: 579-587.

86. Dubois NC, Craft AM, Sharma P, Elliott DA, Stanley EG, Elefanty AG, Gramolini A & Keller G. (2011) SIRPA is a specific cell-surface marker for isolating cardiomyocytes derived from human pluripotent stem cells. Nat Biotechnol, 29: 1011-1018.

87. Rust W, Balakrishnan T & Zweigerdt R. (2009) Cardiomyocyte enrichment from human embryonic stem cell cultures by selection of ALCAM surface expression. Regen Med, 4: 225-237.

88. Elliott DA, Braam SR, Koutsis K, Ng ES, Jenny R, Lagerqvist EL, Biben C, Hatzistavrou T, Hirst CE, Yu QC, Skelton RJ, Ward-van Oostwaard D, Lim SM, Khammy O, Li X, Hawes SM, Davis RP, Goulburn AL, Passier R, Prall OW, Haynes JM, Pouton CW, Kaye DM, Mummery CL, Elefanty AG & Stanley EG. (2011) NKX2-5(eGFP/w) hESCs for isolation of human cardiac progenitors and cardiomyocytes. Nat Methods, 8: 1037-1040.

89. Cao N, Liang H, Huang J, Wang J, Chen Y, Chen Z & Yang HT. (2013) Highly efficient induction and long-term maintenance of multipotent cardiovascular progenitors from human pluripotent stem cells under defined conditions. Cell Res, 23: 1119-1132.

90. Orban TI, Apati A, Nemeth A, Varga N, Krizsik V, Schamberger A, Szebenyi K, Erdei Z, Varady G, Karaszi E, Homolya L, Nemet K, Gocza E, Miskey C, Mates L, Ivics Z, Izsvak Z & Sarkadi B. (2009) Applying a "double-feature" promoter to identify cardiomyocytes differentiated from human embryonic stem cells following transposon-based gene delivery. Stem Cells, 27: 1077-1087.

91. Schwanke K, Merkert S, Kempf H, Hartung S, Jara-Avaca M, Templin C, Gohring G, Haverich A, Martin U & Zweigerdt R. (2014) Fast and efficient multitransgenic modification of human pluripotent stem cells. Hum Gene Ther Methods, 25: 136-153.

92. Xue H, Wu J, Li S, Rao MS & Liu Y. (2014) Genetic Modification in Human Pluripotent Stem Cells by Homologous Recombination and CRISPR/Cas9 System. Methods Mol Biol, Online Ahead of Print.

93. Norrman K, Fischer Y, Bonnamy B, Wolfhagen Sand F, Ravassard P & Semb H. (2010) Quantitative comparison of constitutive promoters in human ES cells. PLoS One, 5: e12413.

94. Chung S, Andersson T, Sonntag KC, Bjorklund L, Isacson O & Kim KS. (2002) Analysis of different promoter systems for efficient transgene expression in mouse embryonic stem cell lines. Stem Cells, 20: 139-145.

95. Alexopoulou AN, Couchman JR & Whiteford JR. (2008) The CMV early enhancer/chicken beta actin (CAG) promoter can be used to drive transgene expression during the differentiation of murine embryonic stem cells into vascular progenitors. BMC Cell Biol, 9: 2.

96. van Laake LW, Passier R, Monshouwer-Kloots J, Verkleij AJ, Lips DJ, Freund C, den Ouden K, Ward-van Oostwaard D, Korving J, Tertoolen LG, van Echteld CJ, Doevendans PA & Mummery CL. (2007) Human embryonic stem cell-derived cardiomyocytes survive and mature in the mouse heart and transiently improve function after myocardial infarction. Stem Cell Res, 1: 9-24.

97. Caspi O, Huber I, Kehat I, Habib M, Arbel G, Gepstein A, Yankelson L, Aronson D, Beyar R & Gepstein L. (2007) Transplantation of human embryonic stem cell-derived cardiomyocytes improves myocardial performance in infarcted rat hearts. J Am Coll Cardiol, 50: 1884-1893.

98. Dai W, Field LJ, Rubart M, Reuter S, Hale SL, Zweigerdt R, Graichen RE, Kay GL, Jyrala AJ, Colman A, Davidson BP, Pera M & Kloner RA. (2007) Survival and maturation of human embryonic stem cell-derived cardiomyocytes in rat hearts. J Mol Cell Cardiol, 43: 504-516.

99. Xue T, Cho HC, Akar FG, Tsang SY, Jones SP, Marban E, Tomaselli GF & Li RA. (2005) Functional integration of electrically active cardiac derivatives from

genetically engineered human embryonic stem cells with quiescent recipient ventricular cardiomyocytes: insights into the development of cell-based pacemakers. Circulation, 111: 11-20.

100. Kita-Matsuo H, Barcova M, Prigozhina N, Salomonis N, Wei K, Jacot JG, Nelson B, Spiering S, Haverslag R, Kim C, Talantova M, Bajpai R, Calzolari D, Terskikh A, McCulloch AD, Price JH, Conklin BR, Chen HS & Mercola M. (2009) Lentiviral vectors and protocols for creation of stable hESC lines for fluorescent tracking and drug resistance selection of cardiomyocytes. PLoS One, 4: e5046.
101. Davis RP, Ng ES, Costa M, Mossman AK, Sourris K, Elefanty AG & Stanley EG. (2008) Targeting a GFP reporter gene to the MIXL1 locus of human embryonic stem cells identifies human primitive streak-like cells and enables isolation of primitive hematopoietic precursors. Blood, 111: 1876-1884.
102. Den Hartogh SC, Schreurs C, Monshouwer-Kloots JJ, Davis RP, Elliott DA, Mummery C & Passier R. (2015) Dual reporter MESP1 -NKX2-5 hESCs enable studying early human cardiac differentiation. Stem Cells, 33: 56-67.
103. Bu L, Jiang X, Martin-Puig S, Caron L, Zhu S, Shao Y, Roberts DJ, Huang PL, Domian IJ & Chien KR. (2009) Human ISL1 heart progenitors generate diverse multipotent cardiovascular cell lineages. Nature, 460: 113-117.
104. Ritner C, Wong SS, King FW, Mihardja SS, Liszewski W, Erle DJ, Lee RJ & Bernstein HS. (2011) An engineered cardiac reporter cell line identifies human embryonic stem cell-derived myocardial precursors. PLoS One, 6: e16004.
105. Anderson D, Self T, Mellor IR, Goh G, Hill SJ & Denning C. (2007) Transgenic enrichment of cardiomyocytes from human embryonic stem cells. Mol Ther, 15: 2027-2036.
106. Xu XQ, Zweigerdt R, Soo SY, Ngoh ZX, Tham SC, Wang ST, Graichen R, Davidson B, Colman A & Sun W. (2008) Highly enriched cardiomyocytes from human embryonic stem cells. Cytotherapy, 10: 376-389.
107. Huber I, Itzhaki I, Caspi O, Arbel G, Tzukerman M, Gepstein A, Habib M, Yankelson L, Kehat I & Gepstein L. (2007) Identification and selection of cardiomyocytes during human embryonic stem cell differentiation. Faseb J, 21: 2551-2563.

108. Gallo P, Grimaldi S, Latronico MV, Bonci D, Pagliuca A, Ausoni S, Peschle C & Condorelli G. (2008) A lentiviral vector with a short troponin-I promoter for tracking cardiomyocyte differentiation of human embryonic stem cells. Gene Ther, 15: 161-170.

109. Fu JD, Jiang P, Rushing S, Liu J, Chiamvimonvat N & Li RA. (2010) Na+/Ca2+ exchanger is a determinant of excitation-contraction coupling in human embryonic stem cell-derived ventricular cardiomyocytes. Stem Cells Dev, 19: 773-782.

110. Evseenko D, Zhu Y, Schenke-Layland K, Kuo J, Latour B, Ge S, Scholes J, Dravid G, Li X, MacLellan WR & Crooks GM. (2010) Mapping the first stages of mesoderm commitment during differentiation of human embryonic stem cells. Proc Natl Acad Sci U S A, 107: 13742-13747.

111. Sundberg M, Jansson L, Ketolainen J, Pihlajamaki H, Suuronen R, Skottman H, Inzunza J, Hovatta O & Narkilahti S. (2009) CD marker expression profiles of human embryonic stem cells and their neural derivatives, determined using flow-cytometric analysis, reveal a novel CD marker for exclusion of pluripotent stem cells. Stem Cell Res, 2: 113-124.

112. Drukker M, Tang C, Ardehali R, Rinkevich Y, Seita J, Lee AS, Mosley AR, Weissman IL & Soen Y. (2012) Isolation of primitive endoderm, mesoderm, vascular endothelial and trophoblast progenitors from human pluripotent stem cells. Nat Biotechnol, 30: 531-542.

113. Blin G, Nury D, Stefanovic S, Neri T, Guillevic O, Brinon B, Bellamy V, Rucker-Martin C, Barbry P, Bel A, Bruneval P, Cowan C, Pouly J, Mitalipov S, Gouadon E, Binder P, Hagege A, Desnos M, Renaud JF, Menasche P & Puceat M. (2010) A purified population of multipotent cardiovascular progenitors derived from primate pluripotent stem cells engrafts in postmyocardial infarcted nonhuman primates. J Clin Invest, 120: 1125-1139.

114. Draper JS, Pigott C, Thomson JA & Andrews PW. (2002) Surface antigens of human embryonic stem cells: changes upon differentiation in culture. J Anat, 200: 249-258.

115. Lin B, Kim J, Li Y, Pan H, Carvajal-Vergara X, Salama G, Cheng T, Lo CW & Yang L. (2012) High-purity enrichment of functional cardiovascular cells from human iPS cells. Cardiovasc Res, 95: 327-335.

116. Wu SM, Fujiwara Y, Cibulsky SM, Clapham DE, Lien CL, Schultheiss TM & Orkin SH. (2006) Developmental origin of a bipotential myocardial and smooth muscle cell precursor in the mammalian heart. Cell, 127: 1137-1150.

117. Skelton RJ, Costa M, Anderson DJ, Bruveris F, Finnin BW, Koutsis K, Arasaratnam D, White AJ, Rafii A, Ng ES, Elefanty AG, Stanley EG, Pouton CW, Haynes JM, Ardehali R, Davis RP, Mummery CL & Elliott DA. (2014) SIRPA, VCAM1 and CD34 identify discrete lineages during early human cardiovascular development. Stem Cell Res, 13: 172-179.

118. Uosaki H, Fukushima H, Takeuchi A, Matsuoka S, Nakatsuji N, Yamanaka S & Yamashita JK. (2011) Efficient and scalable purification of cardiomyocytes from human embryonic and induced pluripotent stem cells by VCAM1 surface expression. PLoS One, 6: e23657.

119. Hirata H, Murakami Y, Miyamoto Y, Tosaka M, Inoue K, Nagahashi A, Jakt LM, Asahara T, Iwata H, Sawa Y & Kawamata S. (2006) ALCAM (CD166) is a surface marker for early murine cardiomyocytes. Cells Tissues Organs, 184: 172-180.

120. Ohneda O, Ohneda K, Arai F, Lee J, Miyamoto T, Fukushima Y, Dowbenko D, Lasky LA & Suda T. (2001) ALCAM (CD166): its role in hematopoietic and endothelial development. Blood, 98: 2134-2142.

121. Scavone A, Capilupo D, Mazzocchi N, Crespi A, Zoia S, Campostrini G, Bucchi A, Milanesi R, Baruscotti M, Benedetti S, Antonini S, Messina G, DiFrancesco D & Barbuti A. (2013) Embryonic stem cell-derived CD166+ precursors develop into fully functional sinoatrial-like cells. Circ Res, 113: 389-398.

122. Hattori F, Chen H, Yamashita H, Tohyama S, Satoh YS, Yuasa S, Li W, Yamakawa H, Tanaka T, Onitsuka T, Shimoji K, Ohno Y, Egashira T, Kaneda R, Murata M, Hidaka K, Morisaki T, Sasaki E, Suzuki T, Sano M, Makino S, Oikawa S & Fukuda K. (2010) Nongenetic method for purifying stem cell-derived cardiomyocytes. Nat Methods, 7: 61-66.

123. Szebenyi K, Pentek A, Erdei Z, Varady G, Orban TI, Sarkadi B & Apati A (2014) Efficient Generation of Human Embryonic Stem Cell-Derived Cardiac Progenitors Based on Tissue-Specific EGFP Expression. Tissue Eng Part C Methods, Online Ahead of Print.

124. Barlow GM, Chen XN, Shi ZY, Lyons GE, Kurnit DM, Celle L, Spinner NB, Zackai E, Pettenati MJ, Van Riper AJ, Vekemans MJ, Mjaatvedt CH & Korenberg JR. (2001) Down syndrome congenital heart disease: a narrowed region and a candidate gene. Genet Med, 3: 91-101.

125. Tavakoli T, Xu X, Derby E, Serebryakova Y, Reid Y, Rao MS, Mattson MP & Ma W. (2009) Self-renewal and differentiation capabilities are variable between human embryonic stem cell lines I3, I6 and BG01V. BMC Cell Biol, 10: 44.

126. Boxall SA & Jones E. (2012) Markers for characterization of bone marrow multipotential stromal cells. Stem Cells Int, 2012: 975871.

127. Varga N, Vereb Z, Rajnavolgyi E, Nemet K, Uher F, Sarkadi B & Apati A. (2011) Mesenchymal stem cell like (MSCl) cells generated from human embryonic stem cells support pluripotent cell growth. Biochem Biophys Res Commun, 414: 474-480.

128. Horton RE & Auguste DT. (2012) Synergistic effects of hypoxia and extracellular matrix cues in cardiomyogenesis. Biomaterials, 33: 6313-6319.

129. Miskon A, Ehashi T, Mahara A, Uyama H & Yamaoka T. (2009) Beating behavior of primary neonatal cardiomyocytes and cardiac-differentiated P19.CL6 cells on different extracellular matrix components. J Artif Organs, 12: 111-117.

130. Xu Y, Zhu X, Hahm HS, Wei W, Hao E, Hayek A & Ding S. (2010) Revealing a core signaling regulatory mechanism for pluripotent stem cell survival and self-renewal by small molecules. Proc Natl Acad Sci U S A, 107: 8129-8134.

131. Braam SR, Nauw R, Ward-van Oostwaard D, Mummery C & Passier R. (2010) Inhibition of ROCK improves survival of human embryonic stem cell-derived cardiomyocytes after dissociation. Ann N Y Acad Sci, 1188: 52-57.

132. Gassmann M, Casagranda F, Orioli D, Simon H, Lai C, Klein R & Lemke G. (1995) Aberrant neural and cardiac development in mice lacking the ErbB4 neuregulin receptor. Nature, 378: 390-394.

133. Burridge PW, Thompson S, Millrod MA, Weinberg S, Yuan X, Peters A, Mahairaki V, Koliatsos VE, Tung L & Zambidis ET. (2011) A universal system for highly efficient cardiac differentiation of human induced pluripotent stem cells that eliminates interline variability. PLoS One, 6: e18293.

134. Cannavo A, Rengo G, Liccardo D, Pagano G, Zincarelli C, De Angelis MC, Puglia R, Di Pietro E, Rabinowitz JE, Barone MV, Cirillo P, Trimarco B, Palmer TM, Ferrara N, Koch WJ, Leosco D & Rapacciuolo A. (2013) beta1-adrenergic receptor and sphingosine-1-phosphate receptor 1 (S1PR1) reciprocal downregulation influences cardiac hypertrophic response and progression to heart failure: protective role of S1PR1 cardiac gene therapy. Circulation, 128: 1612-1622.

135. Communal C, Singh K, Sawyer DB & Colucci WS. (1999) Opposing effects of beta(1)- and beta(2)-adrenergic receptors on cardiac myocyte apoptosis : role of a pertussis toxin-sensitive G protein. Circulation, 100: 2210-2212.

136. Morisco C, Zebrowski DC, Vatner DE, Vatner SF & Sadoshima J. (2001) Beta-adrenergic cardiac hypertrophy is mediated primarily by the beta(1)-subtype in the rat heart. J Mol Cell Cardiol, 33: 561-573.

137. Branco AF, Pereira SL, Moreira AC, Holy J, Sardao VA & Oliveira PJ. (2011) Isoproterenol cytotoxicity is dependent on the differentiation state of the cardiomyoblast H9c2 cell line. Cardiovasc Toxicol, 11: 191-203.

138. Khan M, Mohsin S, Avitabile D, Siddiqi S, Nguyen J, Wallach K, Quijada P, McGregor M, Gude N, Alvarez R, Tilley DG, Koch WJ & Sussman MA. (2013) beta-Adrenergic regulation of cardiac progenitor cell death versus survival and proliferation. Circ Res, 112: 476-486.

139. Yan L, Jia Z, Cui J, Yang H, Zhang Y & Zhou C. (2011) Beta-adrenergic signals regulate cardiac differentiation of mouse embryonic stem cells via mitogen-activated protein kinase pathways. Dev Growth Differ, 53: 772-779.

140. Nakano H, Williams E, Hoshijima M, Sasaki M, Minamisawa S, Chien KR & Nakano A. (2011) Cardiac origin of smooth muscle cells in the inflow tract. J Mol Cell Cardiol, 50: 337-345.

141. Nakashima Y, Yanez DA, Touma M, Nakano H, Jaroszewicz A, Jordan MC, Pellegrini M, Roos KP & Nakano A. (2014) Nkx2-5 suppresses the proliferation of atrial myocytes and conduction system. Circ Res, 114: 1103-1113.

142. Targoff KL, Colombo S, George V, Schell T, Kim SH, Solnica-Krezel L & Yelon D. (2013) Nkx genes are essential for maintenance of ventricular identity. Development, 140: 4203-4213.

143. Watanabe K, Ueno M, Kamiya D, Nishiyama A, Matsumura M, Wataya T, Takahashi JB, Nishikawa S, Muguruma K & Sasai Y. (2007) A ROCK inhibitor permits survival of dissociated human embryonic stem cells. Nat Biotechnol, 25: 681-686.

144. Ardehali R, Ali SR, Inlay MA, Abilez OJ, Chen MQ, Blauwkamp TA, Yazawa M, Gong Y, Nusse R, Drukker M & Weissman IL. (2013) Prospective isolation of human embryonic stem cell-derived cardiovascular progenitors that integrate into human fetal heart tissue. Proc Natl Acad Sci U S A, 110: 3405-3410.

145. Kim HS, Cho JW, Hidaka K & Morisaki T. (2007) Activation of MEK-ERK by heregulin-beta1 promotes the development of cardiomyocytes derived from ES cells. Biochem Biophys Res Commun, 361: 732-738.

146. Suk Kim H, Hidaka K & Morisaki T. (2003) Expression of ErbB receptors in ES cell-derived cardiomyocytes. Biochem Biophys Res Commun, 309: 241-246.

147. Wang Z, Xu G, Wu Y, Guan Y, Cui L, Lei X, Zhang J, Mou L, Sun B & Dai Q. (2009) Neuregulin-1 enhances differentiation of cardiomyocytes from embryonic stem cells. Med Biol Eng Comput, 47: 41-48.

148. Szebényi K, Péntek A, Varga N, Erdei Z, Vőfély G, Orbán TI, Sarkadi B, Apáti Á. Human Stem-Cell-Derived Cardiomyocytes in Drug Discovery and Toxicity Testing. In: Saura C Sahu, Daniel A Casciano (eds.), Handbook of Nanotoxicology, Nanomedicine and Stem Cell Use in Toxicology. John Wiley & Sons, Ltd, Chichester, 2014: Paper in press.

11. List of publications related to this thesis

1 Szebenyi K, Péntek A, Erdei Z, Varady G, Orban TI, Sarkadi B, Apati A. (2014) Efficient Generation of Human Embryonic Stem Cell-Derived Cardiac Progenitors Based on Tissue-Specific EGFP Expression. Tissue Eng Part C Methods, Online Ahead of Print. IF: 4.254*

2 Orbán TI, Apáti Á, Németh A, Varga N, Krízsik V, Schamberger A, Szebényi K, Erdei Z, Várady G, Karászi É, Homolya L, Német K, Gócza E, Miskey C, Mátés L, Ivics Z, Izsvák Z, Sarkadi B. (2009) Applying a "double-feature" promoter to identify cardiomyocytes differentiated from human embryonic stem cells following transposon-based gene delivery. Stem Cells, 27:(5) pp. 1077-1087. IF: 7.747

DOI:10.14753/SE.2015.1764

12. List of publications not directly related to this thesis

1 Erdei Z, Lőrincz R, Szebényi K, Péntek A, Varga N, Likó I, Várady Gy, Szakács G, Orbán TI, Sarkadi B, Apáti Á. (2014) Expression pattern of the human ABC transporters in pluripotent embryonic stem cells and in their derivatives. Cytometry B Clin Cytom, 86: 299-310. IF: 2.283*

2 Apáti A, Pászty K, Hegedus L, Kolacsek O, Orbán TI, Erdei Z, Szebényi K, Péntek A, Enyedi A, Sarkadi B. (2013) Characterization of calcium signals in human embryonic stem cells and in their differentiated offspring by a stably integrated calcium indicator protein. Cell Signal, 25:(4) pp. 752-759. IF: 4.471

3 Erdei Z, Sarkadi B, Brozik A, Szebenyi K, Varady G, Makó V, Pentek A, Orban TI, Apati A. (2013) Dynamic ABCG2 expression in human embryonic stem cells provides the basis for stress response. Eur Biophys J, 42:(2-3) pp. 169-179. IF: 2.474

4 Nagy L, Milano F, Dorogi M, Agostiano A, Laczko G, Szebenyi K, Varo G, Trotta M, Maroti P. (2004) Protein/lipid interaction in the bacterial photosynthetic reaction center: Phosphatidylcholine and phosphatidylglycerol modify the free energy levels of the quinones. Biochemistry, 43:(40) pp. 12913-12923. IF: 4.008

DOI:10.14753/SE.2015.1764

13. Acknowledgement

First of all, I would like to thank my parents, supporting me all the time, even when nobody else did. I am very grateful to them for giving me a good example how to be insistent, consequent and loyal.

I am very grateful for all the help of András Füredi, who is there for me not only as partner for life, but also as partner in scientific projects. His faith in me makes me a better person, and his love makes me stronger and a bit more human at the same time.

I also would like to thank my former teachers in Külvárosi Tankör, since without the help of Györgyi and Co I would have never finished the secondary school and would have not been able to find a lifestyle satisfying me as much as the researcher lifestyle does. I also would like to thank László Nagy, Márta Dorogi and Balázs Rózsa, the people who introduced me to scientific research, as its finest.

I would like to express my special thanks to Ágota Apáti, teaching me that fewer is better and for being a friend through all these years. In addition, she guided my work and helped me through scientific and personal issues. The Pluripotent Stem Cell Laboratory become a second home to me, because of Ágota's attitude.

I am also very grateful to my supervisor, Balázs Sarkadi, who guided and supported my research. I learned a lot from Balázs, among others scientific thinking and publication skills.

I would like to thank those people in the Biomembrane research group, who taught me useful techniques and/or provided access to the necessary means, allowing me to carry out the research required to complete my work. I would like to highlight György Várady, who taught me how to use the flow cytometer, my very favourite technique, not only because of the usefulness of the method itself, but also because I keep a lot of good and happy memories from those times that I spent in the FACS laboratory. Hereby I also would like to thank Gyuri for trusting me and tolerating my sometimes chaotic time schedule. I have to thank Tamás Orbán as well, who taught me how to work with RNA in a precise way and he was also a person to whom I could turn to, whenever I needed advise in scientific issues.

DOI:10.14753/SE.2015.1764

I would like to thank Zsuzsa Erdei, Adrienn Péntek and Nóra Varga for all these years that we spent together and for forming me to a better team player (hopefully). I am also very grateful for the work of Bea Haraszti, who helped me a lot in whatever she could.

I am very grateful for the possibility to participate in the work of the „Őssejt" journal club organized and chaired by Ferenc Uher, who set an example for me how to be a valuable and respectable senior researcher.

I am also very grateful for the existence of Biomembrane group meetings, since the progress reports advanced my presenter skills a lot (from very weak into „still weak, but acceptable" level). Hereby, I have to thank my supervisor, Balázs Sarkadi again, for never hiding his critical opinion, thereby giving me the opportunity to advance. In addition, the group meetings provided an excellent forum for discussions and the questions, valuable comments and advises further advanced my research. For helping me in this way, I am especially thankful to Gergely Szakács.